Fakultät für Medizin

Max-Planck-Institute of Psychiatry

Studies on the role of hypoxia in growth hormone secreting pituitary tumor pathogenesis

Kristin Elizabeth Lucia

Vollständiger Abdruck der von der Fakultät für Medizin der Technischen Universität München zur Erlangung des akademischen Grades eines

Doctor of Philosophy (Ph.D.)

genehmigten Dissertation.

Vorsitzender: Prof. Dr. Roland M. Schmid

Betreuer: Prof. Dr. Günter K. Stalla

Prüfer der Dissertation:

1. Prof. Dr. Dirk Busch

2. Prof. Dr. Roland Rad

Die Dissertation wurde am 17.07.2017 bei der Fakultät für Medizin der Technischen Universität München eingereicht und durch die Fakultät für Medizin am 17.08.2017 angenommen.

Summary

Patients with acromegaly suffer from the endocrine, cardiovascular and psychiatric sequalae of excessive growth hormone secretion caused by somatotroph pituitary tumors. Growth hormone (GH) synthesis is tied to the activity of the cAMP-PKA signaling cascade. To date, overactivation of this cascade has been linked to recurrent somatic mutations in only 40% of patients. The elucidation of non-genomic mechanisms of cAMP-PKA activation in acromegaly may therefore uncover novel therapeutic targets. The present study reveals high levels of the transcription factor HIF-1α, a well characterized effector of the hypoxic cellular microenvironment, in somatotroph pituitary tumors from patients with acromegaly. Further investigation shows that HIF-1α expression under hypoxic conditions increases PKA activity via the transcriptional repression of the PKA regulatory subunit IIβ (PRKARIIβ) through the sequestration of SP1, the major regulator of PRKARIIβ transcription.

As up to 30% of patients with acromegaly do not respond to pharmacological treatment with somatostatin analogs (SSA), the role of HIF-1α expression in SSA resistance was investigated. It was observed that in primary cultures of somatotroph tumor tissue, hypoxic incubation could blunt the response to octreotide on GH secretion. Further analysis revealed that high HIF-1α expression is associated with lower rates of IGF-1 normalization in patients following treatment with somatostatin analogs.

Taken together, this study characterizes a novel molecular mechanism linking the microenvironment of somatotroph pituitary tumors to their secretory behavior and response to pharmacological treatment. These findings may be of particular interest in developing targeted pharmacological therapy for patients suffering from acromegaly.

Zusammenfassung

Patienten mit Akromegalie leiden an den endokrinen, kardiovaskulären und psychiatrischen Folgen einer gesteigerten Waschstumshormon (GH) Sekretion. GH Sekretion ist von der Aktivität der cAMP-PKA Signalkaskade abhängig. In nur 40% der betroffenen Patienten kann jedoch eine somatische Mutation als mögliche Ursache der gestigerten Aktivität der cAMP-PKA Kaskade identifiziert werden. Neue Erkenntnisse bezüglich non-genomische Aktivatoren dieser Signalkaskade könnten daher zur Entwicklung effektiveren therapeutischen Strategien beitragen.

Die vorliegende Studie zeigt gesteigerte Expression des Transkriptionsfaktors HIF-1α im Tumorgewebe von Patienten mit Akromegalie. HIF-1α wurde bereits als wichtiger Mediator des hypoxischen Tumor Microenvironments charakterisiert. Es konnte gezeigt werden, dass unter Hypoxie, HIF-1α den Transkriptionsfaktor Sp1 bindet und von dem Promoter der PKA regulatorischen Untereinheit (Prkar2b) sequestriert. Dies führt zu einer Suppression der PRKAR2B Transkription und ist mit der gesteigerten kalatlytischen Aktivität von PKA verbunden.

Bis zu 30% der Patienten mit Akromegalie zeigen eine therapeutische Resistenz gegen die häufig eingestzten Somatostatin-Analoga (SSA). Die Assoziation von HIF-1α Expression mit SSA Resistenz wurde daher untersucht. In primären Zellkulturen von Tumorgewebe von Patienten mit Akromegalie führte Hypoxie zu einem Wirkungsverlust von SSA auf GH Sekretion. Zudem war eine starke Expression von HIF-1α im Tumorgewebe von Patienten mit Akromegalie mit einer geringeren therapeutischen Effekt auf IGF-1 assoziiert. Zusammengefasst können die vorliegenden Untersuchungen zum Verständis der Pathophysiologe von Akromegalie sowie zur Entwicklung effektiveren pharmakologischen Therapien beitragen

Table of Contents

1. Introduction

1.1. The pituitary gland

The pituitary gland is an endocrine organ located in the sella turcica of the sphenoid bone. It is divided anatomically into the anterior (adenohypophysis) and posterior (neurohypophsis) lobes, with a rudimentary intermediate lobe found in humans. The anterior lobe arises from the oral ectoderm (subsequently Rathke's pouch) and the posterior lobe from the neuroectoderm. As such, the neurohypophysis contains axonal projections from hypothalamic nuclei which run through the infundibulur stalk to release vasopressin, oxytocin and anti-diuretic hormone (ADH) as well as other releasing hormones which target cells of the anterior pituitary (see below). The anterior pituitary contains five types of hormone-producing cells: somatotrophs (produce growth hormone), lactrotrophs (produce prolactin), gonadotrophs (produce LH/FSH), thyrotrophs (produce TSH), and corticotrophs (produce POMC). Stimulation and inhibition of hormone release from cells of the anterior pituitary occur through specific releasing and inhibiting factors produced in the hypothalamus as well as through signals received from peripheral organs. In addition to the hormone producing endocrine cells of anterior pituitary, approximately 5% of the cell population is made up of so-called folliculostellate cells. These non-secreting cells are S100 positive and due to their cytoplasmic projections possess a star-like morphology [1].

1.2. Growth hormone (GH) physiology and regulation

1.2.1. Growth hormone physiology

Growth hormone (GH), a 191 amino acid polypeptide hormone is synthesized by somatotroph cells of the anterior pituitary. These cells arise from the oral ectoderm and differentiate as the result of the expression of various transcription factors such as prophet of Pit1 (Prop-1), Pit1 and ERα [2-4]. Pituitary GH produced by somatotrophs (hGH-N) accounts for approximately 75% of circulating GH with four other isoforms being expressed primarily by tissue of the placenta [5].

GH plays a central role in organ development and metabolic homeostasis throughout the lifespan of an organism. It is generally regarded as an anabolic hormone which

contributes to soft tissue and bone growth, as children with isolated GH deficiency present with growth retardation and delayed onset puberty [6]. In addition, GH regulates central aspects of carbohydrate, lipid and protein metabolism and can act directly or through its effector, Insulin-Like-Growth Factor-1 (IGF-1) [7].

1.2.2. Growth hormone synthesis

GH synthesis in somatotroph pituitary cells is stimulated by the Growth Hormone Releasing Hormone (GHRH) which is synthesized in the hypothalamus and released in a pulsatile fashion through the hypophyseal portal vessel system to the anterior pituitary [8-11]. While GH synthesis and secretion are stimulated by GHRH, inhibition of these processes occurs through several further substrates. Somatostatin (SST) is a peptide hormone produced in the hypothalamus and released via the hypophyseal portal vessel system into the anterior pituitary [12]. Somatostatin is also synthesized by delta cells of the pancreatic islets, gastric mucosa and small intestines [13]. Five somatostatin receptors (Sstr1-5) exist, with Sstr2 having two isoforms due to alternative splicing (Sstr2a and Sstr2b) [14]. Of the five Sstrs, four are expressed in the anterior pituitary [15]. All Sstrs are members of the G-protein coupled receptor superfamily and are coupled to the inhibitory G_i protein causing them to inhibit the activation of adenylyl cyclase [15] which positively regulate GH synthesis. Pituitary GH synthesis is also negatively regulated by the insulin-like-growth factor-1 (IGF-1), a peptide produced mainly by the liver due to GH binding of hepatic GH receptors [16, 17]. Secreted IGF-1 binds its receptor (IGF-1R) and can act directly on somatotroph cells or via inhibition of GHRH synthesis in the hypothalamus [18-21].

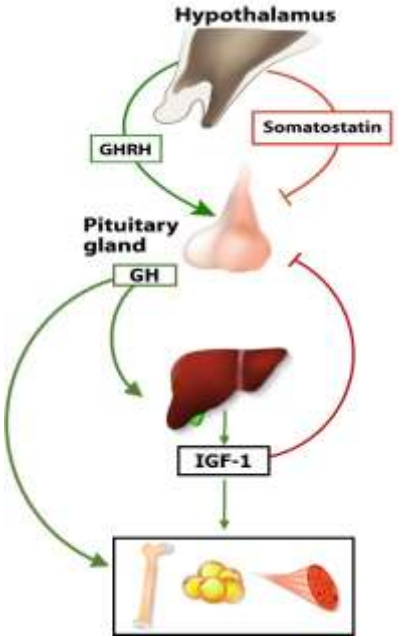

Figure 1.1: Physiological regulation of GH homeostasis: Growth hormone release is stimulated by hypothalamic GHRH release. Once secreted, GH can directly stimulate target organs or can promote the release of IGF-1, which also targets peripheral organs. IGF-1 in turn can inhibit GH release from the anterior pituitary. Hypothalamic somatostatin exerts a suppressive effect on pituitary GH secretion. Image adapted from Designua/Shutterstock.com

1.2.3. The cAMP/PKA signaling cascade in somatotroph cells

GHRH binds to the GHRH-R on the surface of somatotroph cells that belongs to the seven transmembrane domain G-protein coupled receptor, in which the intracellular domain associates with the stimulatory G-protein (Gs). The Gs protein is a heterotrimeric complex composed of an alpha (G_α), beta ($G_{\beta)}$ and gamma (G_γ) subunits. In its inactive state, the Gs protein is associated with guanine diphosphate (GDP). Following ligand binding, GDP is exchanged for GTP by a Guanine Exchange Factors (GEF). Association of the Gs complex with GTP promotes dissociation of Gs_α-GTP from the $G_{\beta\gamma}$ complex. Following its release, Gs_α then allosterically activates the membrane-bound adenyl-cyclase which converts adenosine-5'-triphosphate (ATP) to 3', 5'cyclic adenosine monophosphate (cAMP) [22]. cAMP then binds to and activates the protein kinase A (PKA).

PKA is a tetrameric holoenzyme which transduces signals received through G-protein coupled receptors via the second messenger 3'5'-cyclic adenosine monophosphate (cAMP) [23]. The PKA holoenzyme is composed of regulatory (R) and catalytic (C) subunit dimers, which are each present in alpha (A) and beta (B) isoforms (R1A, R2A, R1B, R2B). When in the R_2C_2 conformation PKA is catalytically inactive. Following the binding of cAMP to the regulatory subunit dimer, a conformational change occurs which allows the active catalytic subunit to dissociate and phosphorylate serine/threonine residues of substrate proteins [24, 25]. The intracellular localization of PKA and therefore its spatio-temporal kinase activity is regulated by a class of scaffold proteins known as AKAPs (A Kinase Anchoring Protein) which bind to the regulatory subunits [26].

In somatotroph pituitary cells the catalytic PKA subunits subsequently phosphorylate and activate the cAMP-responsive element (CRE) binding protein (CREB) at Serine 133 [27]. PKA also phosphorylates the transcriptional coactivator CREB binding protein (CBP). Activated CBP recruits CREB to its canonical CRE sequences at –187/–183 and –99/–95 in the pituitary GH promoter, where it activates GH transcription directly, but also indirectly by promoting the transcription of Pit-1 [28-32]. Two Pit-1 binding sites are also located in the human GH promoter and contribute to promoter activation [33]. In rats, the GH promoter is activated through CREB-mediated Pit-1 expression [34]. One synthesized, GH is stored in secretory vesicles which are released by exocytosis upon activation of voltage-gated L-type Ca^{2+} channels [35].

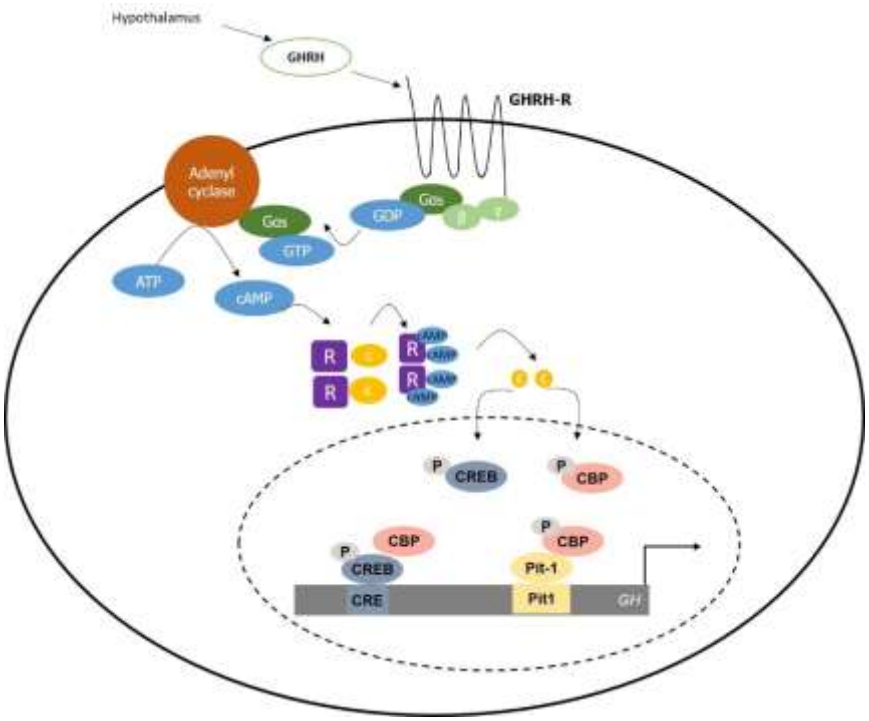

Figure 1.2: Regulation of GH transcription via the cAMP-PKA signaling cascade. Following binding of hypothalamic GHRH to the somatotroph GHRH-R, the $G\alpha_s$ subunit dissociates and activates adenyl-cylcase. This triggers the formation of cAMP, which binds to the regulatory subunits of PKA. Catalyitc PKA subunits are then released and phosphorylate both CREB and CBP which triggers recruitment of Pit-1 and CREB to the GH promoter to initiate transcription.

1.3. GH-secreting pituitary tumors cause acromegaly

Adenomas of the anterior pituitary account for approximately 10% of all surgically resected intracranial tumors and their incidence in post-mortem autopsies ranges from 11-27% [36-39]. Pituitary tumors arising from the somatotroph cell population hypersecrete GH and result in the clinical presentation of acromegaly. As a result of this excessive GH synthesis and secretion, patients with acromegaly display a variety of symptoms including acral and facial changes, hyperhidrosis, headaches, paresthesia, carpal tunnel syndrome, sexual dysfunction, goiter, hypertension, hypertrophic cardiomyopathy, arrhythmia and type 2 diabetes [40, 41]. With an incidence ranging from 0.2 to 1.1 cases/100,000 people, acromegaly is considered a rare disease [42]. However, as tumor growth is usually slow, diagnosis often occurs with a delay of approximately 10 years. At this point patients have already developed significant comorbidities which are associated with a 10-year decrease in lifespan, an increase of the standard mortality rate by 2.5-fold and decreased quality of life [43, 44]. Furthermore, management of the disease has been estimated to cost up to 140 Million USD per year [45].

1.3.1. Pathogenesis of GH-secreting pituitary tumors

The majority of GH-secreting pituitary tumors are sporadic. The most common genetic aberration found in these patients is the activating mutation of the GNAS locus resulting in the gsp-oncogene. This mutation causes the constitutive activation of the G_α subunit of the GHRH-R in somatotrophs leading to overactivation of the downstream signaling cascade promoting GH synthesis. Recent whole genome and exome sequencing has confirmed the presence of the gsp-oncogene in approximately 40% of patients with isolated GH-secreting pituitary tumors [46, 47].

GH-secreting tumors causing Acromegaly can also be found in a familial setting, however these cases account for only 5% of all pituitary tumors [48]. In the autosomal dominant Multiple Endocrine Neoplasia Type I (MEN1), patients present with pituitary tumors, parathyroid and pancreatic neuroendocrine tumors [49]. Carney Complex (CC) is a further autosomal dominant syndrome characterized by cardiac, cutaneous, and neural tumors as well as pigmented lesions of the skin and mucosae in addition to GH-secreting pituitary tumors [50]. Families in which two or more members present with pituitary tumors without the syndromic features of CC or MEN1 are considered to have familial isolated pituitary adenoma (FIPA) [51]. Some FIPA patients may not display genetic aberrations, whereas others have been found to carry germline AIP (Aryl hydrocarbon interacting protein) mutations [52].

1.3.2. Treatment of GH-secreting pituitary tumors

Treatment options for GH-secreting pituitary tumors consist of surgical resection, pharmacological treatment and/or radiotherapy [53]. The primary goal of all approaches is to achieve biochemical control of GH and IGF-1 defined as a random GH of < 1ng/ml and a normal age- and gender-specific IGF-1 value [53].

Transsphenoidal tumor resection is considered to be the primary treatment approach for most patients [54]. Pharmacological treatment may be considered as a neoadjuvant or adjuvant therapy. The first-line option for the pharmacological treatment of acromegaly is synthetic somatostatin analogs (SSA) such as octreotide and lanreotide. These SSA preferentially bind to the somatostatin receptor (SSTR) type 2 (SSTR2), and up to 70% of patients treated with these substances display biochemical normalization [55-57]. More recently, the multi-ligand SSA, SOM230 (Pasireotide) which binds SSTR 1,2,3 and 5, has been shown to suppress GH synthesis even in patients resistant to octreotide [58, 59]. However, SOM230 has also been associated

with treatment-resistant hyperglycemia prompting discontinuation in approximately 10% of patients [60]. A further pharmacological approach to treatment of acromegaly is the use of the GH receptor antagonist Pegvisomant which can quickly lower systemic IGF-1 levels in patients with severe disease [61].

Overall, up to 40-60% of acromegalic patients do not achieve biochemical normalization and/or tumor shrinkage with tumor-targeting pharmaceuticals, therefore necessitating the better understanding of tumor pathophysiology as a basis to improve treatment outcomes [62-65].

1.4. Vascularization & hypoxia

1.4.1. Normal pituitary

An important component of pituitary anatomy and physiology is the hypothalamic-hypophyseal portal vessel system [66] which consists of two capillary beds primarily supplied from the superior hypophyseal arteries arising from the ophthalmic segment of the internal carotid artery. The first capillary bed (primary capillary network) resides in the median eminence of the hypothalamus, which then drains into portal veins through the infundibulum directly into the second capillary bed of the anterior pituitary. Studies employing cellular *in vivo* imaging on pituitary somatotrophs have demonstrated the critical importance of intact microvasculature in coordinating the GH secretory response transmitted by hypothalamic signals [67, 68]. Bypassing systemic circulation via the portal vessel system therefore allows for direct signal transmission between the hypothalamus and pituitary, and plays critical role in maintaining endocrine homeostasis via releasing (i.e. GHRH) and inhibiting (i.e. somatostatin) factors.

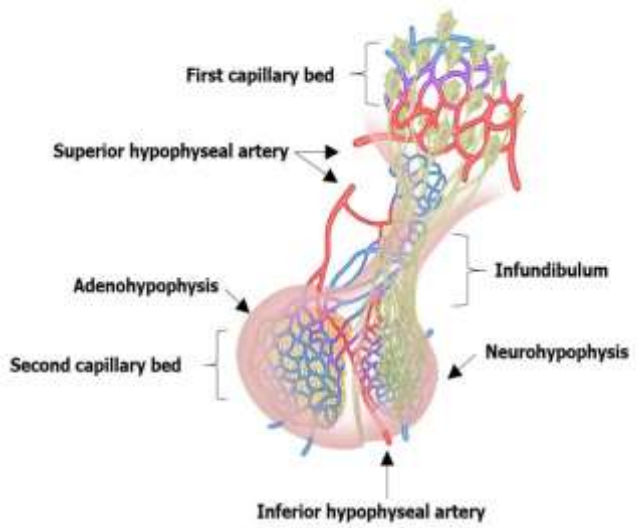

Figure 1.3: The hypothalamic-hypophyseal portal vessel system: blood containing hypothalamic releasing/inhibiting factors drains directly from the first capillary bed in the median eminence into the second capillary bed located in the anterior pituitary via portal veins passing through the infundibulum. Blood from peripheral organs supplies the hypothalamus and anterior pituitary via the superior hypophyseal artieries. The neurohypophysis is supplied with blood primarly from the inferior hypophyseal artery. Image adapted from Alexilusmedical/shutterstock.com

1.4.2. GH-secreting pituitary tumors

The importance of the hypophyseal portal vessel system for physiological regulation of somatotroph function was outlined above. In pituitary tumors, several studies have not only demonstrated a reduction in the vascular density of adenomas versus the normal pituitary, but also that among adenoma subtypes, GH-secreting tumors display the lowest vascular density [69-71]. Furthermore, ultrastructural analysis of the vessels in pituitary tumors have shown signs of beginning necrosis including thick and swollen endothelium with a fragmented basal membrane and only few sprouting capillaries [72, 73]. As decreased vascular density in solid tumors promotes the presence of intratumoral hypoxia, it was hypothesized for this thesis that pituitary adenomas, and in particular GH-secreting tumors, are also hypoxic [74].

1.5. The physiological response to cellular hypoxia

An adequate supply of molecular oxygen (O_2) is essential for a multitude of cellular processes in mammalian cells, the most vital being the synthesis of adenosintriphosphate (ATP). At the cellular level, the physiological response to transient states of decreased oxygen supply (hypoxia) as it occurs in processes such as organogenesis and wound healing is tightly regulated. Ultimately, oxygen homeostasis can be maintained by increasing the efficiency of ATP production and decreasing its expenditure [75].

In oxygenated cells ATP production occurs mainly through mitochondrial oxidative phosphorylation. Here, molecular oxygen is required for the transfer of electrons from NADH or $FADH_2$ which provides energy for synthesis of ATP—this process is maintained over several steps throughout the inner and outer mitochondrial membranes and is known as mitochondrial respiration. When cellular oxygen concentrations drop, mitochondrial respiration is slowed and ATP synthesis is diverted to glycolysis, a process which generates less ATP but requires less oxygen. Figure 1.4 illustrates three mechanisms through which cellular metabolism is shifted from oxidative phosphorylation towards glycolysis. First, upregulation of glucose transporters (Glut1) ensures increased uptake of extracellular glucose. The expression of Pyruvate dehydrogenase kinase-1 (PDK1) inhibits the activity of pyruvate dehydrogenase which catalyzes the oxidative decarboxylation of pyruvate to Acetyl-CoA used in the mitochondiral TCA cycle, ultimately providing $NADH_2$ for oxidative

phosphorylation. Upregulation of LDH-A (lactate dehydrogenase A) instead converts the pyruvate resulting from glucose metabolism to lactate.

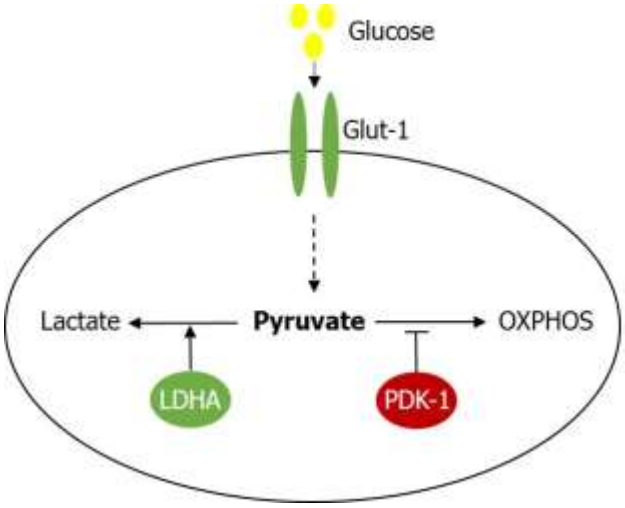

Figure 1.4: Regulation of the metabolic shift found in hypoxia. Hypoxia promotes the expression of Glut-1 glucose transporters as well as enzymes such as LDHA and PDK-1 which promote utilization of pyruvate for the production of lactate.

The expenditure of ATP is also found to be decreased in response to hypoxia. It has been demonstrated that cells “prioritize” functions which can be shut down first in response to decreased ATP production, and those which must be maintained to retain viability, a process known as oxygen conformance [76]. Among these processes, RNA and DNA synthesis are the first to be suspended with the maintenance of Na+/K+ pumping and Ca2+ cycling being the most critical. Furthermore, hypoxia leads to cell cycle arrest at the G1/S phase in a p27-dependent manner, ultimately resulting in growth arrest and reduced ATP expenditure in order to maintain cell viability even under adverse environmental conditions [77, 78].

1.6. Hypoxia in solid tumors

Hypoxia has been implicated as a characteristic of solid tumors since the 1950s [79]. In non-tumorous tissues, a pO_2 of 25-65 mmHg (3-9%) can be considered physiological whereas many solid tumors display decreased oxygenation (hypoxia) of <2.5 mmHg in up to 25% of the total tumor mass [80]. Development of tumor hypoxia can be attributed to the initial outgrowth of tumor cells beyond their original blood supply. This reduced microvessel density therefore results in greater diffusion distances between blood vessels. The subsequent development of new vasculature (angiogenesis), to compensate for tumor cell growth and reduced microvessel density often proves to be abnormal and not as effective as in non-tumorous tissue therefore promoting sustained hypoxia [81]. The development of new blood vessels (angiogenesis) to maintain oxygen and nutrient supplies is a processes triggered by hypoxia and plays an

important role in maintaining tumor cell survival [82]. The effects of tumor hypoxia have been demonstrated to reach beyond triggering angiogenesis and to promote multiple processes closely linked to tumor biology and disease progression.

The hypoxic tumor microenvironment has been shown to provide a survival advantage through several mechanisms. In human colon cancer cells it has been shown that hypoxia leads to decreased expression of the pro-apoptotic proteins Bid and Bax which ultimately suppressed apoptosis, but also reduced the sensitivity of these cells to etoposide [83]. Hypoxia has also been shown to promote the selection and clonal expansion of transformed tumor cells which carry p53 mutations and are therefore resistant to apoptosis [84]. Tumor cells undergoing hypoxia have also been shown to upregulate lysosomal autophagy, which may provide a survival advantage through the ability to recycle amino acids to maintain ATP and protein synthesis [85, 86].

Another major feature of the hypoxic tumor microenvironment is the alteration of metabolic profiles which can also have farther reaching effects than the immediate generation of ATP. The shift from oxidative phosphorylation to glycolysis, for example, results in the increased production and accumulation of lactate. This promotes a decreases of the pH of the tumor microenvironment which has been shown to suppress the activity of cytotoxic T-lymphocytes, thereby suppressing the anti-tumor immune response allowing tumor cells to evade immune detection [87, 88]. Furthermore, de-novo fatty acid synthesis required for the generation of cell membranes of replicating tumor cells is downregulated under hypoxia. Instead, alternative serum phospholipids (lysophospholipids) are scavenged and used for fatty acid synthesis, allowing cells to bypass the need for acetyl-CoA, whose generation is oxygen-dependent [89].

Intratumoral hypoxia has also been implicated in promoting the epithelial-mesenchymal trasition (EMT) and metastasis of tumor cells [90-93]. Several mechanisms have been elucidated including upregulation of the *met* protooncogene [94] and key EMT transcription factors such as Twist, Snail and Zeb1 under hypoxic conditions [95-97]. Furthermore, EMT is promoted by hypoxia through activation of multiple signaling pathways such as Notch [98, 99] and TGF-β [100].

Given the multifaceted effects of the hypoxic tumor microenvironment on promoting tumor cell survival, the presence of intratumoral hypoxia has been found to confer resistance to radiation and pharmacological therapy in several tumor entities [101, 102]. Furthermore, the presence of hypoxia in solid tumors has been associated with worse clinical outcomes in cancer patients [103-107].

1.7. HIF-1α regulates the cellular response to tissue hypoxia

1.7.1. Oxygen-dependent regulation of HIF-1α stabilization

Many of the outlined pro-survival responses triggered by intratumoral hypoxia are mediated by a key transcription factor, the hypoxia inducible factor 1-α (HIF-1α). Initiation of the cellular adaptation to hypoxia first requires a molecular mechanism which can detect changes in oxygen availability. In metazoan cells, this function is fulfilled by a family of transcription factors known as Hypoxia Inducible Factors (HIFs). HIFs are basic helix-loop-helix DNA binding proteins of the PER-ARNT-SIM family (bHLH-PAS) [108]. HIF-1 was the first HIF member to be identified, purified and cloned and has since been characterized as a key oxygen sensor in mammalian cells.

HIF-1 is a heterodimeric protein which is composed of an alpha (HIF-1α) and beta (HIF-1β) subunit [109]. The amino-terminals of both subunits contain the bHLH-PAS domains which mediate heterodimerization and DNA binding [110]. Only the carboxy-terminal of HIF-1α contains two transactivation domains that mediate interactions with transcriptional coactivators [111].

Whereas HIF-1β is found to be constitutively expressed, the protein stability of HIF-1α is tightly regulated by cellular O_2 concentrations. Under non-hypoxic conditions, HIF-1α is post-transcriptionally hydroxylated at Pro-402 and Pro-564 by prolyl-4-hydroxylases [112-115]. Prolyl hydroxylation marks HIF-1α for recognition by the von-Hippel-Lindau (VHL) E3 ubiquitin ligase complex which triggers its proteasomal degradation [116-118]. The activity of prolyl-4-hydroxylases is dependent upon iron, α-ketoglutarate, ascorbate and molecular oxygen, so that the hydroxylation decreases when oxygen concentrations are depleted and HIF-1α is no longer degraded [119]. Upon its stabilization, HIF-1α translocates to the nucleus where it binds with the co-factors CBP/p300 to its cognate DNA motif known as the hypoxia-responsive-element (HRE) and initiates the transcription of target genes [108, 120].

To date, the role of HIF-1α in transcriptional repression has remained less well characterized than its role as a direct transcriptional activator [121]. Genome-wide association studies of HIF-1α DNA binding and transcription profiling have shown that HIF-1α-dependent gene suppression most commonly occurs through indirect mechanisms [122] such as the HIF-1α mediated upregulation of a transcriptional repressor [123]. A less well-characterized mechanism of HIF-1α-mediated

transcriptional repression occurs through its physical interaction and sequestration of a transcription factor from a promoter sequence required for gene expression [124].

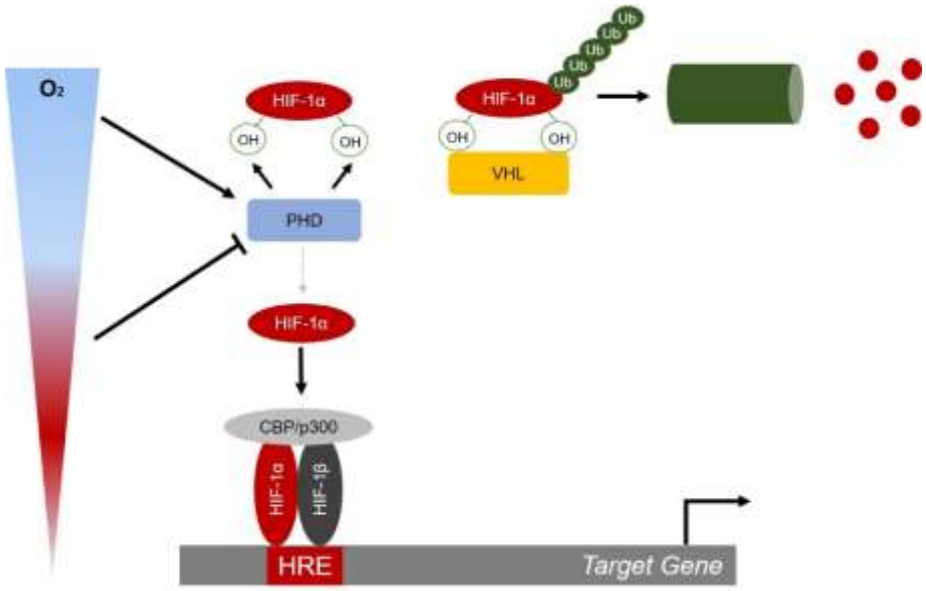

Figure 1.5: Oxygen-dependent regulation of HIF-1α. Under normoxic conditions, HIF-1α is hydroxylated at proline residues by the prolyl-hydroxylase (PHD) family of enzymes. HIF-1α-OH is recognized by the ubiquitin-ligase VHL marked for proteasomal degredation. PHD activity is decreased under hypoxia, allowing for stabilization of HIF-1α and its translocation to the nucleus where it activates target gene transcription by binding to the HRE with HIF-1β and CBP/p300.

1.7.2. HIF-1α in disease

As intratumoral hypoxia is a common finding among solid tumors, strong of HIF-1α in multiple tumor entities has also been observed compared to non-tumorous tissues [125, 126]. HIF-1α has been implicated in directly activating the transcription of over 60 target genes [120] and has been shown to play a central role in several disease pathologies involving tissue hypoxia coronary artery disease, peripheral artery disease and heart failure [127-129] To date, strong focus has been placed primarily on the role of HIF-1α in cancer and tumorigenesis. Here, HIF-1α has been shown to transcriptionally regulate the expression of genes coordinating metabolic reprogramming, pH regulation and nutrient uptake which help to ensure cell viability [130-133]. Beyond maintaining cell viability, HIF-1α can also contribute to mitogenic signaling in tumor cells by triggering the expression of growth factors and their receptors on tumor cells such as IGF-2 and TGF-α [134, 135].

HIF-1α can also influence the behavior of stromal cells in the tumor microenvironment by targeting cancer-associated fibroblasts (CAFs) which themselves are an important source of mitogenic signals for tumor cells. As such, HIF-1α can directly promote the transcription of TGF-β, endothelin and CXCL2 in tumor cells, which then promote the differentiation of precursor cells to CAFs. [136, 137]. In addition, the development of tumor fibrosis has also been contributed in part to the transcriptional activation of a family of HIF-1α target genes known as lysyl oxidases (LOX) in CAFs. These enzymes are responsible for the crosslinking of collagen fibers and their activity can contribute to the stiffening of the collagen matrix in tumor tissue which ultimately leads to formation of a protective niche for a growing, and ultimately metastasizing tumor mass [83, 138, 139].

The extensive nature of HIF-1α's action in solid tumors also makes it a promising target in anticancer therapies. Although several existing chemotherapeutic drugs affecting the PI3K-AKT-mTOR and RAS-RAF-MEK-ERK pathways have been shown to decrease HIF-1α protein expression, no specific HIF-1α inhibitors are currently in clinical use [140]. A major hurdle in targeting HIF-1α lies within the heterogeneity of the solid tumor cell population, as hypoxia and therefore HIF-1α are not expressed in the same temporal or spatial manner throughout the tumor mass. Furthermore, while HIF-1α largely acts in a pro-tumorigenic manner, it can also promote tumor cell death in certain cell types [141]. Further understanding of the nature of HIF-1α's action in solid tumors may therefore provide insight into potential therapeutic targets which are tailored to target the pathophysiology of an individual tumor entity.

2. Aim of the study

Genetic aberrations associated with the development of GH-secreting pituitary tumors causing acromegaly are rare. A unique feature of these tumors is the reduced microvessel density compared to the normal anterior pituitary, suggesting the presence of tissue hypoxia. Given the paucity of evidence supporting driving genetic mutations in the pathogenesis of these tumors, the aim of the current study was therefore to assess the effects of an environmental stressor in the form of intratumoral hypoxia on the pathophysiology of GH-secreting pituitary tumors.

While the reduced microvessel density in GH-secreting pituitary tumors has been previously described, little is known about the consequences of tissue hypoxia on GH-secreting pituitary tumor pathophysiology. Therefore, primary cultures of human GH-secreting tumors were first utilized to characterize the effects of hypoxia on important parameters of GH-secreting pituitary tumor pathophysiology including proliferation, cell viability, metabolic gene expression, response to the somatostatin analogue octreotide, and GH secretion. Given the evidence that the transcription factor HIF-1α is upregulated in hypoxic tumor tissue and may contribute to drug resistance, its tissue expression and association with clinical parameters of drug resistance in patients with acromegaly were examined [125, 126]. This first characterization pointed towards the upregulation of HIF-1α expression in GH-secreting pituitary tumors as well as the stimulatory effects of hypoxia on GH secretion.

In a second step, the molecular mechanisms behind the stimulatory effects of hypoxia on GH synthesis were analyzed. In both human tumor tissue and the rat lactosomatotroph GH3 cell line, hypoxic incubation and transient HIF-1α overexpression were utilized to pinpoint the molecular target of HIF-1α within the PKA-CREB signaling cascade. The putative target of HIF-1α could be confirmed in tissue samples from GH-secreting pituitary tumors and subsequent rescue experiments in GH3 cells confirmed the specificity of its role in GH synthesis.

3. Materials and methods

3.1. Chemicals and reagents

Chemicals and Reagents	Manufacturer
1 Kb Plus DNA Ladder	Thermo Fischer Scientific (Waltham, MA USA)
ABC (Avidin-Biotin Complex) blocking kit	Vector laboratories (Burlingane, CA, USA)
Acetic acid	MERCK (Darmstadt, Germany)
Acridine orange	Sigma (St.Louis. MO, USA)
Acrylamide	Sigma (St.Louis. MO, USA)
Ammonium persulfate	Sigma (St.Louis. MO, USA)
Amphotericin B	Biochrom (Berlin, Germany)
Agar	Life Technologies (Paisley, Scotland, UK)
Agarose	Carl Roth (Karlsruhe, Germany)
β-mercaptoethanol	MERCK (Darmstadt, Germany)
Beetle-Juice firefly luciferase kit	PJK (Kleinblittersdorf, Germany)
Bovine serum albumin (BSA)	Invitrogen Corp.(Paisley, Scotland, UK)
Bradford protein assay	Biorad (Munich, Germany)
cAMP [125I] determination RIA kit	Perkin Elmer (MA,USA)
Chloroform	Sigma (St.Louis. MO, USA)
Clarity Western ECL Blotting Substrate	Bio-Rad (Munich, Germany)
Collagenase	Worthington Biochemical Corp. (Lakewood, NJ, USA)
Diaminobenzidine (DAB)	Sigma (St.Louis. MO, USA)
Developer Solution	Kodak (Stuttgart, Germany)
Diethyl-pyrocarbonate (DEPC)	Sigma (St.Louis. MO, USA)
Dimethyl sulfoxide (DMSO)	Sigma (St.Louis. MO, USA)
DNase I	Invitrogen Corp.(Paisley, Scotland, UK

Chemicals and Reagents	Manufacturer
dNTP Mix	MBI Fermentas (Vilnius, Lithouania)
Dulbecco's modified Eagle medium (DMEM)	Invitrogen Corp.(Paisley, Scotland, UK)
Dulbecco's modified Eagle medium (DMEM) with D-valine	Invitrogen Corp.(Paisley, Scotland, UK)
EDTA	Sigma (St.Louis. MO, USA)
Entellan	MERCK (Darmstadt, Germany)
Ethanol 100%	Carl Roth (Karlsruhe, Germany)
Ethidium bromide	Sigma (St.Louis. MO, USA)
Fetal calf serum	Gibco (Karlsruhe, Germany)
Fixer solution	Kodak (Stuttgart, Germany)
Formaldehyde 37%	Sigma (St.Louis. MO, USA)
Forskolin	Sigma (St.Louis. MO, USA)
Glycerol	Sigma (St.Louis. MO, USA)
HCl	Carl Roth (Karlsruhe, Germany)
Hyaluronidase	Sigma (St.Louis. MO, USA)
Hydrogen Peroxide Solution 30%	Sigma (St.Louis. MO, USA)
Isopropanol	Sigma (St.Louis. MO, USA)
L-Glutamine	Biochrom AG (Berlin,Germany)
Magnesium chloride	MERCK (Darmstadt, Germany)
Milk powder	Roth (Karlsruhe, Germany)
[methyl-^{3}H]-Thymidine	Amersham Biosciences (Uppsala, Sweden)
Nitrocellulose membrane Hybond-ECL	Amersham Biosciences (Uppsala, Sweden)
Okadaic acid	Calbiochem (Darmstadt, Germany)
ONPG	Sigma (St.Louis. MO, USA)
Paraformaldehyde	Sigma (St.Louis. MO, USA)
Passive Lysis Buffer	Promega (Madison, WI, USA)

Chemicals and Reagents	Manufacturer
Penicillin+Streptomycin mix	Biochrom AG (Berlin, Germany)
Phenol Roth	(Karlsruhe, Germany)
Phosphatase inhibitor cocktail	Roche (Mannheim, Germany)
Plasmid Maxi Kit	Qiagen (Hilden, Germany)
Polyacrylamide	Invitrogen Corp.(Paisley, Scotland, UK)
Potassium chloride (KCl)	MERCK (Darmstadt, Germany)
Propidium Iodide	Sigma (St.Louis. MO, USA)
Protease inhibitor cocktail	Sigma (St.Louis. MO, USA)
Protein G Dynabeads	Invitrogen Corp.(Paisley, Scotland, UK)
QuantiFAST SYBR Green PCR Kit	Qiagen (Hilden, Germany)
QuantiTect Reverse Transcription Kit	Qiagen (Hilden, Germany)
QuikChange Lightning Multi Site-Directed Mutagenesis Kit	Agilent Technologies, Inc. (CA, USA)
rGH [125I]	BIOTREND (Cologne, Germany(
rGH standard	National Institute of Diabetes, Digestive & Kidney Disease (CA, USA)
Rotiload	Carl Roth (Karlsruhe, Germany)
Ser/Thr phosphatase Kit	Upstate (MA, USA)
Sodium chloride (NaCl)	Carl Roth (Karlsruhe, Germany)
Sodium hydrogen phosphate dehydrate	MERCK (Darmstadt, Germany)
Sodium Dodecyl Sulphate (SDS)	Carl Roth (Karlsruhe, Germany)
Sodium hydroxide (NaOH)	Carl Roth (Karlsruhe, Germany)
Superfect Transfection Reagent	Qiagen (Hilden, Germany)
Taq DNA polymerase	MBI Fermentas (Vilnius, Lithouania)
TEMED	Sigma (St.Louis. MO, USA)
Toluidin Blue	Sigma (St.Louis. MO, USA)
Trichloracetic acid	Carl Roth (Karlsruhe, Germany)
Trypsin inhibitor	Sigma (St.Louis. MO, USA)

Tris Base	Carl Roth (Karlsruhe, Germany)
Triton X-100	Carl Roth (Karlsruhe, Germany)
TriZol	Invitrogen Corp.(Paisley, Scotland, UK)
Trypsin	Sigma (St.Louis. MO, USA)
Tween-20	Sigma (St.Louis. MO, USA)
WST-1 cell proliferation reagent	Roche (Mannheim, Germany)
Xylol	Carl Roth (Karlsruhe, Germany)

3.2. Solutions

Solution	Composition
Cell Lysis Buffer for ChIP	10mM Hepes pH 7.9: 238mg/100 ml $MgCl_2x6H_2O$ 1.5 mM: 30.4mg/100 ml KCl 10mM: 74.5 mg/100 ml NP-40 0.5%
Dilution Buffer	SDS 0.01% Triton X-100 1.1% 1.2 mM EDTA pH 8.0 16.7 mM Tris-HCl pH 8.0 NaCl 167 mM
Elution Buffer For ChIP	SDS 1% $NaHCO_3$ 50mM 50 mM Tris-HCl pH 8.0 1mM EDTA pH 8.0 To each 100µl add 5mg/ml of Proteinase K
HDB$^+$ buffer	Glucose: 10 mM NaCl: 137 mM KCl: 5 mM Na_2HPO_4: 0.7 mM HEPES: 25 mM Adjust pH 7.3 with NaOH Partricin: 500 µg/L Penicillin/Streptomycin:10^5 U/L
High Salt Wash Buffer for ChIP	SDS 0.1% Triton X-100 1% 2 mM EDTA pH 8.0: 74.4 mg/200 ml 20 mM Tris-HCl pH 8.1: 242 mg/200 ml NaCl 500 mM: 2.92g/200ml
LB medium	Peptone: 10 g/L Yeast extract: 5 g/L NaCl: 5 g/L

	NaOH 1M: 2 ml/L Adjust to pH 7.0
LiCl Wash Buffer for ChIP	LiCl 0.25 mM: 1.06g/200 ml NP-40 1% Sodium Deoxycholate 1% 1mM EDTA pH 8.0: 37.22mg/200 ml 10mM Tris-HCl pH 8.1: 121mg/200 ml
Low Salt Wash Buffer for ChIP	SDS 0.1% Triton X-100: 1% 2mM EDTA pH 8.0: 7.4 mg/200 ml 20mM Tris-HCl pH 8.1: 242 mg/200 ml NaCl 150mM: 876.87mg/200 ml
Lower Tris Buffer	Tris pH 8.8: 182 g/L SDS: 4 g/L
Medium for tumor primary cell culture	DMEM Foetal Calf Serum (FCS) :10% v/v Glutamine: 2.4g/L Partricin: 500 µg/L Penicillin/Streptomycin: 10^5 U/L MEM 1x Non-essential aminoacids (NEAA) 1x Insulin: 5 mg/L T3: 60 pmol/L Transferrin: 5 mg/L Sodium Selenate: 20 µg/L
NP-40 lysis buffer for immunoprecipitation	Hepes pH 7.4: 20 mM NaCl: 100 mM EDTA: 1 mM Nonidet P-40: 1% v/v
Nuclear Lysis Buffer for ChIP	SDS: 1% EDTA 10mM: 372 mg/100 ml Tris-HCl pH 8.1: 605 mg/100ml
ONPG buffer 2x	Na2HPO4 1M: 55.3 ml NaH2PO4 1M: 29.3 ml Water: 339.2 ml MgCl2x6H2O: 154.5 mg ONPG: 500.0 mg 40 minutes stirring β-Mercaptoethanol 14M: 2.5 ml Freeze aliquots at -20 °C
Paraformaldehyde 4% (PFA)	paraformaldehyde:4 g/100 ml Sodium phosphate buffer: 20 ml/100 ml solution DDW: 80 ml Add 1M NaOH to pH 7.4 Heat at 56°C to dissolve

	Filter and cool before usage Store at +4°C for maximum 2 days
Phosphate based buffer 1x (PBS)	NaCl: 8 g/L KCl: 0.2 g/L $Na_2HPO_4.2H_2O$: 1.44 g/L KH_2PO_4: 0.2 g/L Adjust to pH 7.4
RIPA cell lysis buffer	Tris HCl pH 8: 50 mM NaCl: 150 mM NP-40:1% Sodium Deoxycholate: 0.5% SDS: 0.1%
Running Buffer for gel electrophoresis	Tris-base: 3.03 g/L Glycine: 14.42 g/L SDS: 1.00 g/L Adjust to pH 8.3
SDS-PAGE (SDS-Polyacrylamide gel electrophoresis) running gel 10%	DDW: 6.6 ml Acrylamide: 8 ml Lower Tris buffer:5 ml Ammonium persulfat 10%:0.2 ml Temed:0.008 ml
SDS-PAGE (SDS-Polyacrylamide gel electrophoresis) stacking gel 4%	DDW :4.1 ml Acrylamide:1 ml Upper Tris buffer: 0.75 ml Ammonium Persulfate 10%:0.06 ml Temed:0.006 ml
Sodium acetate 2M	Sodium acetate trihydrate: 272 g/ 1L DEPC: 200 µl / 1 L Add acetic acid to pH 4.0 Leave at room temperature overnight
SOC Medium	0.5% Yeast Extract 2% Peptone 10mM NaCl 2.5 mM KCl 10mM $MgCl_2$ 10mM$MgSO_4$ 20mM Glucose
Sodium phosphate buffer 50 mM	$Na_2HPO_4.2H_2O$: 7.06 g/L NaH_2PO_4. H_2O: 1.32 g/L Adjust to pH 7.4
TE Buffer for ChIP	10 mM Tris-HCl pH 8.0: 121 mg/200 ml 1mM EDTA pH 8.0: 37.22mg/200 ml

Transfer Buffer for gel electrophoresis	Tris-base: 3.03g/L Gycine: 14.42 g/L Methanol: 200 ml/L pH automatically adjusts to 8.3
Tris-acetic EDTA buffer (TAE) 50x	Glacial acetic acid: 57.1 ml/L EDTA 0,5M pH 8: 100 ml/L Tris pure: 242 g/L Adjust to pH 8.0
Tris buffer	Tris pure: 12.114 g/L Adjust to pH 7.6
TBS 1x	Tris pure : 2.42 g/L NaCl: 8 g/L Adjust to pH 7.6
TBST	Tris pure: 2.42 g/L NaCl: 8 g/L Tween 20: 1ml/L
TEGDM Buffer	10mM Tris-HCl pH 7.4 50mM NaCl 4mM EDTA 10 mM Na_2MoO_4 Glycerol: 10% DTT: 1mM add freshly prior to use
Tris-HCl 1M	Tris pure: 121.14 g/L Add 25% HCl to a pH 8.2
Upper Tris Buffer	Tris-Base pH 6.8: 60.5 g/L SDS: 4.0 g /L

3.3. Antibodies

Target	Manufacturer	Cat. Nr.	Application	Dilution
B-Actin	Millipore	MAB-1501	WB	1:10.000
CREB	Cell Signaling	86B10	WB, IP, ChIP	1:2000 (WB) 0.5µg/Rx (IP) 5µg/Rx (ChIP)
FLAG-M2	Sigma	F3165	WB, IP	1:5000 (WB) 0.5µg/Rx (IP)
HIF-1α	Novus	NB-100-134	WB, IHC, IP, ChIP	1:5000 (WB) 1:100 (IHC) 0.5µg/Rx (IP) 5µg/Rx (ChIP)
pCREBSer133	Cell Signaling	87G3	WB	1:1000

Pit1	Santa Cruz	Sc-442	WB, ChIP	1:2000 (WB) 5µg/Rx (ChIP)
PP1α	Santa Cruz	Sc-7482	WB	1:1000
Sp1	Santa Cruz	Sc-59X	ChIP	5µg/Rx
Mouse-IgG (HRP)	Cell Signaling	7076S	WB	1:2000
Rabbit-IgG (HRP)	Cell Signaling	7074S	WB	1:2000
Non-immune	Santa cruz	Sc-2027	IP, ChIP	0.5µg/Rx (IP) 5µg/Rx (ChIP)
Rabbit-IgG (biotinylated)	Vector	BA1000	IHC	1:300

3.4. Oligonucleotides

Primers for Real-Time PCR (human targets)		
Target	**Sequence (5'-3')**	**Product size (bp)**
GLUT1	F: GGTTGTGCCATACTCATGACC R: CAGATAGGACATCCAGGGTAGC	66
GNAI1	F: GCCCTCTCACTATATGCTATCCAG R: TTGAGGTCTTCAAACTGACATTG	91
GNAI2	F: TCTAAGATGATCGACAAGAACCTG R: GATGGTGCTCTTCCCTGACT	102
GNAI3	F: TGTGCCACAGACACGAAGAA R: CATTCCCTGGTCCCGTTCAT	197
GNAS	F: GTGAGGCCAACAAAAAGATCGAG R: ACTTTGGTTGCCTTCTCACCA	217
HIF1A	F: TTTTTCAAGCAGTAGGAATTGGA R: GTGATGTAGTAGCTGCATGATCG	66
LDHA	F: CGTCAGCATAGCTGTTCCAC R: TGGAACCAAAAGGAATCGGGA	138
PDK1	F:GAGTCTTCAGGAGCTTCTTGATTT R:TGCAACCATGTTCTTCTAGGC	87
PRKAR1A	F: GTCAGTAGCCGAACGCTGAT R: GGCACAAAAGTCAACTGGGG	178
PRKAR1B	F: GGTCCCCCAATGAGGAGTA R: TTCAGCAGCAGTGCAATCTC	79
PRKAR2A	F: AGTCTGGCGAAGTGAGCATC R: TCCAAAGTACTGCCCCTTATG	107

PRKAR2B	F: CTGCTACCTCTCCTGGTGCT R: TTTTTGGCATTGTTTTTCACA	79
SP1	F: CTATAGCAAATGCCCCAGGT R: TCCACCTGCTGTGTCATCAT	89
SSTR1	F:GTCTGGAGGTTGCGCACT R:CGGCTCTGGACTGGTAAATG	71
SSTR2	F:GGAGCTAGCGGATTGCAG R:TCACCTTAATGGACCCTGGA	73
B-Actin	F:ACAGAGCCTCGCCTTTGCCG R:ACATGCCGGAGCCGTTGTCG	104

Primers for Real-Time PCR (rat targets)

Target	Sequence (5'-3')	Product size (bp)
Gh	F: AAAGAGTTCGAGCGTGCCTA R: ATGTCAGTTCTCTGCTGGGC	131
Glut1	F: ACGTCCATTCTCCGTTTCAC R: TCCCACGGCCAACATAAG	107
Gnai1	F: GCCCTGAGTGACTATGACCTG R: CTTCATGCTTTCATGCATCC	69
Gnai2	F: TCAATGACTCAGCCGCTTACAC R: GATGCCTGTGGTCTTCACAC	110
Gnai3	F: TGGGACGGTTGAAGATTGAT R: ATAACTGTCGGGCATCATCC	60
Gnas	F: CCGTGTCTTCAACGACTGC R: CAGCTCGTATTGGCGAAGAT	61
Hif1a	F: AAGCACTAGACAAAGCTCACCTG R: TTGACCATATCGCTGTCCAC	75
Ldha	F: GATCTCGCGCACGCTACT R: CACAATCAGCTGGTCCTTGAG	111
Pdk1	F: TTTATCCCCCGATTCAAGTTC R: CTCCCCGGTCACTCATCTT	72
Pppca	F: TTGCAGCCATTGTAGATGAGA R: CATGGATTGCAAGTCTGGAG	68
Prkaca	F: CGGGGTCCTCATCTACGA R: TGAAGTGGGATGGGAACC	113
Prkar1a	F: GGATCCCTCGACACCTGAGAA R: TCGAGTCTGTACGAATGCCG	255
Prkar1b	F: CGGGGTCCTCATCTACGA R: TGAAGTGGGATGGGAACC	72
Prkar2a	F: TGGATGTGATCGGGGAAA R: AAGCTGTCGGCCTTTTCA	73

Prkar2b	F: GATGCTGTGAACCTGTGTACCT R: TCAGGATTATAAGCTTCTGCACATA	95
Sp1	F: GCTATAGCAAACACCCCAGGT R: GATCAGGGCTGTTCTCTCCTT	115
Sstr2	F: TGCTCGTGGAAAAGCAAGAT R: CTTCAGTCCGCCTAGAACCA	100
TfIIB	F: AAGCACTAGACAAAGCTCACCTG R: TTGACCATATCGCTGTCCAC	135
Primers for Chromatin-Immunoprecipitation (rat targets)		
Target	**Sequence (5'-3')**	**Product size (bp)**
***Gh* Promoter**	F: GTGACCATTGCCCATAAACC R: TGCATGCCCTTTTTATACCC	400
***Pit1* Promoter**	F: TGACGTCAAATAAAGTTTCTGTTTT R: TGTTAACCCGAACTGTCTTTCTTAC	120
***Prkar2b* Promoter**	F: CACCAATGTGGAGGCTGAAGT R: GCAAATCCCACGCTTCTTTCT	84
Primers for Site-Directed Mutagenesis		
Vector	**Sequence (5'-3') Mutation underlined**	**Source of Primers**
pCMV-3x FLAG-HIF1αR30A	GCAGCCAGATCTCGGGCGAGTAAAGAATCTG	
RNA-Interference Oligonucliotides		
Target		**Source**
Rat *Hif1α*		Santa Cruz (sc-45919)
Rat *Creb1*		Dharmacon siGENOME (81646) siRNA

3.5. Plasmid Constructs

Expression Vectors and Reporter Constructs	
Vector	**Source**
pCMV-3x FLAG 7.1-HIF1α	Origene, USA
pCMV-Myc	Origene, USA
RSV CREB M1	Marc Montminy (Addgene plasmid # 22395)
RSV CREB	Marc Montminy (Addgene plasmid # 22394)
pCMV6XLS-PRKARIIB	Origene, USA
M7 pdnPKA-GFP	Randall Moon (Addgene plasmid # 16716)

pa3rGH-Luciferase	A. Gutierrez-Hartmann, University of Colorado, Denver, CO, USA
pCRE-Luciferase	Mercury pathway profiling system; Clontech Laboratories, Mountain View, CA, USA
Pit1-Luciferase	C. Alvarez, Univ. of Santiago de Compostela, Spain
HRE-Luciferase	Navdeep Chandel (Addgene plasmid # 26731)
B-Galactosidase	D. Spengler, MPI of Psychiatry, Germany

3.6. Methodology

3.6.1. Immunohistochemistry

To investigate the expression of HIF1α and in normal and tumorous human pituitary tissue, fresh samples were snap-frozen and cut into 8 µm thick sections (Leica CM3050 S). Two adjacent sections were bedded on each poly–L–lysine-coated slide and then fixed in 4% freshly prepared ice-cold paraformaldehyde, dehydrated and stored in 96% ethanol, at +4°C until further processing. At the time of the experiments, sections were incubated in TBS for 5 minutes, followed by 30 minutes blocking performed in TBS with 20% goat serum. After blocking, the sections were incubated overnight with the desired primary antibody (see 3.3) at 4°C in a dampened chamber. As each slide contained two adjacent sections, one section was incubated with the primary antibody, while the other was incubated with TBS to control for background.

The next day, after washing three times with TBS (5 minutes each), the sections were incubated for 30 minutes with the secondary antibody at room temperature. The slides were then washed 3 more times and incubated with the ABC complex for 30 minutes (prepared in saline-free Tris Buffer 30 minutes prior to use to allow for complex formation). The use of ABC complex facilitates the binding of biotinylated motifs in the secondary antibody to ensure optimal signal strength versus HRP-containing antibodies alone. After washing three times in TBS the slides were immersed in freshly prepared DAB (1 mg/ml) supplemented with 0.01% hydrogen peroxide. As DAB is light sensitive the reaction was carried out in semi-darkness. The time of incubation in DAB varied and was determined for each primary antibody separately. The optimal time was the one giving the strongest expected signal with the lowest possible background. Only slides in which the TBS-incubated samples were showed no signal were considered for analysis. After achieving a satisfactory signal level, the slides were washed three times in TBS and counterstained with toluidine-blue (which stains the cell nuclei pale blue) in order to

visualize the tissue organization. Excess staining was removed by immersing the slides in 70% ethanol supplemented with acetic acid, and the sections were dehydrated, fixed in xylol and coverslipped using Entellan. Evaluation of immunohistochemistry was performed using the Axioscop II microscope (Zeiss).

3.6.2. Cell culture: GH3 cell line

The immortalized rat lactosomatotroph GH3 cell line was used in this study. Cells were obtained from ATCC (American Type Culture Collection) and grown for maintenance in what will be referred to as cell culture medium: DMEM (Gibco 41965) supplemented with 10% FCS (heat-inactivated), 2mM L-Glutamine and 100 U ml^{-1} penicillin/streptomycin at 37°C in a humidified atmosphere with 95% air and 5% CO_2. As GH3 cells do not grow to confluency, cells were split every 4 days (approximately 70-80% confluency) at a ratio of 1:5. Splitting was performed following washing with pre-warmed PBS, followed by incubation with 0.05%/0.02% trypsin/EDTA (w/v) until cells were fully detached from the culture flask and could be recovered by centrifugation.

3.6.3. Cell culture: primary cultures of human GH-secreting tumors

GH-secreting pituitary tumors were obtained from patients who underwent transsphenoidal surgery. Tumor tissue was washed with HDB buffer and mechanically dispersed into small fragments, which was followed by enzymatic digestion for 45 minutes at 37°C in a solution containing 4g l^{-1} collagenase, 0.01 g l^{-1} DNAse II, 0.1 g l^{-1} soybean trypsin inhibitor and 1 g l^{-1} hyaluronidase II. Cell viability was determined by acridine orange/ethidium bromide staining and only cultures with viability scores above 90% were further cultured in medium for tumor primary cell culture. All experiments with human material were performed after approval of the local ethics committee of the Ludwig-Maximilian-University of Munich, Germany, and with informed written consent from each patient whose tissue was received.

3.6.4. WST-1 cell viability assay

Cell viability was determined using the WST-1 assay (Roche). The WST-1 assay is based upon the reduction of the stable tetrazolium salt added to cell cultures to a soluble formazan dye dependent upon the activity of a complex cellular mechanism relying mainly on the glycolytic production of NAD(P)H in cells. Therefore, the amount of formazan dye which can be measured correlates directly to the number of metabolically active cells. Cells were seeded in a 96-well culture plate and following completion of

treatment, medium was aspirated and replaced with 90µl cell culture medium/well. 10µl WST-1 reagent was added to each well (including blank controls containing only cell culture medium without cells), and incubated in the dark at 37°C for 30 minutes. Absorption was measured using a plate reader at 450 nm.

3.6.5. ^{3}H-Thymidine incorporation assay

The use of ^{3}H-Thymidine incorporation allows for the measurement of cellular proliferation rates as reflected by the amount of ^{3}H-Thymidine integrated into newly synthesized DNA in multiplying cells. In primary cell cultures from human pituitary adenomas ^{3}H-Thymidine incorporation was performed in 10% cell culture medium supplemented with D-Valine to suppress the growth of fibroblasts in culture. Following treatment, ^{3}H-Thymidine (0,5µCi/mL) was added directly to the cell culture medium and left to incubate for 24 hours. Supernatants were then removed and cells were precipitated with 10% ice-cold trichloroacetic acid and washed with cold PBS. DNA was hydrolyzed using 0.5 mol l^{-1} NaOH and 0.1% Triton X-100. Cells were collected and added to 4 ml scintillation fluid, vortexed and measured in a beta counter (Beckman LS6000IC). All measurements were carried out in triplicate.

3.6.6. Western Immunoblot

3.6.6.1. Protein Extraction

The western immunoblot allows for the determination and quantitation of cellular proteins. Following electrophoretic separation of protein lysates according to size, samples are transferred onto a membrane which binds the proteins present in the gel under the influence of an electric field. The membrane can now be incubated with a specific antibody (primary antibody) to recognize the desired protein. Following the incubation of the primary antibody, a secondary antibody, which is coupled to HRP, is added to the membrane to recognize the Fc-Region of the primary antibody. By adding ECL substrate to the membrane, HRP is activated and results in a chemiluminescent reaction which can be detected by film. The signal intensity can be measured, as it directly correlates with the amount of a specific protein present in a sample, allowing for quantitation of protein levels in a particular lysate.

In this study, two forms of protein lysate were used for western immunoblot: whole cell lysates and isolated nuclear fraction. For preparation of whole cell lysates, cell culture plates were immediately placed on ice and washed once with ice-cold PBS. Cells were

then scraped and collected in RIPA cell lysis buffer supplemented with protease and phosphatase inhibitors. The cell mixture was mechanically lysed by pipetting up and down 5 times using a 20G insulin syringe. Cell membranes were pelleted by centrifuging the lysates for 10 minutes at 12.000g. The supernatant was transferred to a new tube and protein content was quantitated using the Bradford Protein Assay. Using this assay, samples were diluted 1:100 in RIPA lysis buffer and a standard curve using BSA was prepared at concentrations of 0, 5, 10, 20, 25 µg/ml. 100µL of samples and standards were pipetted in triplet to a 96-well plate. The Bradford reagent was diluted 1:1 in ddH_2O and 50µL was added to each well. After 5 minutes of incubation at room temperature the absorbance was read at 595nm. The concentration of each sample could then be calculated using the values determined by the standard curve and all samples were normalized to contain the same amount of total protein (10-30µg).

The preparation of nuclear fraction lysates was performed as follows: cells were washed twice with ice-cold PBS and collected by careful scraping. Cells were pelleted by centrifugation at 4.200g for 5 minutes at 4°C. The cell pellet was carefully resuspended in hypotonic cell lysis buffer (10mM HEPES, pH 7.9, 1.5mM $MgCl_2$, 10mM KCl and 0.1 mM DTT) supplemented with proteinase inhibitor cocktail (Sigma) and incubated on ice for 15 minutes. Following centrifugation at 4.200g for 5 minutes, the supernatant was decanted and cells were disrupted again in hypotonic lysis buffer using a 20G insulin syringe and centrifuged at 10.000g for 20 minutes. The supernatant (now containing the cytoplasmic fraction) was separated and 75µl of cell extraction buffer (20mM HEPES, pH 7.9, 1.5 mM $MgCl_2$, 0.42 M NaCl, 0.2 mM EDTA, 25% Glycerol and 0.1 mM DTT) was used to resuspend the pellet. A final centrifugation step at 16.000g for 5 minutes at 4°C was performed and the supernatant containing the nuclear fraction was separated to a clean tube and subjected to preclearing for 30 minutes at 4°C using 10µL Protein G Dynabeads per 10^6 cells. The immunoprecipitation (IP) reaction was performed using Protein G Dynabeads coupled to the primary antibody in a separate reaction. In brief, for each IP 1µg of primary antibody was given to 10µL Protein G Dynabeads (Thermo Fischer) in a total volume of 300µL TEG buffer (10 mM Tris, 50 mM NaCl, 4 mM EDTA, 10% glycerol, and 0.1% NP-40) and rotated at 4°C for 90 minutes. Complexes were then washed 3 times in TEG buffer and resuspended in a total volume of 10µL per IP. 10 µL of the complexes were given to 30µL of pre-cleared lysates and brought up to a volume of 500µL using TEG buffer. Following rotation overnight at 4°C, immune complexes were washed 2 times in TEG supplemented with 0.01% Tween-20 and once

without detergent then suspended in sample buffer (RotiLoad 1, Roth) and boiled at 95°C for 5 minutes.

3.6.6.2. Immunoblotting

Following protein extraction and quantification using the Bradford Assay, denaturing sample buffer containing β-Mercaptoethanol and SDS was added to the samples containing equal amounts of protein and boiled at 95°C for 5 minutes. Samples were then allowed to cool and centrifuged for 5 minutes at 12.000g. Depending on the size of the protein to be detected, samples were loaded onto an SDS-PAGE gel containing varying concentrations of acrylamide. The samples which have been boiled in an SDS-containing buffer are now linearized and contain a net negative charge allowing the protein to be resolved by size in the gel. Samples were run at a constant voltage of 120V for approximately 1 hour. Following electrophoresis, proteins were transferred onto a nitrocellulose membrane under a constant current of 400mA for 2 hours with the transfer chambers packed in ice. After completion of the protein transfer, the nitrocellulose membrane was washed briefly in TBST and unspecific binding was blocked using 5% Milk for 1 hour at room temperature under gentle shaking. Following blocking, the primary antibody was added (see 3.3 for dilutions) and the membrane was covered and left to shake overnight. The next day, the membrane was washed 3 times for 5 minutes using TBST, followed by incubation with the secondary antibody for 1 hour at room temperature. A final washing step was performed using TBST, and the chemiluminescent ECL substrate was pipetted on top of the membrane and left to incubate in the dark for 5 minutes. Excess substrate was removed and the membrane was incubated in a cassette with light-sensitive film until a desired signal was obtained.

3.6.7. RNA Extraction and Reverse-Transcriptase Polymerase Chain Reaction (RT-PCR)

For the purpose of quantifying mRNA expression in cell culture and tissue samples, reverse-transcriptase polymerase chain reaction (RT-PCR) was used. In this procedure, after isolating RNA from samples the addition of a reverse transcriptase enzyme allows for the amplification of cDNA. In a further step, specific primers targeting a gene of interest can be used to amplify a product through either semi-quantitative or quantitative real-time PCR. For RNA extraction, following treatment according to the experiment, cells were washed once with 1x PBS and 1mL of TriZol Reagent was added to each sample. Cells were left to incubate in TriZol for 5 minutes at room temperature. Following

incubation, cells were collected into RNAse-free tubes and 200 µl of chloroform was added and briefly vortexed to mix. The samples were left to incubate for 3 minutes at room temperature followed by centrifugation at 12.000g for 15 minutes at 4°C. After centrifugation, the upper phase which now contains the RNA was removed into a clean tube and 500 µl of isopropanol was added to precipitate RNA. After incubation at room temperature for 10 minutes, samples were centrifuged at 10.000g for 10 minutes at 4°C and the supernatant was decanted. Precipitated RNA was washed by adding 1 ml of 70% EtOH, briefly vortexing and centrifuging at 7.600g for 5 minutes at 4°C. Following centrifugation, the ethanol was carefully decanted from the pelleted RNA and the samples were left to air-dry for 10 minutes and then resuspended in 40 µl DEPC water.
For reverse-transcription using the Qiagen QuantiTect Reverse Transcriptase Kit, 1 µg of total RNA in a volume of 12 µl was used per sample. In an initial step, genomic DNA was eliminated from the reaction mixture by adding 1µL of gDNA wipeout buffer and incubating at 42°C for 2 minutes. Samples were then placed on ice and a mastermix containing 4µL of Reverse Transcriptase Buffer, 1 µl of primer mix and 1µl of Reverse Transcriptase was added to each sample and incubated at 42°C for 15 minutes. The reaction was inactivated by incubation at 95°C for 3 minutes and samples were immediately placed on ice and stored at -80°C until further use.
For purposes of semi-quantitative PCR reactions, 1µl reverse-transcribed cDNA was added to a master mix containing:

- 1.5 µl 10x PCR buffer
- 0.9 µl 25 mM MgCl2
- 1.5 µl 2 mM dNTP Mix
- 0.5 µl amplification primer 1 (10 pmol/µl)
- 0.5 µl amplification primer 2 (10 pmol/µl)
- 0.15 µl Thermus aquaticus (Taq) DNA polymerase 10x
- 8.95 µl autoclaved, distilled water

The PCR reaction was conducted under the following conditions: denaturation at 95°C for 1 minute, annealing at 55-65°C for 1 minute, polymerization at 72°C for 1 minute, repeating these steps for 30-35 cycles. PCR products were then separated on a 1.2% agarose gel prepared with TAE buffer and 0.04% ethidium bromide. The gels were run at 100V for 20-30 minutes and products were visualized under UV light.
For quantitative real-time PCR using the Qiagen QuantiFAST SYBR Green Kit, master mix containing 5 µl of 2x Reaction Buffer, 1 µl of ddH_2O, and 1 µl of amplification primers

1 and 1 µL of SYBR Green Enzyme was prepared at pipetted into glass capillaries (Roche) in a Light Cycler Carousel. 2 µl of cDNA were added to each capillary and briefly centrifuged using the Roche Light Cycler 2.0 carousel centrifuge. Real time reactions were carried out in a Light Cycler 2.0 (Roche) under the following cycling conditions according to the manufacturers' instructions: initial activation at 95°C for 5 minutes, denaturation at 95°C for 10 seconds, combined annealing/extension at 60°C for 30 seconds for 35-40 cycles. Following completion of cycling, the baseline and threshold values were set manually and kept constant across different runs for samples from the same experiment. Data analysis was performed with the $2^{(\Delta\Delta Ct)}$ method using a pooled standard as the reference for target gene and housekeeping gene expression. All experiments were repeated three times and technical duplicates were included in each experiment. Results are expressed as fold increase versus control.

3.6.8. Co-Immunoprecipitation

Co-immunoprecipitation (Co-IP) studies allow for the investigation of protein-protein interactions. After isolating a protein I, the detection of a protein II would indicate the interaction of these two target proteins. After incubating a cellular lysate with a primary antibody directed towards protein I, magnetic beads coated with recombinant protein G, a high-affinity binder of the immunoglobulin Fc-Region, are added to the lysate-antibody mixture. Protein I bound by the antibody (including any interaction partners of protein I) can be isolated from the lysate by using a magnet which pulls down the beads. Protein complexes are then washed and separated by SDS-PAGE gel electrophoresis and immunoblotted for protein II. Using this method, it is possible to determine possible interaction partners of a target protein.

In this study, GH3 cells were seeded in 10 cm petri dishes ($1.2x10^6$ cells/petri). Following completion of the particular experiment, cells were placed on ice and nuclear protein lysates were extracted according to the procedures described in 3.6.5. Following isolation of lysates a preclearing step was performed using 10 µl of Protein G Dynabeads (pre-washed three times using TEGDM with 0.1% Tween-20) per sample for 30 minutes on a rotating platform at 4°C. Beads were pulled down and the supernatant was transferred to a fresh tube and 0.5 µg of the target antibody was added to each tube and incubated overnight on a rotating platform at 4°C. The following day, immune complexes were washed three times using TEGDM and captured using 8 µl of Protein G Dynabeads per sample. After two washing steps using TEGDM with 0.1% Tween-20 and one wash with TEGDM without detergent, samples were denatured by

addition of sample buffer containing SDS and β-Mercaptoethanol and boiling at 95°C for 5 minutes. Samples were then immunoblotted according to the procedure described in 3.6.5. Non-immune IgG antibody as well as 1% input controls were included in each experiment.

3.6.9. Chromatin Immunoprecipitation (ChIP)

Through chromatin-immunoprecipitation (ChIP) it is possible to detect the interactions between specific proteins (transcription factors) and a target region of DNA, therefore providing insight into the dynamics of transcriptional regulation. In order to study such interactions, proteins present on DNA at a particular moment must be “fixed” to the DNA in order to preserve this interaction throughout the following sample preparation. For this purpose, crosslinking agents such as formaldehyde can be used. Following crosslinking of proteins and DNA, cells are lysed and the chromatin is sheared using ultrasound disruption in order to facilitate pull-down of protein-bound DNA fragments. After measuring and normalizing the amount of DNA in each sample to be analyzed, samples are pre-cleared using Protein G Dynabeads to reduce background signal caused by unspecific antibody binding. A small aliquote (1% of total lysate) is removed from the samples to later be used as an input control for final data analysis. Each sample is then incubated with a specific primary antibody to pull down a particular protein (transcription factor) of interest and pulled down with protein G coated magnetic beads. Following further washing steps, the addition of proteinase K allows for the digestion of all proteins in the sample, leaving only DNA as a final product. The DNA won from this procedure can then be amplified using primers targeting regulatory regions of interest by quantitative real-time PCR to gain insight into absolute changes in the amount of a particular transcription factor bound to the specific DNA sequence of interest.

In this study, ChIP was performed on GH3 cells seeded in at a density of 3.5×10^5 in 6-well culture plates and allowed to attach overnight. On the following day, cells were transfected according to the procedure described in 3.7.12 with three wells of each plate used for each transfection condition and left to recover for 16 hours. To crosslink, 37% formaldehyde was added directly to the cell culture medium to a final concentration of 1% and allowed to incubate at room temperature for 10 minutes. Cells were then washed 3 times with 1x PBS and placed on ice. For each condition, cells were collected by careful scraping into 1 ml of PBS supplemented with protease inhibitor cocktail. The cells were then collected by centrifugation at 4.000g for 5 minutes at 4°C and the

supernatant was decanted. The cell pellet was gently resuspended in 300 µl cell lysis buffer supplemented with protease inhibitor cocktail and left to incubate on ice for 30 minutes with gentle vortexing every 10 minutes. The cells were spun down at 4.000g for 5 minutes and the resulting pellet was resuspended in 500 µl of nuclear lysis buffer. The lysates were then sonicated on ice to shear the cross-linked chromatin with a Sonifier Cell Disruptor B15 (output control 6, duty cycle 40%) applying pulses for 10 seconds followed by 1 minute of recovery to allow for heat dissipation. This cycle was repeated 12 times for each sample to acquire DNA fragments between 200 and 1000 bp. The lysates were then centrifuged at 12.000g for 10 minutes at 4°C and the supernatant was collected into fresh tubes. DNA concentration in each sample was measured and normalized using dilution buffer to contain 10µg chromatin in 500 µl total volume per immunoprecipitation to be performed. Samples were precleared by adding 5 µl of Protein G Dynabeads under gentle rotation for 30 minutes at 4°C. Following removal of Dynabeads, 5 µl of the lysate was retained for later comparison as a 1% input control and a total of 5 µg of antibody (specific and non-immune IgG) was added to the samples and allowed to incubate on a rotating platform overnight at 4°. The next day, 5 µl of Dynabeads were added to each sample tube and allowed to rotate for 30 minutes at 4°C. Samples were then washed under gentle rotation according to the following scheme:

- 2x 10 minutes in Low Salt Buffer
- 2x 10 minutes in High Salt Buffer
- 1x 5 minutes in LiCl Buffer
- 1x 5 minutes in TE Buffer

Following the last washing step, samples were resuspended in 100 µL of Elution Buffer and incubated in a shaking heat block at 62°C for 2 hours at 450 rpm. The reaction was inactivated by incubating samples at 95°C for 10 minutes. The eluted DNA was removed from the magnetic beads and cleaned using a commercial kit (Qiaquick PCR Purification Kit) The final purified DNA product was then used for real-time PCR analysis using specific primers designed to target the promoter regions of genes of interest (see table 3.4). Normalization of ChIP results was performed in a two-step process using the percent input method which divides signals obtained from the specific ChIP reaction by the signals obtained from an input sample according to the following formula:

1). Ct Input – 6.644 = adjusted input control

2). $2^{(\text{adjusted input control} - \text{Ct (IP)})} \cdot 100$

Calculations were performed for all specific as well as non-immune control antibodies. All experiments were performed in duplicate.

3.6.10. Site-directed mutagenesis

The use of site-directed mutagenesis enables both the alteration of a specific nucleotide sequence by introducing point mutations as well as the insertion or deletion of entire amino acids in a template DNA sequence. Site-directed mutagenesis is a valuable method for characterizing relationships between protein structure and function as well as studying the regulatory function of specific DNA sequences on gene expression. In this study, the role of HIF-1α as a transcriptional regulator of growth hormone expression was examined by mutating the known DNA-binding sequence of the HIF-1α vector used for overexpression studies.

To introduce mutations, the QuikChange Lightening Multi Site-Directed Mutagenesis Kit (Agilent Technologies, Cat. No 210516) was used. For each mutagenesis reaction, 100ng of the pCMV-3x FLAG 7.1-HIF1α expression plasmid and 100 ng of mutagenesis primers (see table 3.4) were incubated along with the other PCR reagents according to the manufacturers' instructions under the following cycling conditions: 1 initial cycle at 95°C for 2 minutes followed by 30 cycles of: 95°C for 20 seconds; 55°C for 30 seconds; 65°C for 220 seconds and one final cycle at 65°C for 5 minutes. To eliminate non-mutated dsDNA, 1 µl of DpnI restriction enzyme was added to the reaction product and incubated at 37°C for 5 minutes. Following this reaction, only linearized mutated amplicons should remain for subsequent processing. To propagate the mutagenesis product, transformation reactions were performed by adding 5 µl of the reaction product to 50 µl *E. coli* XL1-blue and incubated on ice for 30 minutes. Vials were then incubated in a 42°C water bath for 30 seconds and placed immediately on ice. 250 µl pre-warmed S.O.C medium was added to the vial and were placed on a shaking incubator at 37°C for 1 hour at 225 rpm. To confirm successful mutagenesis, 250 µl of this reaction volume was plated onto LB agar plates containing 50 µg ml^{-1} Ampicillin and incubated at 37°C overnight. The next day, 4 clones were picked and propagated in LB medium supplemented with 50 µg ml^{-1} Ampicillin and plasmids were purified using the Qiagen Mini-Prep kit. Successful mutation was confirmed by sequencing performed by SequiServe (Vaterstetten, Germany).

3.6.11. Transfection

Cell transfection for the purposes of RNA-interference, overexpression as well as reporter assays was performed in cells seeded in a 48-well cell culture plate at a density of 1 x 10^5 cells per well. After splitting, cells were left to attach overnight. The next day, cells were transfected with either 10 µM siRNA or 0.4 µg DNA/1 x 10^5 cells using the SuperFect (Qiagen, Hilden, Germany) transfection reagent. In the case of reporter assays, 0.05 µg β-Galactosidase/ 1 x 10^5 cells was included to monitor transfection efficiency. Following 3 hours of incubation with the transfection complexes, cells were washed once with 1x PBS and cell culture medium was added to allow cells to recover overnight. According to the experiment, cells were either treated or harvested for analysis 24 hours post-transfection.

In the case of reporter assays, cells were washed once with 1x PBS and 75 µl passive lysis buffer (Promega) were added to each well. Cells were then frozen at -80°C until measurement. To measure luciferase activity, cell lysates were unthawed and collected in 1.5 ml tubes and centrifuged at 12.000 x g for 5 minutes. The supernatant was distributed between a luminometer plate (20 µl lysate / well) and a transparent ELISA reader plate (30 µl ddH_2O + 20 µl lysate + 50 µl ONPG). The transparent plate for β-Galactosidase measurement was incubated in the dark at 37°C for 30-90 minutes. Luciferase signals were measured using the Berthold TriStar luminometer and β-Galactosidase was measured in an ELISA plate reader at 420 nm. All transfection reactions were performed in triplicate and data are expressed as the ratio of relative luciferase activity of plasmid to β-galactosidase activity.

3.6.12. Protein-phosphatase 1α activity assay

Protein-phosphatase 1α (PP1α) activity was measured using the Ser/Thr phosphatase Kit 1 (Upstate, MA, USA), which is based on the malachite green phosphatase assay. Following completion of treatment, cells were washed twice with TBS and collected in 150 µl of NP40 lysis buffer. Cells were disrupted using a 20G insulin syringe. Following centrifugation for 10 minutes at 12.000 g (4°C) the supernatant was saved to a fresh tube on ice. Prior to measurement a standard curve was prepared using a phosphate standard to range from 0-200 pmol.. Phosphatase activity in samples was measured in a 96 well plate using 25 µl of sample lysate + 25 µl of assay buffer (provided in the kit) + 8,8 µl phosphopeptide [500 µM] following incubation for 30 minutes at room temperature. Absorbance was then measured at 630 nm in an ELISA plate reader.

Absorbance of blank (buffer containing enzyme in the absence of phosphopeptide) was subtracted from the absorbance of the wells containing the enzyme and phosphopeptide. The amount of phosphate released by the enzyme could then be determined using using the standard curve ranging from 0 – 2000 pmol of free phosphate. All samples were measured in triplicate.

3.6.13. PEP-TAG PKA activity assay

The measurement of PKA activity in the study was performed using the PepTag Assay Kit (Promega, Madison USA). This kit allows for the nonradioactive measurement of PKA activity based on the use of a fluorescent peptide substrate specific for PKA. Following phosphorylation of the peptide by PKA, the net charge changes from +1 to -1. Phosphorylated and non-phosphorylated substrates can then be separated using agarose gel electrophoresis. The phosphorylated, negatively charged substrate subsequently migrates towards the positive electrode whereas the non-phosphorylated substrate migrates towards the negative electrode. Following separation, gels can be qualitatively imaged or quantitatively measured using densitometry (Bio-Rad ChemiDoc MP Imaging System).

3.6.14. Radioimmunoassay of growth hormone

To determine the growth hormone (rGH) secretion in GH3 cells the radioimmunoassay (RIA) was performed. The RIA assay is based on the competition for binding of a fixed concentration of anti-rGH antibody by the rGH in a sample and ^{125}I-rGH. The more rGH is in the sample, the less ^{125}I-rGH binds to the anti-rGH antibody. To increase complex size, a secondary antibody is bound to the primary anti-rGH antibody, allowing for the precipitation of larger immunoglobulin complexes. Using a polyethylene glycol buffer, the specific residual ^{125}I-rGH bound to the antibody complex can be separated from unbound ^{125}I-rGH in solution. Radioactivity can then be measured using a gamma counter, and the rGH concentration can be calculated using a standard curve.

In detail, the supernatant from GH3 cells seeded in 96-well cell culture plates at a density of 1 x 10^4 was incubated with ^{125}I-rGH (BIOTREND, Germany) and an anti-rGH antibody overnight. The standard curve was set up using serial dilutions of [1 mg ml^{-1}] unlabeled rGH (NIDKK, USA) in DMEM to 10.000 – 5000 – 2500 – 1250 – 625 – 312 – 156 – 78 – 0 pg ml^{-1} and incubated ON at 4°C with 20.000 – 25.000 cpm per 100 µl tracer and primary antibody directed against rGH. The next day, secondary antibody (anti–rabbit IgG) was added for 1.5h at RT. The resulting immunocomplexes were precipitated with

PEG 6%, the pellet was washed, and radioactivity was measured. Characteristics of the GH secretory pattern (mean rGH levels, area under the curve and amplitude) were assessed using the ULTRA program (kindly supplied by E Van Cauter; Van Cauter, 1988).

Figure 3.1 shows a typical RIA standard curve. The X-axis depicts the concentration of the standard and the Y-axis (Bound/Ttotal) is calculated for each value by the measurement of radioactivity for each concentration of standard used, minus the unspecific signal (primary antibody omitted). The uppermost value of 0.1 represents 100% binding of ^{125}I-rGH when 0 pg ml^{-1} standard is present. This binding signal decreases accordingly with increasing concentrations of the standard. The sample values calculated from the fitted regression curve correspond to pg ml^{-1}. As rGH secretion may be skewed by increased cell proliferation, WST-1 analysis was performed in all samples and rGH measurements were divided by WST-1 values to correct for such effects.

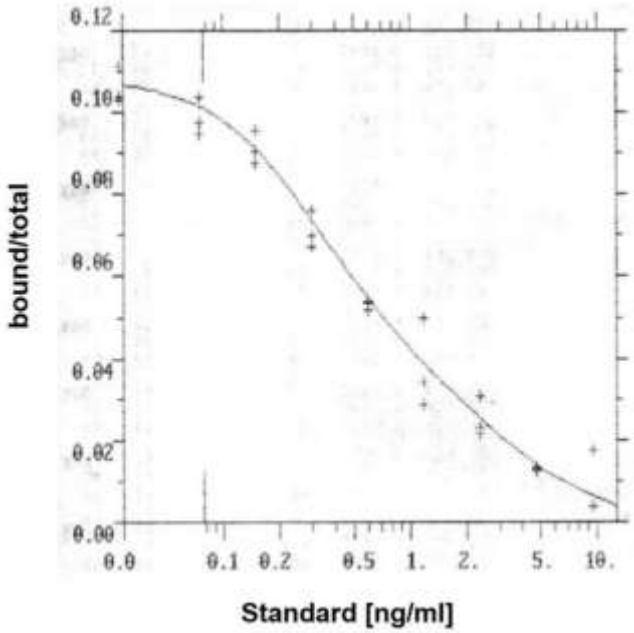

Figure 3.1: Representative RIA standard curve. RIA was implemented to measure hGH and intracellular cAMP..

3.6.15. Radioimmunoassay of intracellular cAMP

GH3 cells were seeded (1 x 10^5 cells per well) in 48 well plates in DMEM medium without antibiotics, with glutamine, and with 0.1% BSA and 0.5 mM IBMX. Following treatment specified in the particular experiment, culture medium was carefully aspirated without disturbing the cells. Cold 5% trichloroacetic (TCA) acid (500 µl/well) was added and the place was incubated on ice overnight.

After overnight incubation, the TCA was transferred from the wells into 10 ml glass tubes. TCA was extracted from the samples with 3 ml of diethyl ether saturated with water. The diethyl ether was then aspirated and discarded. This extraction was performed twice. Samples were then frozen at -80°C overnight and next day they were lyophilized overnight in a P3K-S50 Lyophilizer.

cAMP determination was performed with a commercial kit from Perkin Elmer following the same principle as outlined for RIA measurement of growth hormone. In all experiments forskolin 5 µM, a potent activator of adenylate cyclase, was used as a positive control.

3.6.16. Hypoxia chamber treatment

The hypoxic treatment of cells was performed in a modular hypoxia incubator chamber (StemCell Technologies, Cat. 27310). For hypoxic incubation, cells were placed in the center of the chamber which was sealed shut and connected via a flow meter (StemCell Technologies, Cat. 27311) to a gas tank containing 1% O_2, 5% CO_2 and 94% N_2. The modular chamber was placed in a standard humidified incubator at 37° for 6-12 hours. A normoxic control was placed in the same incubator outside of the hypoxia chamber. Control of hypoxia was performed either by western blot for HIF-1α protein expression or HRE-luciferase assay.

Figure 3.2: Modular hypoxia chamber used for hypoxic incubation. The chamber (left) containing cell culture plates was flooded with a gas mixture containing 1% O_2, 5% CO_2 and 94% N_2 using the flow meter (right). Images from stemcelltechnologies.co

4. Results

4.1. The hypoxic response in GH-secreting pituitary tumors

4.1.1. Vascular density in GH-secreting pituitary tumors and the normal pituitary

Previous studies on the vascularization pattern in pituitary tumors have demonstrated a reduction in the vascular density of tumors versus the normal pituitary [69-71]. Furthermore, among tumor subtypes, GH-secreting tumors from patients with acromegaly were found to display the lowest vascular density therefore pointing towards relative tissue hypoxia in these tumors. Prior to characterizing the effects of hypoxia on GH-secreting pituitary tumor cells, it was confirmed whether our cohort of pituitary tumors and normal pituitaries indeed displays a similar pattern of vascularization as described in the literature. To this end immunohistochemistry against the endothelial-specific antigen CD-31 was performed to visually assess vascular density in normal and tumorous human pituitaries. To assess whether GH-secreting tumors indeed display lower vascular density compared to other pituitary tumor entities, non-secreting pituitary tumors were also examined (Fig. 4.1).

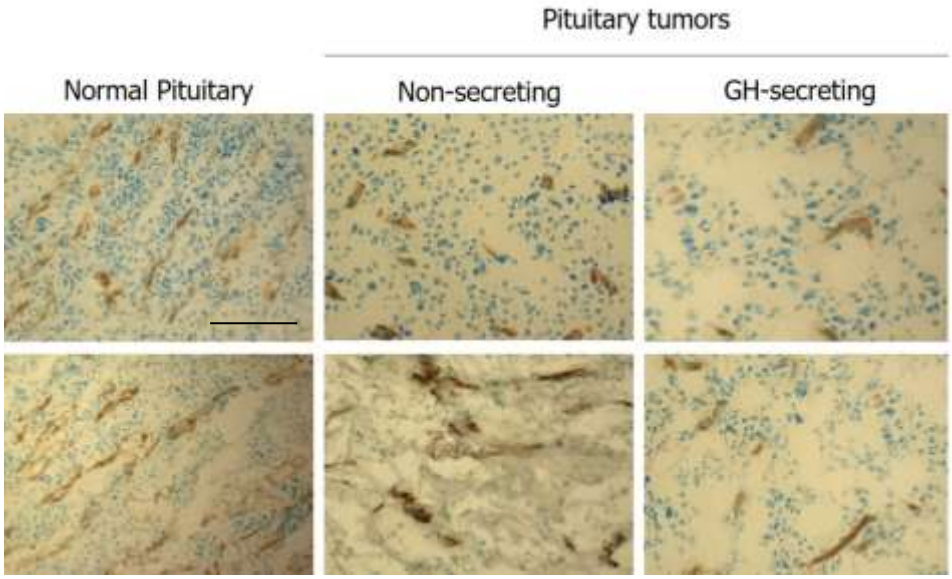

Figure 4.1: GH-secreting tumors display lower vascular density compared to the normal pituitary and non-secreting pituitary tumors. Representative images of CD-31 immunoreactivity in normal pituitary (n=4), non-secreting (n=11) and GH-secreting (n=11) pituitary tumors. CD-31 signal is visualized with diaminobenzidine (DAB) staining (brown nuclei) (scale bar 40µm). Counterstaining with toluidine blue (blue nuclei).

The resulting staining patterns could confirm the previous reports that pituitary tumors indeed show lower vascular density compared to the normal pituitary with the GH-secreting pituitary tumors displaying the lowest pattern of vascularization also compared to another, non-secreting pituitary tumor entity. As tissue hypoxia can result from greater diffusion distances for molecular oxygen, low vascular density is associated with decreased oxygen availability for individual tumor cells. Taken together with the confirmatory findings of lower vascular density in GH-secreting pituitary tumors, it was hypothesized that these tumors are exposed to relative tissue hypoxia.

4.1.2. HIF-1α is overexpressed in GH-secreting pituitary tumors

The cellular response to tissue hypoxia as it is found in solid tumors involves the oxygen-dependent stabilization and activation of a family of transcription factors known as Hypoxia Inducible Factors (HIFs), with HIF-1α being the most well-characterized member. Taken together with the evidence of decreased vascular density pointing towards tissue hypoxia, as well as the upregulation of HIF-1α target genes under hypoxic incubation of GH-secreting tumor cells, it was next questioned whether HIF-1α itself is indeed present at higher levels in GH-secreting pituitary tumors.

To this end, immunohistochemical analysis of HIF-1α expression was performed on archival paraffin embedded tissue from patients with GH-secreting tumors (n=40) and normal autoptic pituitary samples (n=6). HIF-1α immunoreactivity (IR) of all samples was scored as 1 = 0-30% IR, 2 = 31-60% IR and 3 = 61-100% IR. Figure 4.2 depicts the percentage of each immunoreactivity score in the collective of all samples. Overall, GH-secreting tumors displayed a clear and abundant nuclear staining pattern of HIF-1α in GH-secreting tumors with virtually absent staining in the normal pituitary.

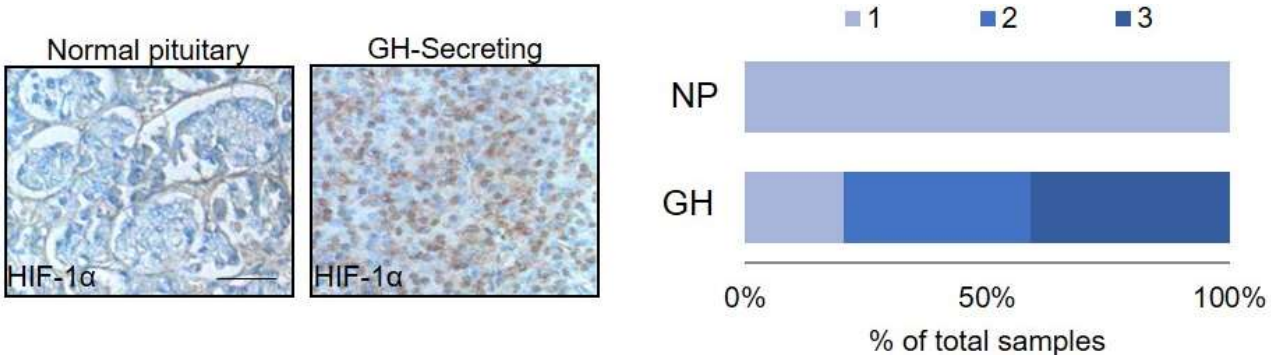

Figure 4.2: HIF-1α expression is higher in GH-secreting pituitary tumors than the normal pituitary. HIF-1α immunoreactivity in representative normal pituitary gland and a GH-secreting tumor. Signal is visualized with diaminobenzidine (DAB) staining (brown nuclei) (scale bar 40µm). Counterstaining with toluidine blue (blue nuclei). The graph shows the distribution of the HIF-1α immunoreactivity (IR) score on normal pituitary glands (n= 5) and acromegalic tumors (n= 39). 1 = 0-30% IR, 2 = 31-60% IR and 3 = 61-100% IR.

To address the question whether HIF-1α expression is specific for GH-secreting tumors, additional samples from patients with non-secreting pituitary tumors were used for confirmation in western blot analysis. Densitometric quantification of signal strength showed that GH-secreting tumors strongly express HIF-1α (7-fold vs. normal pituitary), while it is low or absent in non-secreting pituitary tumors (Fig. 4.3 a,b). These findings showed that GH-secreting tumors selectively overexpress HIF-1α compared to the normal non-tumorous pituitary and other pituitary tumors (non-secreting pituitary tumors), thereby pointing towards a specific role for HIF-1α in the pathophysiology of GH-secreting tumors.

HIF-1α stability is mainly post-transcriptionally regulated through prolyl hydroxylation which marks it for proteasomal degradation under normoxic conditions. While HIF-1α transcripts were detected in both normal pituitaries and acromegalic tumors, no significant differences were measured (Fig 4.3c) indicating that increased HIF-1α transcription *per se* is not responsible for the abundant protein expression observed in acromegalic tumors.

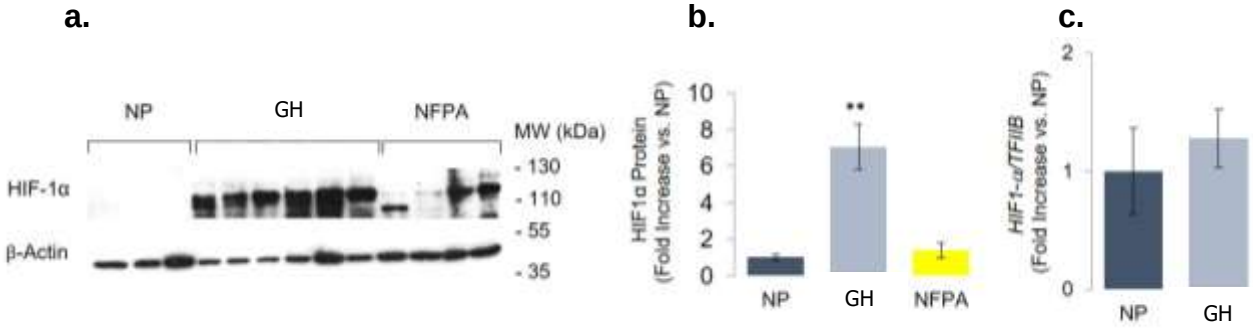

Figure 4.3: HIF-1α protein is strongly and selectively expressed in acromegalic tumors. (a). Representative immunoblot for HIF-1α on normal pituitary glands (n=3) and acromegalic tumors (n=6) and non-functioning pituitary tumors (n=4) **(b).** Densitometric Quantification of HIF-1α western blot signal on the larger set of samples containing 5 normal pituitaries, 25 acromegalic tumors and 8 non-functioning pituitary tumors. Values are given as HIF-1α to β-actin signal ratio and presented as fold increase versus the mean normal pituitary values. Error bars: s.d. ***P*<0.01 to normal pituitary glands (Mann-Whitney U-test). **(c).** qPCR quantification of HIF-1α transcripts collected from RNA from the same samples as in b. Data are means ± standard deviation of 2 measurements and presented as HIF1α/TFIIB fold increase versus the mean normal pituitary values.

As GH-secreting tumors carry oncogenic gsp mutations in 40% of cases [142], the possible association between gsp status and HIF-1α protein levels was examined in 21 patient cases (Table 1). Linear regression analysis showed no significant predictive

value of the presence of the gsp oncogene on HIF-1α protein expression (F(1,20) = 0.479, P=0.497, R2=-0.025). However, linear regression analysis revealed that mRNA transcript levels for *GNAS*, the gene encoding for Gsα, statistically significantly predict HIF-1α protein expression (F(1,20) = 5,962, P=0.024, R^2 = 0.233). These data suggest that the increased HIF-1α expression does not occur secondary to gsp oncogenic mutations, and most likely results from the presence of tissue hypoxia.

Case Nr.	Sex	Age	Grade	Gsp Status	Gsa mRNA	HIF-1α Protein
1	M	61	II	-	557	113
2	M	31	II	-	57	196
3	M	50	III	+	475	200
4	M	38	II	+	729	188
5	F	54	III	-	755	161
6	F	37	III	-	99	348
7	F	30	III	-	175	216
8	F	51	III	-	170	180
9	M	51	III	-	684	231
10	M	49	III	-	668	5
11	M	24	II	-	288	429
12	M	43	III	-	858	56
13	M	46	III	-	734	80
14	M	34	II	+	330	190
15	M	83	III	-	168	332
16	M	72	II	-	324	162
17	F	38	III	+	207	147
18	M	36	II	+	332	168
19	M	57	I	-	997	322
20	M	42	III	-	174	165
21	M	32	III	+	239	123

Table 1. Characteristics of tissue used for mRNA and protein screening. Clinical characteristics of patients whose tissue was used for mRNA and protein screening. Tumor grade according to the modified Hardy Classification Scale. Gsa mRNA expressed as transcript numbers after normalization to a houskeeping gene compared to an internal standard used in qPCR analysis. HIF-1α protein expression as determined by densitometric quantification of western blot signals normalized to β-Actin. Values expressed as percent increase versus normal pituitary.

4.1.3. Hypoxia promotes the expression of glycolytic enzymes in human acromegalic pituitary tumor cells

Decreased oxygen availability as a result of decreased vascular density can promote the metabolic adaptation of hypoxic cells towards a glycolytic phenotype requiring less molecular oxygen for ATP generation compared to oxidative phosphorylation. This process is coordinated by the transcriptional activity of HIF-1α which promotes the

transcription of key glycolytic enzymes (*Ldha*, *Glut1*, *Pdk1*). To validate whether the increased HIF-1α expression found in acromegalic tumors also results in the expression of HIF-1α target genes under hypoxia, qPCR analysis on the expression of genes encoding for major glycolytic enzymes was performed in primary cultures of acromegalic tumors.

To this end, GH-secreting tumor tissue from patients who underwent transsphenoidal tumor resection was enzymatically digested and divided in half, with one half being cultured under normoxic conditions, and the other half cultured under hypoxia (1% O_2) for 12 hours. The mRNA expression of key glycolytic enzymes was assessed via real-time PCR (qPCR) (Fig.4.4). Hypoxic acromegalic tumor cells showed significantly increased transcription of three key glycolytic enzymes (*Ldha*, *Glut1*, *Pdk1*) under conditions of 1% O_2 incubation versus normoxic conditions.

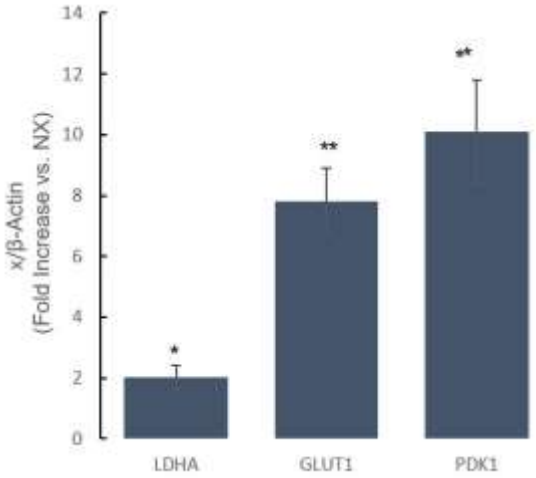

Figure 4.4: Hypoxia increases glycolytic gene expression in human acromegalic tumors. Effect of hypoxia on endogenous *LDHA*, *GLUT1* and *PDK1* transcription as determined by real time qPCR in primary cultures of human acromegalic tumors (n=5). Data are <*gene*>/β-Actin and presented as fold increase to each normoxic control. **P*<0.05; **P*<0.01 (Mann-Whitney U-test).

These findings are in line with observations that tumor cells preferentially utilize glycolysis under states of hypoxia by upregulating key enzymes of the glycolytic pathway. The response of GH-secreting pituitary tumor cells to hypoxia together with the observed decreased vascular density and increased HIF-1α expression indicate that these tumors are also governed by the general adaptive mechanisms of eukaryotic cells to oxygen deprivation.

4.1.4. Hypoxia does not affect cell viability or DNA synthesis in human acromegalic tumors

While tissue hypoxia promotes the adaptation of a glycolytic phenotype to maintain ATP synthesis, cell proliferation and DNA synthesis can be hampered due to decreasing energy reserves. Tumor cells can remain viable under decreased oxygen concentrations

in part due to the activity of HIF-1α in inhibiting apoptosis and regulating autocrine growth signals. As acromegalic tumors were found to express high levels of HIF-1α, it was next questioned whether hypoxia may also promote cell viability and proliferation in acromegalic tumor cells.

Cell viability was assessed using the colorimetric WST-1 assay and DNA synthesis using ^{3}H-thymidine incorporation assay (Fig. 4.5) Tumor tissue from acromegalic patients (n=5) was enzymatically digested and half of the tumor was cultured under normoxic conditions and the other half under hypoxic conditions for 24 hours. Tumor cells incubated under hypoxic conditions showed a tendency towards increased WST-1 (155%) and ^{3}H-thymidine incorporation (126%), which did not reach statistical significance (*P*=0.24, *P*=0.37, respectively).

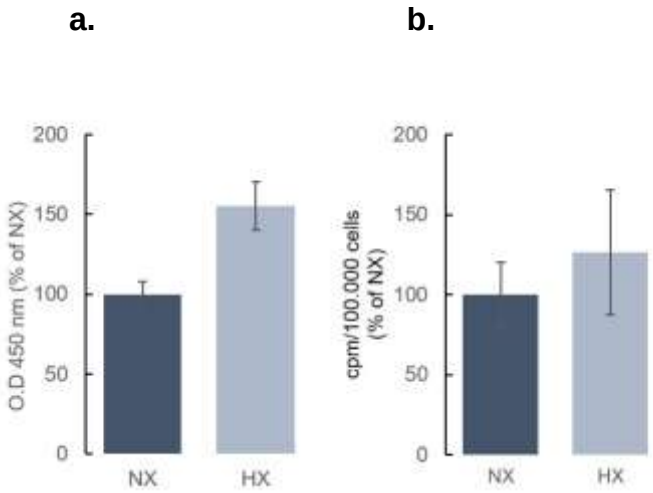

Figure 4.5 (a) WST-1 and **(b)** ^{3}H-thymidine incorporation assay in human acromegalic tumors (n=5). Incubation of enzymatically dispersed tumor tissue showed no significant difference (Mann-Whitney U-Test) in cell viability or DNA synthesis between normoxia (NX) and hypoxia (HX).

4.1.5. Hypoxia stimulates GH synthesis in human acromegalic tumors

GH hypersecretion is the pathological landmark of acromegalic tumors. It was therefore questioned whether HIF-1α may contribute to GH hypersecretion as the central pathophysiological characteristic of these tumors. To this end, enzymatically digested tumor tissue from patients who underwent transsphenoidal tumor resection was divided in half, with one half being cultured under normoxic conditions, and the other half cultured under hypoxia (1% O_2) for 18 hours. GH was then measured in the supernatant by RIA and normalized to WST-1 values to compensate for any changes in viability induced by the different treatments (normoxia vs. hypoxia).

In all human tumors (n=9) a significant increase in GH secretion among the hypoxic cultures versus those incubated under normoxic conditions was observed (*P*=0.008) (Fig. 4.7). These findings indicate that hypoxia indeed promotes the secretion of GH in human GH-secreting tumors and may therefore be of pathophysiological relevance.

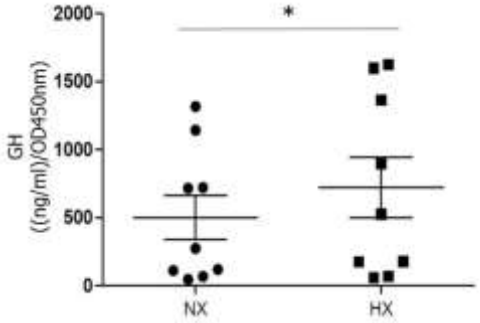

Figure 4.7: Hypoxia promotes GH secretion in human GH-secreting tumors. Effect of hypoxia (1% O2 for 18 hours) on GH secretion on 9 human acromegalic tumors in primary cell culture. For all cell culture experiments, each GH RIA value was divided by cell viability counts as determined by WST-1 at OD450nm. Each condition was measured in technical quadruplicates and data are means ±SEM.*P<0.05 (Mann-Whitney U-Test).

4.2. Hypoxia and HIF-1α stimulate GH synthesis

4.2.1. HIF-1α mediates the effects of hypoxia on GH synthesis

To examine whether HIF-1α mediates the stimulatory effects of hypoxia on GH synthesis, GH3 cells transiently transfected with either HIF-1α siRNA or control siRNA were incubated under hypoxic and normoxic conditions and *Gh* promoter activity, transcription and hormone secretion was measured (Fig. 4.8). Hypoxic incubation of GH3 cells transfected with control siRNA stimulated the activity of the GH-luciferase promoter construct as well as *Gh* transcription measured by qPCR and secretion determined by RIA. The effects of hypoxia on all three parameters of GH synthesis was abrogated in GH3 cells transfected with siRNA targeting HIF-1α pointing towards the specificity of HIF-1α in mediating the effects of cellular hypoxia on GH synthesis.

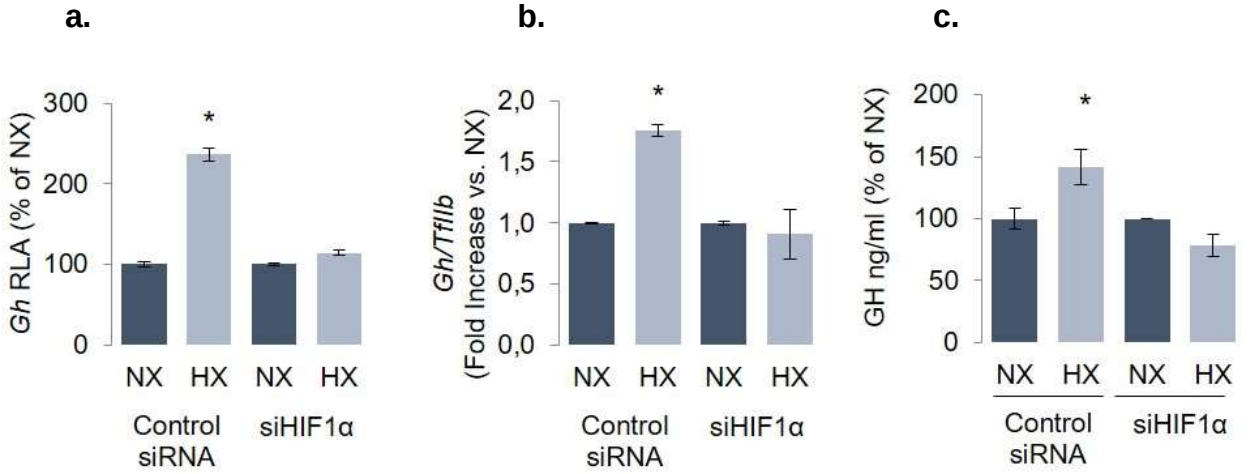

Figure 4.8: HIF-1α mediates the effects of hypoxia on GH synthesis. (a). Effect of 18 hours hypoxia on Gh promoter activity in GH3 cells transfected with the rat *Gh*-luc plasmid (pA3GHluc). Luc/βGal: luciferase to β-galactosidase ratio. Data are means±SEM from 3 experiments and are presented as percentage of each normoxic (NX) control. *P<0.05 (t-test). RLA, relative luciferase activity. **(b).** Effect of hypoxia on endogenous rat Gh transcription as determined by real time RT-PCR. Data are *Gh/TfIIb* and presented as fold increase to each normoxic control. *P<0.05 (t-test). **(c).** Effect of

hypoxia on GH secretion. In c, d, and e transfection with 100nM HIF-1α siRNA for 48 hours abolished the effect of hypoxia.

4.2.2. HIF-1α promotes GH synthesis

Following the observations in primary cultures of human acromegalic tumors, it was next asked whether the increased expression of HIF-1α also observed in tissue specimens may contribute to the ability of hypoxia to stimulated GH synthesis. To this end, the rat lactosomatotroph cell line GH3 was transiently transfected to overexpress HIF-1α. Co-transfection with the pA3GHluc reporter plasmid was performed to monitor the effect of HIF-1α on *Gh* promoter activity. *Gh* transcript levels were measured using qPCR and GH secretion quantified with RIA (Fig. 4.9 a-c). HIF-1α overexpression increased rat *Gh* promoter activity which also translated into increased endogenous *Gh* mRNA synthesis and finally, GH secretion. These findings pointed towards the role of HIF-1α in promoting GH synthesis as it was observed in hypoxic acromegalic tumors.

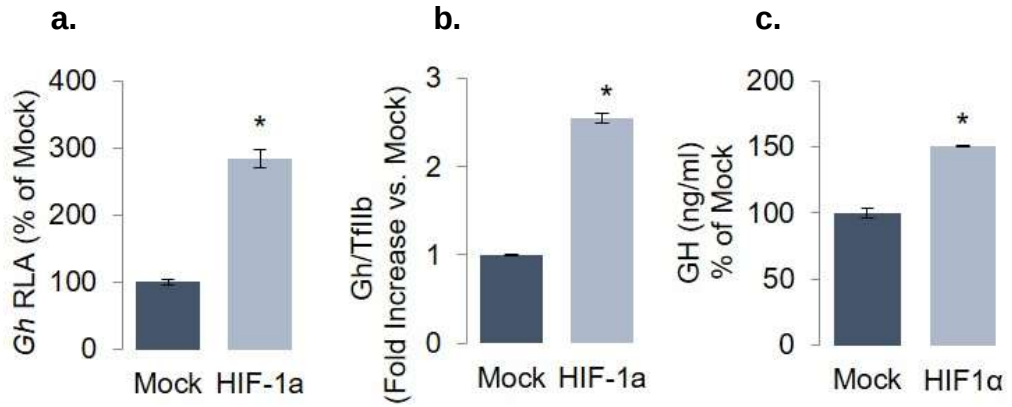

Figure 4.9: HIF-1α stimulates GH synthesis Effect of HIF-1α overexpression on **(a).** rat Gh promoter activity, **(b).** endogenous rat Gh transcription and **(c).** secretion. Data are presented as fold increase versus mock control (pCMV empty vector). *P<0.05 to mock (t-test).

4.2.3. HIF-1α stimulates growth hormone synthesis independently of its DNA-binding activity

HIF-1α is a transcriptional activator of over 60 putative target genes [120]. It was therefore speculated that HIF-1α may also activate *Gh* transcription via direct DNA binding. To this end, chromatin immunoprecipitation of HIF-1α on the *Gh* promoter was performed in GH3 cells exposed to 18 hours of either hypoxia or normoxia using binding of Pit1 as a positive control [39]. This analysis showed no enrichment of HIF-1α on the *Gh* promoter in contrast to the abundant binding of Pit1 (Fig. 4.10).

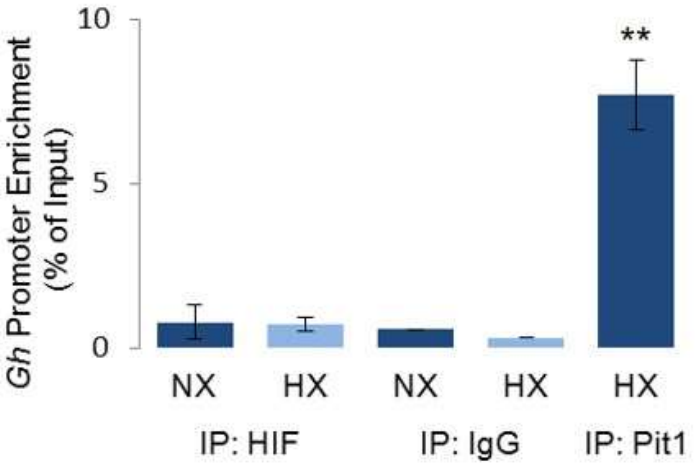

Figure 4.10: HIF-1α does not enrich on the GH promoter. Chromatin immunoprecipitation showing absence of HIF-1α binding to the endogenous rat Gh promoter in GH3 cells under normoxia or hypoxia, in contrast to the positive control Pit-1 (shown in hypoxic cells). Rabbit IgG was used as a control. ***P*<0.01 (t-test)

These findings were validated in a second approach in which a HIF-1α construct unable to bind to its consensus hypoxia responsive element (HRE) due to a single amino acid mutation (Arg30Ala) in its DNA binding domain was generated using site-directed mutagenesis [143]. The inability of the HIF-1α^{R30A} mutant construct to bind to the HRE element was confirmed in GH3 cells expressing either HIF-1α^{R30A} or wild type HIF-1α together with an HRE-luciferase reporter plasmid (Fig. 4.11a). Western blot analysis using an antibody recognizing an unaltered epitope (amino acids 432 – 528) confirmed that the mutation does not alter the protein expression and stability (Fig. 4.11b).

HIF-1α^{R30A} and wild-type HIF-1α constructs were transiently transfected into GH3 cells together with the pA3GHluc reporter plasmid with the pCMV-Myc backbone plasmid used as a control (Fig. 4.11c). *Gh* promoter activity was similarly stimulated in both wild-type and HIF-1α^{R30A} expressing Gh3 cells indicating that HIF-1α is not promoting *GH* transcription via promoter binding**.** Taken together these findings point to an integration point of HIF-1α on the GH synthesis pathway upstream to its transcriptional activation.

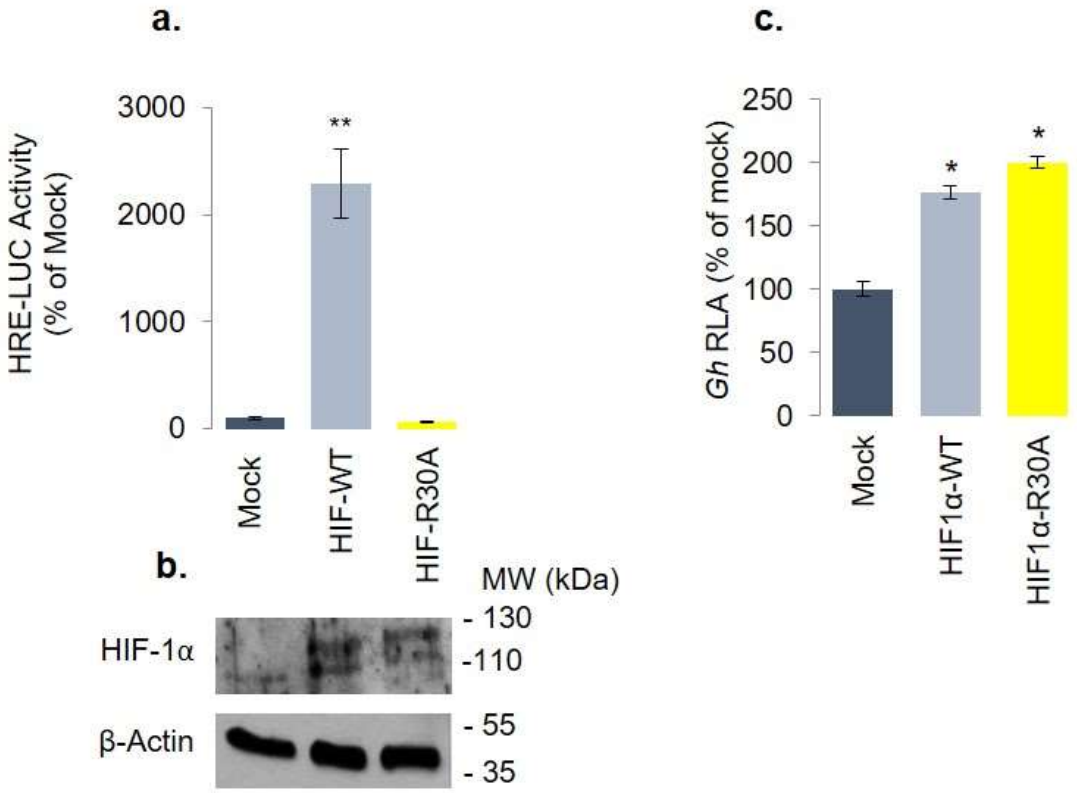

Figure 4.11: HIF-1α^{R30A} stimulates *Gh* promoter activity in GH3 cells. **(a).** HIF-1α^{R30A} versus wild-type HIF-1α on HRE-luciferase activity. **(b).** Immunoblot for HIF-1α in the HIF-1α^{R30A} and wild-type overexpressing cells. The antibody used recognizes an epitope (aa 432 – 528) expected to be unaffected by site-directed mutagenesis. **(c).** Effect of the HIF-1α mutant HIF-1α^{R30A} on rat *Gh* promoter activity. **P*<0.05 ***P*<0.01 (t-test).

4.2.4. HIF-1α stimulates CREB transcriptional activity and phosphorylation

The main signaling events regulating pituitary GH transcription involve the canonical cAMP-PKA-CREB signaling cascade [30, 144, 145]. GH transcription is stimulated by CREB both directly, through the binding to its canonical CRE promoter sequences, and indirectly by promoting the transcription of *POU1F1* which encodes for Pit1 [35, 39, 40]. It was therefore first examined whether HIF-1α can induce CRE-transcriptional activity in GH3 cells. To this end, GH3 cells transiently transfected with either HIF-1α siRNA or control siRNA together with the pCRE-luciferase reporter construct were incubated under hypoxic conditions (normoxic incubation as control) for 18 hours and CRE-luciferase activity was measured. (Fig. 4.12a) CRE transcriptional activity was increased under hypoxia and that this effect was abrogated when HIF-1α was silenced. Similarly,

transient HIF-1α overexpression in GH3 cells also increased CRE transcriptional activity (Fig. 4.12b).

Furthermore, the effects of HIF-1α overexpression on CREB recruitment to the Pit1 promoter were examined using chromatin immunoprecipitation in GH3 cells (Fig. 4.12c). HIF-1α overexpressing GH3 cells showed significantly more CREB enrichment to the endogenous Pit1 promoter compared to mock transfected cells using the pCMV-Myc backbone plasmid.

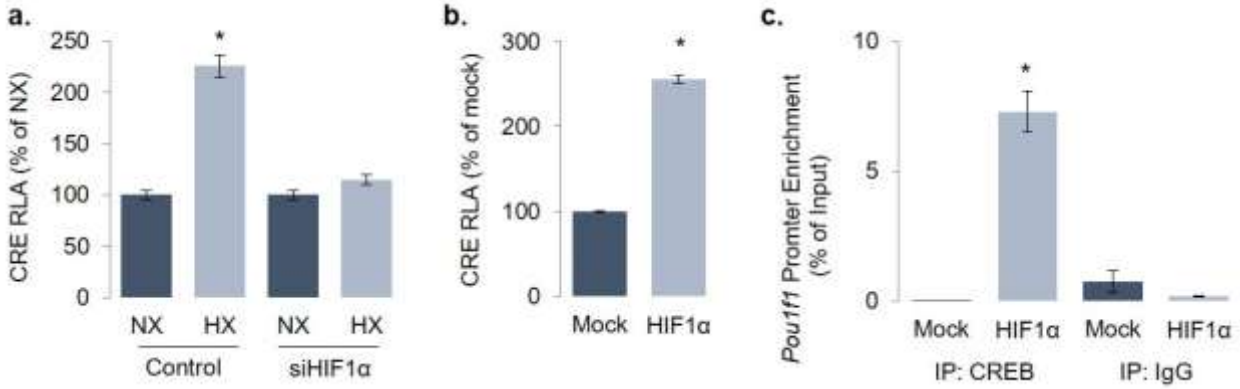

Figure 4.12: HIF-1α promotes CRE-transcriptional activity. (a). effect of hypoxia (1% O2 for 18 hours) on CRE induced luciferase activity. Transfection with 100nM HIF-1α siRNA for 48 hours abolished the effect of hypoxia. Luc/βGal: luciferase: β-galactosidase ratio. Data are means±SEM of three experiments and expressed as percentage of each normoxia control. **(b).** Effect of HIF-1α overexpression on CRE luciferase activity. *P<0.05 (t-test). **(c).** Chromatin immunoprecipitation showing increased CREB binding to the endogenous rat *Pou1f1* (encoding for Pit-1) promoter in GH3 cells overexpressing HIF-1α. Rabbit IgG was used as a control**.** **P*<0.05 (t-test).

4.2.5. HIF-1α stimulates CREB phosphorylation

A prerequisite for CREB promoter binding and transcriptional activity is the phosphorylation of its serine 133 residue by PKA [27]. CREB is not continually phosphorylated, but rather displays a burst-attenuation kinetic [146] with maximal phosphorylation occurring at approximately 1 hour, followed by sequentially decreasing phosphorylation returning to baseline after approximately 6 hours. The decrease in CREB phosphorylation and ultimately transcriptional activity is due to the action of the serine/threonine phosphatase PP1, which returns CREB to basal phosphorylation levels at approximately 6 hours [147-149]. As HIF-1α was shown to increase CRE-transcriptional activity it was next asked whether the phosphorylation status of CREB is similarly upregulated. To this end, a forskolin attenuation experiment was performed.

Here, GH3 transiently transfected with HIF-1α or a mock plasmid were stimulated with 5 µM forskolin for different time points (0, 1, 3 and 6 hours) and protein was collected for western immunoblot of CREB-Ser133-CREB (Fig. 4.13a). The results of this experiment showed that HIF-1α overexpression indeed increased basal phosphorylation of CREB and blunted the physiological attenuation of forskolin-induced Ser133 phosphorylation. HIF-1α expressing cells showed elevated CREB phosphorylation levels even after 6 hours whereas the mock transfected cells they had returned to their basal status similar to 0 hours.

The increased basal CREB phosphorylation led to the hypothesis that the activity or absolute expression levels of the protein phosphatase 1 (PP1) may be decreased when HIF-1α is overexpressed, therefore allowing for sustained phosphorylation of Ser133 CREB. Therefore, PP1 protein levels were assessed by immunoblot in transiently transfected GH3 cells expressing either HIF-1α or the pCMV-Myc empty backbone plasmid. (Fig. 4.13b) This analysis showed no difference in PP1 protein expression between HIF-1α or mock-transfected cells. To exclude the possibility of altered phosphatase activity despite the equal presence of PP1 protein, phosphatase activity was measured in the same cells that were used for the western immunoblot (Fig. 4.13c). No difference in PP1 phosphatase activity could be detected in HIF-1α and mock-transfected cells, indicating that HIF-1α does not increase CREB phosphorylation by interfering with its PP1-mediated dephosphorylation.

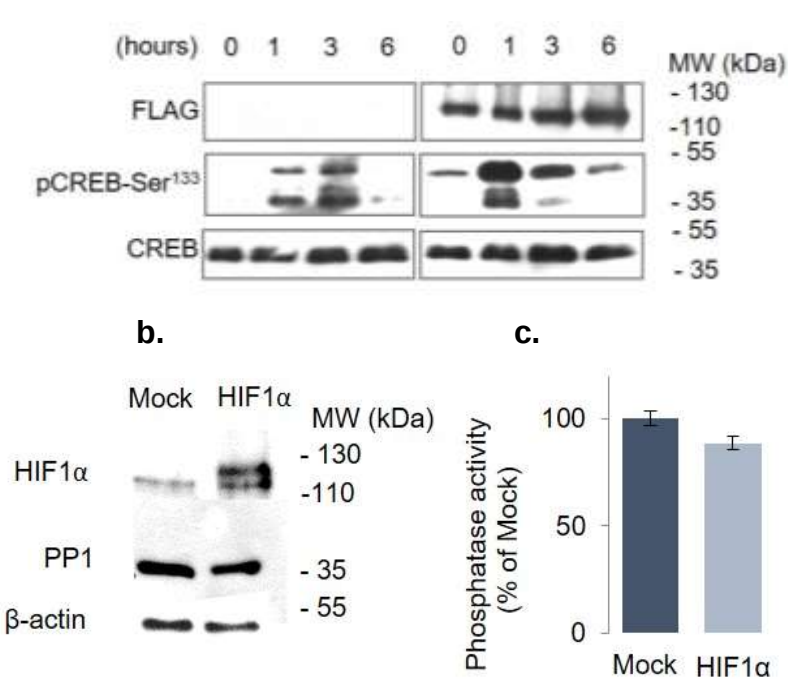

Figure 4.13: HIF-1α stimulates CREB phosphorylation. (a). Immunoblot showing that HIF-1α overexpression (here against the FLAG-tag of HIF-1α expression plasmid) increases basal and forskolin (5µM, 1-6 hours)-induced pCREB-Ser133 levels. It also shows that forskolin-induced CREB-Ser133 levels remain elevated in HIF-1α overexpressing GH3 cells, while it is back to basal after 6 hours in the mock plasmid control transfected cells. **(b).** HIF-1α does not affect PP1 protein levels as determined by western blot and phosphatase activity assay.

4.2.6. Hypoxia acts through CREB and Ser133 phosphorylation to stimulate GH synthesis

It was next examined whether the stimulatory effects of hypoxia acting through HIF-1α indeed requires phosphorylated CREB to affect GH synthesis. GH3 cells were therefore transiently transfected with siRNA targeting CREB and were exposed to hypoxia or normoxia for 18 hours (Fig. 4.14a). It was observed that GH3 cells lacking CREB indeed showed a blunted response to hypoxia as was reflected by decreased *Gh* transcript levels.

Finally, the role of CREB phosphorylation in mediating the effects of hypoxia was examined by overexpressing in GH3 cells a $CREB^{S133A}$ mutant (CREB-M1) which cannot be phosphorylated by PKA due to a Serine133-to-Alanine point mutation [27] (Fig. 4.14b). Hypoxia could not increase *Gh* transcription in cells expressing CREB-M1 contrary to the stimulatory action observed in the mock-transfected (RSV control plasmid) counterparts. Taken together, these results illustrate not only the importance of CREB expression, but also of active Ser133 phosphorylation in mediating the stimulatory effects of hypoxia and HIF-1α on GH synthesis indicating the importance of CREB phosphorylation in hypoxia's action.

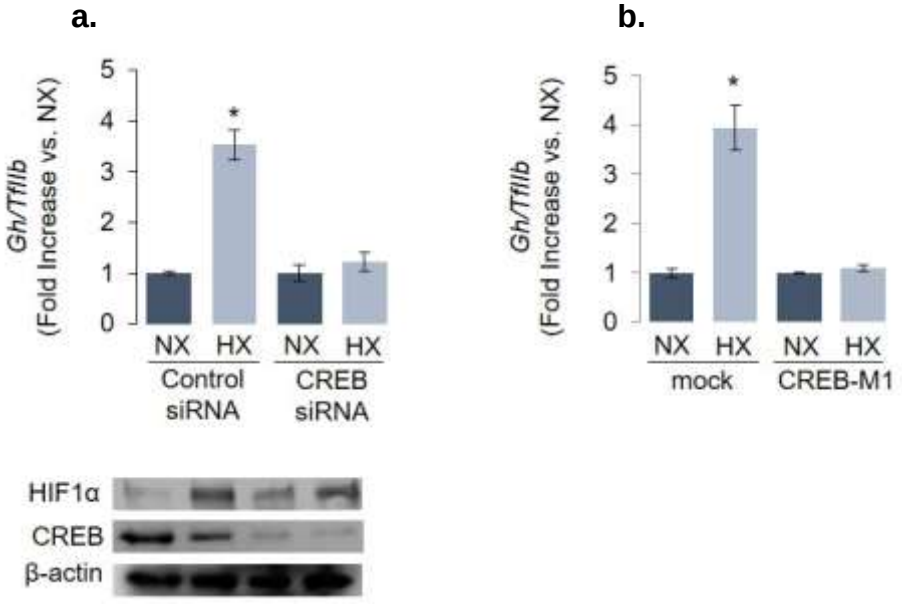

Figure 4.14: HIF-1α promotes GH synthesis in a CREB-dependent manner. (a). knocking down CREB with siRNA abolishes the effect of hypoxia on endogenous rat *Gh* transcription in GH3 cells as determined by real time RT-PCR. Immunoblot shows the knockdown efficacy of the CREB siRNA. **(b).** Hypoxia fails to increase rat *Gh* transcription in GH3 cells overexpressing CREB-M1 ($CREB^{S133A}$) a mutant that cannot be phosphorylated by PKA. Data are Gh/TfIIb and presented as fold increase to each normoxia (NX). *P<0.05 to each normoxia (t-test).

4.2.7. HIF-1α and hypoxia activate PKA

Within the cAMP cascade, PKA is the major kinase which phosphorylates CREB at Serine 133. Having established the importance of phosphorylated CREB in mediating the effects of hypoxia on GH synthesis it was next hypothesized that HIF-1α may act on CREB and ultimately GH via PKA. It was therefore questioned whether hypoxia and HIF-1α can stimulate the catalytic activity of PKA. GH3 cells exposed to hypoxia for 18 hours as well as cells transiently transfected with the HIF-1α expression plasmid indeed showed significantly increased PKA activity compared to the normoxic and mock transfected counterparts, respectively (Fig. 4.15).

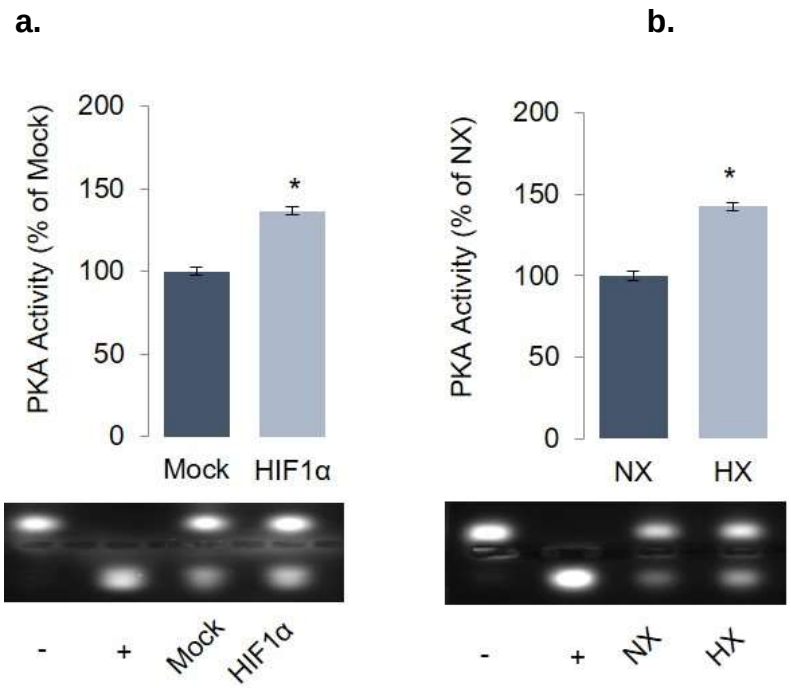

Figure 4.15: Hypoxia and HIF-1α stimulate PKA activity. The effect of **(a)** HIF-1α and **(b**) hypoxia on PKA activity as determined with a non-radioactive commercial kit (Promega). Blots show imaging of the phosphorylated peptide substrate. Data are arbitrary units presented as % of mock (empty pCMV plasmid) control or normoxia (NX) *P=0.040 to mock and P=0.019 to normoxia (t-test).

To determine whether HIF-1α acts through PKA, a dominant negative catalytically inactive PKA expression plasmid (pdn-PKA) was transiently transfected into GH3 cells and GH promoter activity, mRNA synthesis and secretion were measured following exposure to hypoxia or normoxia for 18 hours (Fig. 4.16). Cells expressing the pdn-PKA plasmid showed a blunted response to the hypoxic induction of *Gh* promoter activity,

mRNA synthesis and secretion which could be observed in the control plasmid transfected cells.

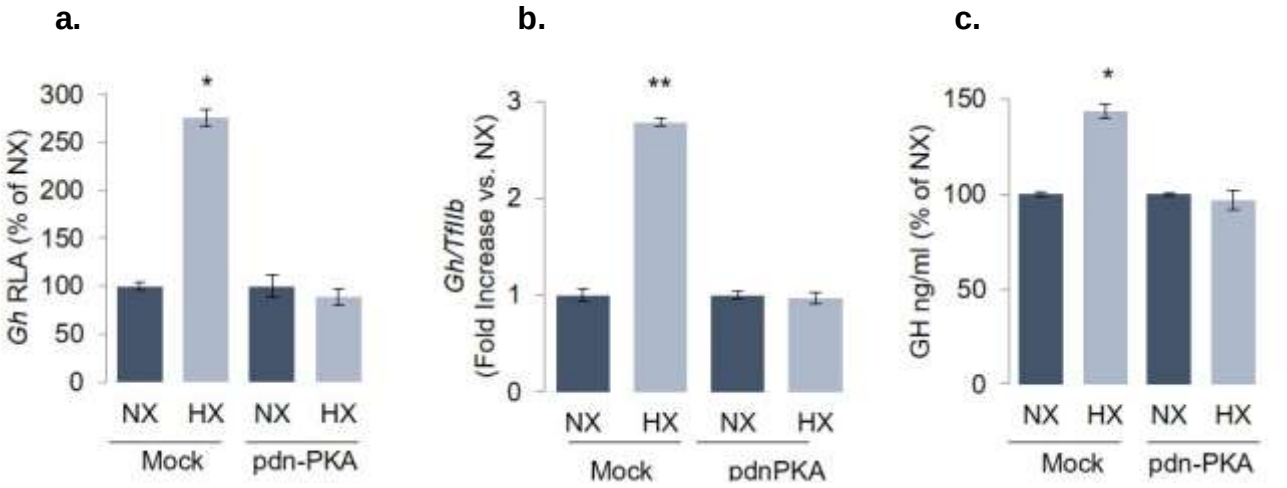

Figure 4.16: Hypoxia requires PKA to stimulate GH synthesis. Overexpression of a dominant negative catalytically inactive PKA (pdn-PKA) abolishes the stimulatory action of hypoxia on **(a)** Gh promoter activity, **(b)** endogenous rat Gh transcription and **(c)** GH secretion. Data are means±SEM from 2 experiments and presented as percentage of fold increase to each normoxia (NX). *P<0.05 to each normoxia (t-test).

4.2.8. HIF-1α and hypoxia do not alter intracellular cAMP concentrations

Given the observed necessity of catalytically active PKA for the stimulatory effects of HIF-1α on GH synthesis, it was next questioned whether the increased PKA activation may be promoted by increases in intracellular cAMP, as cAMP binding to the regulatory PKA subunits initiates its catalytic activation. However, neither HIF-1α inhibition with RNA interference nor hypoxic incubation were found to affect basal or forskolin-induced intracellular cAMP levels (Fig. 4.17). These findings therefore pointed towards the target of HIF-1α's stimulatory action on GH synthesis lying within the PKA holoenzyme itself.

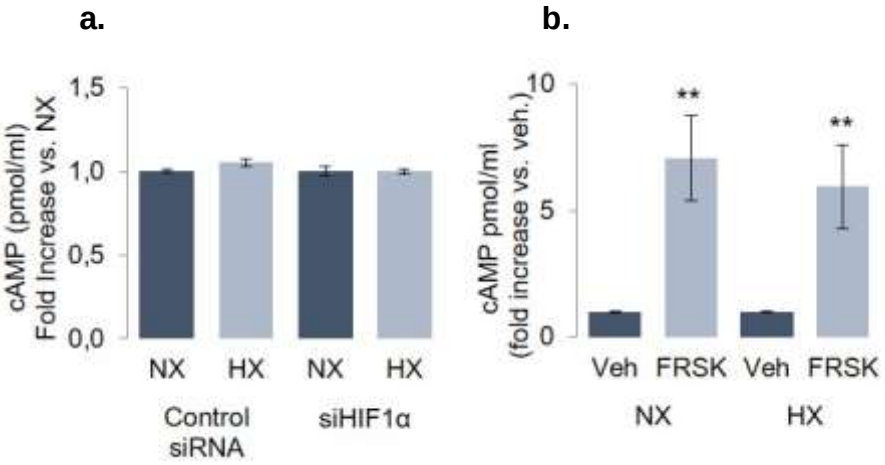

Figure 4.17 Hypoxia has no effect on basal and forskolin-induced cAMP levels. Data are means±SEM of two experiments. Forskolin 5μM was added 15 minutes prior to stopping the experiment **P<0.001 to vehicle (t-test).

4.2.9. Hypoxia and HIF-1α suppress *Prkar2b* transcription

In addition to the PKA catalytic subunit, two distinct subclasses of regulatory dimers have been described (RI and RII) [150], each of which is present in an alpha or beta isoform (RIα/β; RIIα/β) [151, 152]. PKA activity can be dysregulated as a result of altered patterns of regulatory subunit expression [153, 154].It was therefore speculated that in its function as a transcription factor, HIF-1α may affect the transcription of the regulatory or catalytic PKA subunits which could cause elevated catalytic activation.

To examine the effects of HIF-1α on the components of the PKA holoenzyme, GH3 cells were either transiently transfected to overexpress HIF-1α or incubated under hypoxic conditions for 18 hours and the transcript levels of all regulatory and catalytic subunits were analyzed by qPCR. This analysis showed that hypoxia significantly suppressed the expression of the gene encoding for RIIβ (*Prkar2b*) while genes encoding for the rest of the regulatory subunits (*Pkar1a*, *Prkar1b*, *Prkar2a*) and the catalytic subunit (*Prkaca*) were not significantly affected (Fig. 4.18).

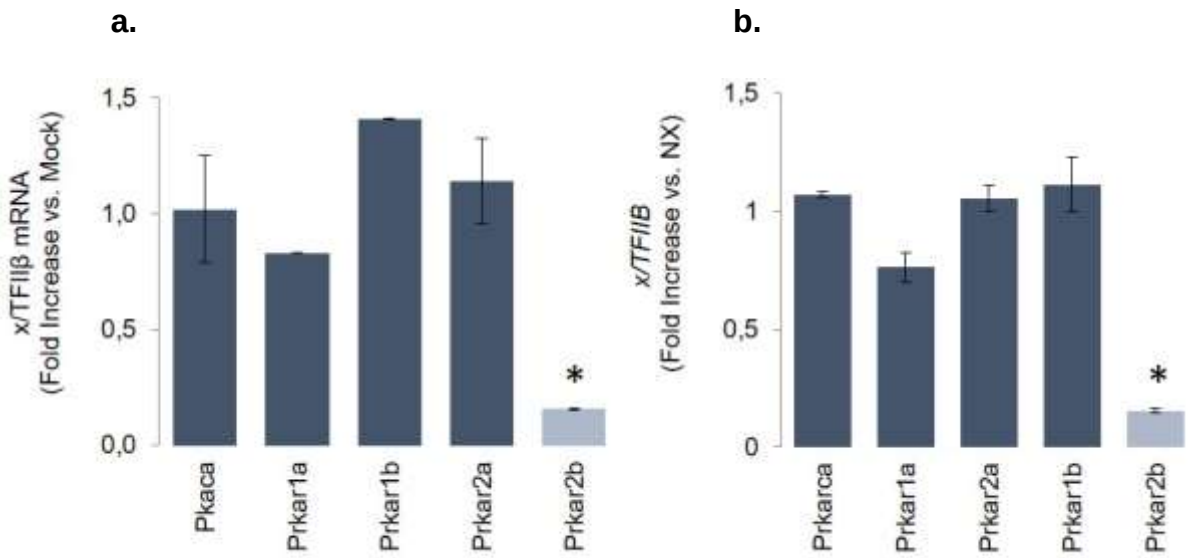

Figure 4.18: Hypoxia and HIF-1α downregulates the transcription of gene encoding for the PKA regulatory subunit RIIB. Expression of the genes encoding for PKA regulatory and catalytic subunits in GH3 cells grown under **(a)** HIF-1α overexpressing or **(b)** hypoxic conditions (1% O_2 for 18 hours) as determined by real time RT-PCR. Data are <*gene*>/*TfIIb*, means±SEM from 2 experiments and presented as fold change to each mock or normoxia, respectively. ***P*<0.01 to each Mock or normoxia (NX), respectively. (*t*-test).

The nature of the relationship between *Prkar2b* and HIF-1α expression was confirmed under varying conditions including hypoxia, HIF-1α silencing, and overexpression of

both wild-type and HIF^{R30A} (Fig. 4.19). Overall, conditions in which HIF-1α was present, including the HIF^{R30A} mutant, *Prkar2b* transcripts were found to be suppressed. Targeting HIF-1α with RNA interference, however, restored the level of *Prkar2b* mRNA to near baseline levels compared to control siRNA transfected cells. Therefore, all approaches confirmed the suppressive effects of HIF-1α on the transcription of the RIIB subunit.

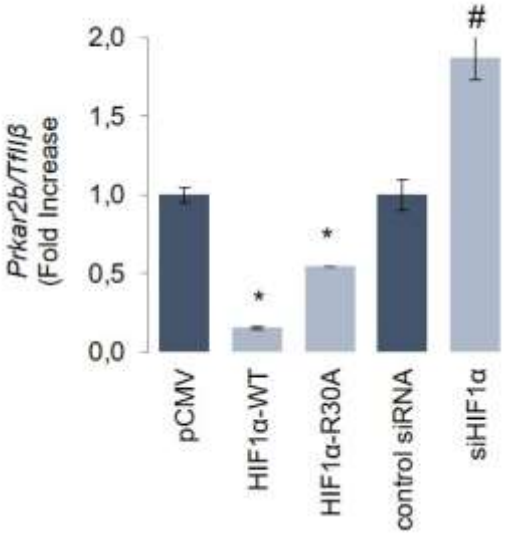

Figure 4.19: Effect of HIF-1α overexpression or knockdown with siRNA on *Prkar2b* transcription. *Prkar2b* transcripts measured using real-time PCR**.** *P<0.05 to pCMV empty vector; # P<0.05 to scrambled siRNA control (t-test).

4.2.10. GH-secreting tumors from patients with acromegaly show decreased *PRKAR2B* expression

GH-secreting pituitary tumors from patients with acromegaly (n=10) were used to confirm whether the suppression of *PRKAR2B* is also a relevant finding in human tumors. Transcript levels of all regulatory and catalytic subunits were measured in tumor samples as well as in a collective of normal pituitary glands (n=6). This analysis showed a significant decrease in *PRKAR2B* expression among GH-secreting tumors compared to normal pituitary glands (*P*=0.006; Fig. 4.20a), whereas no significant changes were observed in the expression of the genes encoding for all the other subunits. In addition, a significant negative correlation was observed between HIF-1α protein and *PRKAR2B* mRNA levels in the GH-secreting pituitary tumors (Kendall's Tau = -0,533, *P*=0.009) (Fig. 4.20b). Taken together, these findings point towards the relevance of *PRKAR2B* downregulation in human GH-secreting pituitary tumors.

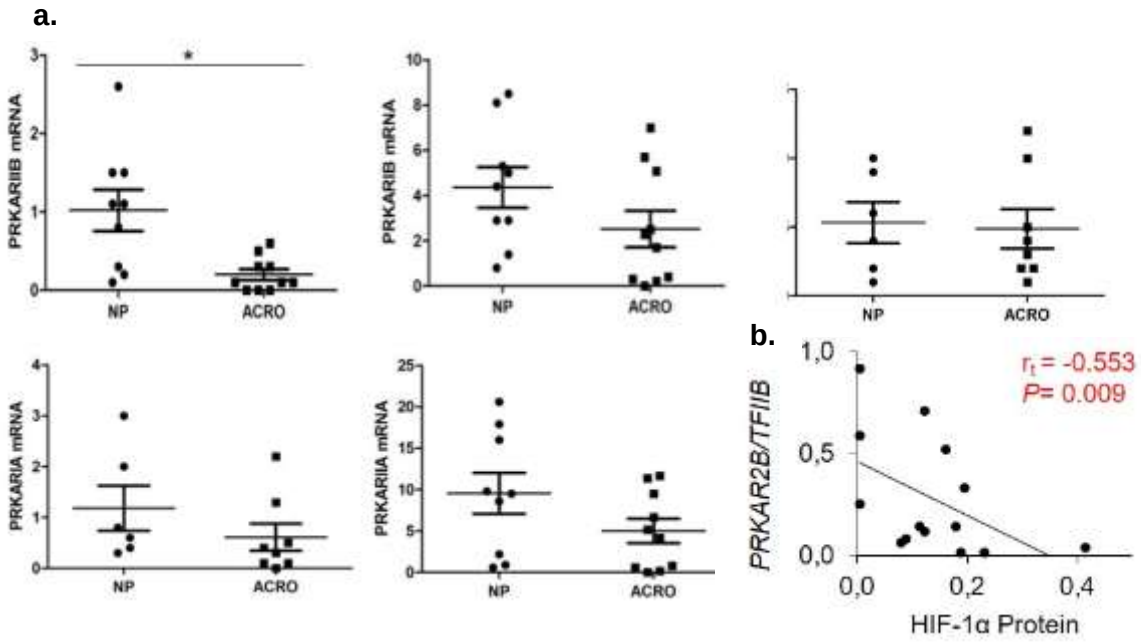

Figure 4.20: *PRKAR2B* expression is suppressed in human acromegalic tumors. **(a)** Expression levels of the PKA regulatory and catalytic subunits in normal pituitaries (NP) and acromegalic tumors (ACRO) as determined by real time RT-PCR. Data are <gene>/TFIIB *P*<0.05 (Mann-Whitney U-Test) **(b)** linear regression analysis of *PRKAR2B* transcript and HIF-1α protein levels in 14 acromegalic tumors. *PRKAR2B* was determined by real time RT-PCR and values are *PRKAR2B*/TFIIB arbitrary units. HIF-1α protein was quantified from immunoblots (Chemidoc, BioRad). Kendall's Tau= -0,553, P=0.009; Spearman's rho=-0.663, P=0.007

4.2.11. Expression of PRKARIIβ in GH3 cells rescues the effect of hypoxia on GH synthesis

It was next questioned whether the transcriptional suppression of the *Prkar2b* subunit mediated by HIF-1α was indeed sufficient to increase PKA activity and subsequently GH synthesis. To this end, GH3 cells were transiently transfected with a PRKARIIβ expression plasmid and incubated under hypoxic conditions for 18 hours, after which PKA activity was measured (Fig. 4.21). It was observed that the selective overexpression of PRKARIIβ indeed abrogated the stimulatory effects of hypoxic incubation on PKA activity observed in control transfected cells.

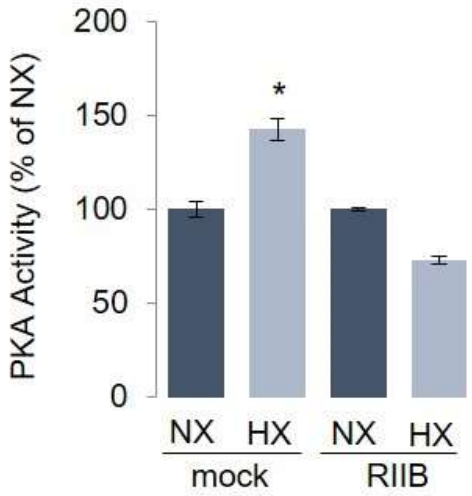

Figure 4.21: PRKARIIβ expression blunts increased PKA activation under hypoxia. Hypoxia ((1% O_2 for 18 hours) has no effect on PKA activity in GH3 cells overexpressing the regulatory subunit RIIB. Data are means±SEM from 3 experiments and are presented as fold of each normoxia (NX). * P<0.05 to each normoxia (NX) (t-test).

In a further step, the effects of PRKARIIβ overexpression on GH synthesis in GH3 cells exposed to hypoxia were examined (Fig. 4.22). In contrast to control transfected cells, those expressing PRKARIIβ showed no response to hypoxic incubation at the level of rat *Gh* promoter activity, mRNA synthesis or secretion. These findings pointed towards the apparent importance of the PRKARIIβ subunit in regulating PKA catalytic activity which ultimately promotes GH synthesis in GH-secreting pituitary tumor cells.

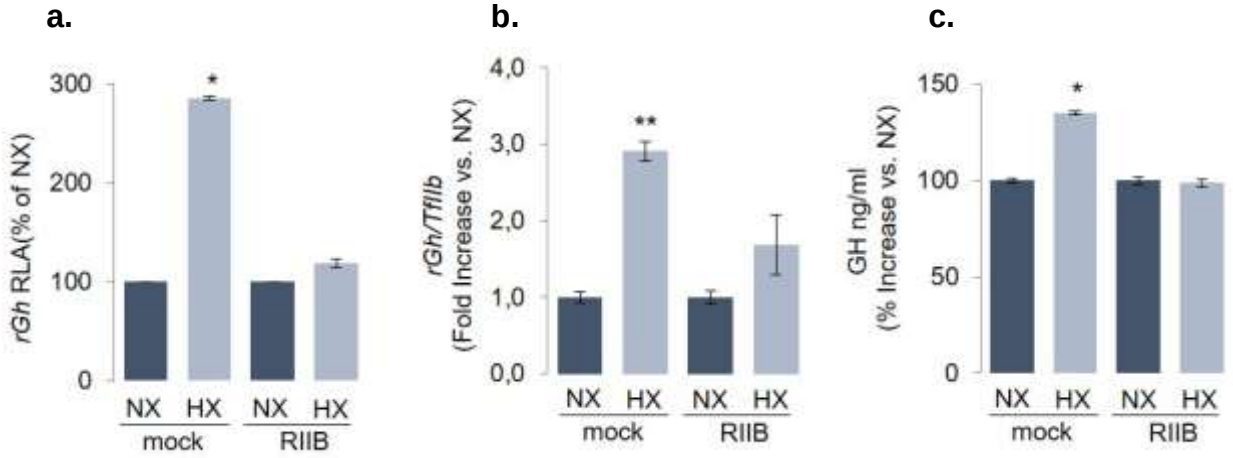

Figure 4.22: PRKARIIβ expression blunts the stimulatory effects of hypoxia on GH synthesis. Hypoxia (1% O_2 for 18 hours) has no effect on **(a)** rat *Gh* promoter activity, **(b)** endogenous rat *Gh* transcription, and **(c)** GH secretion in GH3 cells overexpressing the regulatory subunit PRKARIIβ. Rat *Gh* promoter activity is luciferase to β-galactosidase ratio and shown as RLA (relative luciferase units). *Gh* gene transcription was quantified by real time PCT and shown as *Gh/TfIIb*. Data are means±SEM from 3 experiments and are presented as fold or percentage of each normoxia (NX). * *P*<0.05 to each normoxia (NX) (*t*-test).

4.2.12. HIF-1α inhibits transcription via sequestration of Sp1 on the Prkar2b promoter

Having identified a putative target of hypoxia and HIF-1α within the PKA-CREB signaling cascade, it was next asked through which mechanism of action HIF-1α may suppress *Prkar2b* transcription.

The promoter of the *Prkar2b* gene contains GC-rich promoter sequences known to be bound by the transcription factor SP1 which positively regulates its transcription [155, 156]. As previous studies have shown that HIF-1α can physically interact with Sp1, it was hypothesized that HIF-1α may interact with and sequester Sp1 from the *Prkar2b* promoter, thereby resulting in transcriptional repression.

Chromatin immunoprecipitation was therefore performed in GH3 cells exposed to hypoxia or normoxia for 18 hours. It was observed that hypoxia indeed resulted in decreased Sp1 enrichment to the *Prkar2b* promoter compared to normoxic controls (Fig. 4.23a). In the same experiment, the possibility of HIF-1α binding to the *Prkar2b* was also examined, however no enrichment could be detected indicating that HIF-1α does not exert its repressive effects through direct promoter binding. Subsequent co-immunoprecipitation the Sp1- HIF-1α complex in hypoxic cells confirmed the physical interaction between Sp1 and HIF-1α in GH-secreting pituitary tumor cells. The HIF1a^{R30A} mutant also showed binding to Sp1 confirming that the action of HIF-1α occurs independently of DNA binding. (Fig. 4.23b).

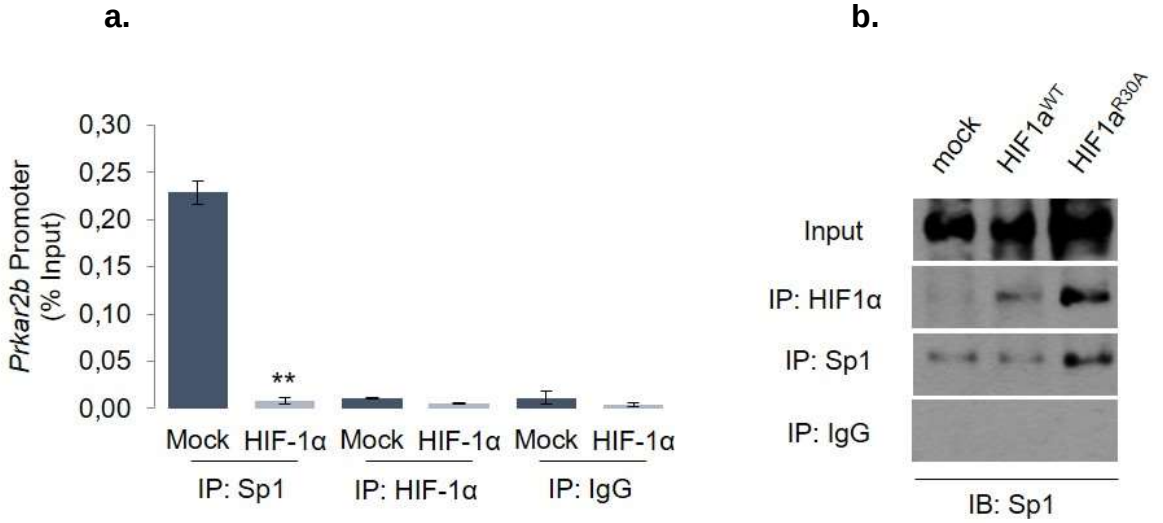

Figure 4.23: HIF-1α sequesters Sp1 from the *Prkar2b* promoter. (**a**) Chromatin immunoprecipitation showing decreased Sp1 binding on the *Prkar2b* promoter in GH3 cells overexpressing HIF-1α. No DNA binding was quantified with HIF-1α. Rabbit IgG was used as control. **(b)** Co-immunoprecipitation experiment showing that both HIF-1α and HIF-1α^{R30A} physically associate with Sp1. HIF-1α and Sp1 immunoprecipitates were blotted for Sp1. Proteins immunoprecipitated with rabbit IgG were used as controls.

Finally, to rule out the possibility that HIF-1α was affecting the absolute levels of Sp1, mRNA and protein levels of Sp1 were measured in GH3 cells subjected to hypoxia, HIF-1α silencing and transient overexpression of HIF-1α (Fig. 4.24). None of these conditions led to a change in Sp1 mRNA or protein expression in GH3 cells, effectively ruling out changes in Sp1 expression level as the cause of its decreased binding to *Prkar2b* promoter.

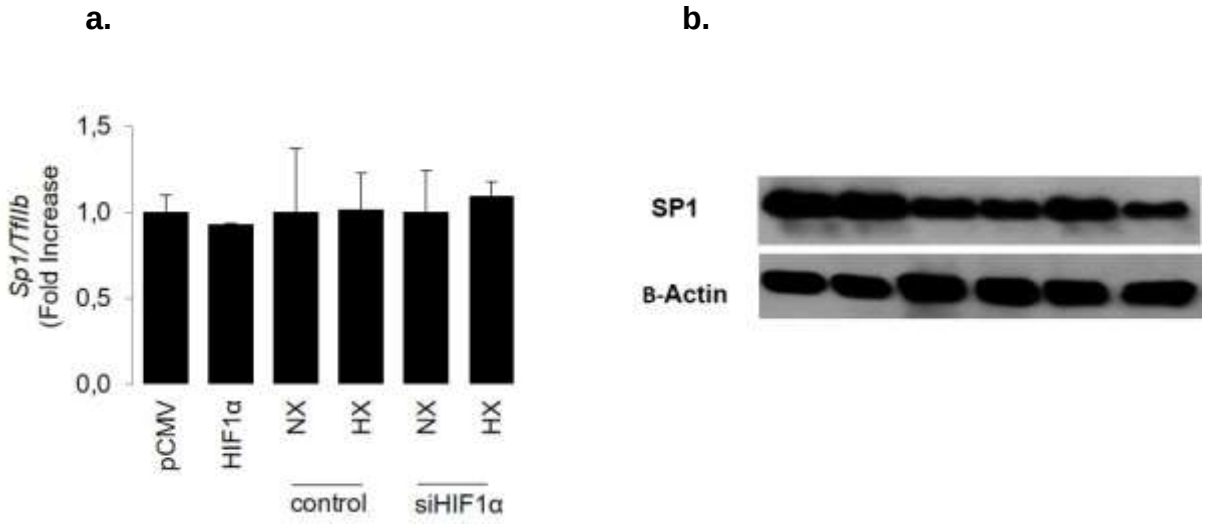

Figure 4.24: Neither HIF-1α nor hypoxia affects Sp1 expression. (a) Sp1 mRNA and **(b)** protein levels as determined by real time PCR and western blot. Real-Time data are means±SEM from 3 experiments and the western blot is representative of 2 experiments.

4.2.13. HIF-1α is associated with resistance to somatostatin analogue treatment in acromegalic patients

The clinical management of patients diagnosed with acromegaly consists mainly of surgical tumor excision and/or pharmacological therapy with somatostatin analogs (SSA). Under SSA therapy up to approximately 30% of patients do not achieve biochemical control of GH or IGF-1 production [41]. It was therefore examined whether HIF-1α and the hypoxic tumor microenvironment may contribute to the development of SSA resistance in patients with GH-secreting pituitary tumors.

To this end, primary cell cultures of GH-secreting pituitary tumors from SSA-naïve patients were treated with 10^{-9}M of the SSA octreotide under normoxic or hypoxic conditions, and GH secretion was measured. Each tumor was divided and half was cultured under normoxic and half under hypoxic conditions (1% O_2) for 24 hours. Three out of 4 responded to octreotide treatment by significantly decreasing GH secretion when cultured under normoxic conditions, whereas hypoxic cultures of the same tumors

showed no response to treatment (Fig. 4.6). As HIF-1α is stabilized under hypoxic conditions, these results pointed towards the possible role of HIF-1α in SSA resistance.

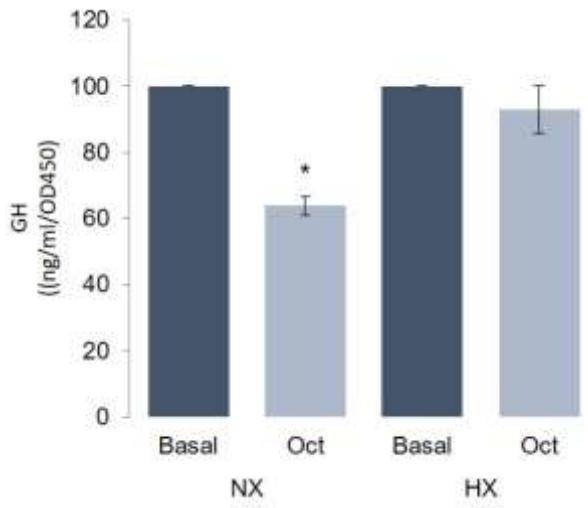

Figure 4.6: The response of GH-secreting tumors to octreotide is blunted by hypoxia. Primary cultures of GH-secreting tumors (n=4) treated with vehicle (basal) or 10^{-9}M octreotide and exposed to hypoxia for 24 hours. hGH was measured by RIA. **P*<0.05. (Mann-Whitney U-Test).

To further pursue the possible role of HIF-1α in SSA resistance, a cohort of 20 patients that received adjuvant (post-surgical) SSA therapy was examined for HIF-1α immunoreactivity and correlated to clinical data regarding GH and IGF-1 normalization after treatment. Statistical analysis of cohort data revealed a significant negative correlation between IGF-1 normalization and HIF-1α immunoreactivity (r=-0.466, *P*=0.029) (Table 2). No correlation was seen between HIF-1α immunoreactivity and GH normalization or patient gender. Taken together, both *in vitro* data from primary tumor material as well as retrospective analysis of SSA response rates corroborate a potential role for HIF-1α in the pathophysiology of GH-secreting tumors.

HIF-1a Immunoreactivity	**Weak (≤40%positive nuclei)**	**Strong (≥41%positive nuclei)**		***P*-Value**	**Spearman r**
Gender			**Total**		
Male (P=0.979)	7	6	**15**	*0.979*	-0,55
Female	8	7	**13**		
Total	**15**	**13**			
GH Normalization (P=0.214)			**Total**		-0.239
Yes (≤2.0)	1	1	**2**	*0.542*	
No	10	4	**14**		
Total	**11**	**5**			
IGF Normalization (P=0.29)			**Total**	*0,042*	-0.466
Yes	13	6	**19**		
No	2	7	**9**		
Total	**15**	**13**			

Table 2. HIF-1α immunoreactivity is associated with SSA response. HIF-1α immunoreactivity was classified as weak (less than 40% positive nuclei) and strong (over 40% positive nuclei). GH normalization following SSA treatment was classified as an OGTT nadir value of ≤2.0 µg/L. IGF-1 levels were evaluated as high or low based on age and gender-normalized values. No significant difference was found between high and low HIF-1α immunoreactivity groups in regards to gender or GH normalization. However, rates of IGF-1 normalization were significantly higher in the low HIF-1α immunoreactivity group. *P≤0.05, Spearmans r was used to determine the strength of correlation between analyzed groups.

5. Discussion

Patients with acromegaly suffer from the endocrine, cardiovascular and psychiatric sequalae of excessive growth hormone secretion caused by GH-secreting pituitary tumors. GH synthesis is tied to the activity of the cAMP-PKA signaling cascade. To date, overactivation of this cascade has been linked to recurrent somatic mutations in only 40% of patients. The elucidation of non-genomic mechanisms of cAMP-PKA activation in acromegaly may therefore uncover novel therapeutic targets. As GH-secreting tumors have been found to display decreased microvessel density compared to the normal pituitary, the role of hypoxia as a non-genomic effector of GH-secreting pituitary tumor pathophysiology was investigated.

The present study reveals the presence of high protein levels of the transcription factor HIF-1α in GH-secreting pituitary tumors from patients with acromegaly. Accordingly, hypoxic incubation of primary cultures of GH-secreting pituitary tumors showed an increase in HIF-1α target gene expression and maintenance of cell viability. Interestingly, hypoxia also promoted the synthesis of GH, prompting further investigation into the nature of the hypoxia-HIF-1α-GH interaction.

Using hypoxic incubation and HIF-1α overexpression the PKA-CREB signaling cascade was systematically analyzed to identify the point of interaction between the hypoxic microenvironment, revealing a link between HIF-1α and the regulatory subunit RIIB (*PRKAR2B*) of the PKA holoenzyme. The stimulatory effects of hypoxia on GH synthesis could be explained by the HIF-1α-mediated sequestration of the transcription factor Sp1 from the promoter of the *Prkar2b* gene, as reintroduction of this subunit abrogated the effects of hypoxia on GH promoter activity, transcription and secretion.

As up to half of patients with acromegaly do not respond to pharmacological treatment with somatostatin analogs, the role of HIF-1α expression in SSA resistance was investigated. It was observed that in primary cultures of GH-secreting pituitary tumors, hypoxic incubation could blunt the response to octreotide on GH secretion. Further analysis revealed that high HIF-1α expression is associated with lower rates of IGF-1 normalization in patients following treatment with somatostatin analogs.

5.1. The GH-secreting pituitary tumor cell response to hypoxia

The microvessel architecture of the normal pituitary plays a central role in the physiological regulation of endocrine homeostasis [66]. Somatotroph tumors display a lower microvessel density and high HIF-1α expression compared to the normal pituitary indicating the presence of intratumoral hypoxia [157]. While hypoxia has long been considered a contributing factor to sustained survival of tumor cells [158], little is known about the role of tissue hypoxia in the pathogenesis of pituitary tumors.

While commonly characterized as a regulator of the formation of new blood vessels (neoangiogenesis) in response to tissue hypoxia [159], HIF-1α has since been implicated in a variety of further processes which ultimately support the cellular adaptation to the hypoxic tumor microenvironment [160]. The rising importance of the non-angiogenic role of HIF-1α is underscored by findings from several tumor entities such as lung, mammary, renal cell and colon carcinomas in which HIF-1α expression is associated with worse clinical outcomes [74, 161-163] although these tumors display lower vascular densities than their non-tumorous tissue counterparts [164]. As such, HIF-1α target genes (*LDHA*, *GLUT1*, *PDK1*) were upregulated in hypoxic versus normoxic GH-secreting pituitary tumor cells indicative of a “metabolic switch” from mitochondrial oxidative phosphorylation towards glycolysis.

The apparent discrepancy between low microvessel density and high HIF-1α therefore poses the question of how the decreased vascularization may provide an advantage to the developing GH-secreting tumor. As the physiological inhibition of GH synthesis and proliferation is coordinated by hypothalamic somatostatin release delivered through the hypothalamic-hypophyseal portal vessel system and IGF-1 from peripheral organs, it can be hypothesized that the absence of angiogenesis provides the tumorous somatotroph cells with a potential escape mechanism. Evidence for this hypothesis has been provided by studies employing cellular *in vivo* imaging on pituitary somatotrophs which could demonstrate the critical importance of intact microvasculature in coordinating the GH secretory response transmitted by hypothalamic signals [67, 68]. Furthermore, the decrease in GH feedback regulation has been associated with the development of hypersecretory somatotrophs [165]. The reduction of microvascular density in somatotroph tumors may therefore provide a mechanism of escape, thereby conferring a survival advantage for transformed somatotroph tumor cells.

Taken together, it can be hypothesized that the somatotroph cell may respond to hypoxia in a manner derived from its physiological regulation. The observed stimulatory

effects of hypoxia on GH synthesis through PKA may therefore also be considered part of a “somatotroph-specific” response to hypoxia.

5.2. PKA in GH-secreting pituitary tumor pathophysiology

While PKA is ubiquitously present in mammalian cells, the expression and tissue-specific balance of RI and RII enzyme isoforms has been shown to be essential in shaping the specificity and degree of PKA activity [166, 167]. Given the diversity tissue-specific cellular processes which are coordinated by PKA [168], it can be expected that the consequences of altering its composition will be equally as diverse [169]. Accordingly, in neoplasms displaying pathologically altered activity of PKA, disturbances of the tissue-specific physiological balance of regulatory and catalytic subunits have been identified [153, 170-173].

In the pituitary, the regulatory RIα subunit has been of particular interest as mutations mapping to its locus at 17q22-24 are commonly found in patients with Carney complex, a multiple neoplasia syndrome associated with abnormal GH and prolactin secretion [172]. While a previous study has shown significantly decreased RIα subunit immunoreactivity in all hormone-secreting and non-secreting subtypes of pituitary tumors despite high mRNA expression, several subsequent mouse models of *Prkar1a* deficiency have since not been able to demonstrate clear pituitary abnormalities [174, 175]. Studies in pituitary specific *Prkar1a*$^{-/-}$ mice have shown increased serum GH levels, however these mice show no pituitary lesions or tumors indicating that the pituitary loss of *Prkar1a* is not directly involved in tumorigenesis [176]. Furthermore, a large-scale genetic screening of patients with sporadic acromegaly found no loss of *PRKAR1A* gene expression indicating that *PRKAR1A* mutations are not involved in GH hypersecretion outside of the Carney complex [46, 47, 177].

5.3. PKA- HIF-1α interactions in disease

As a major regulatory protein kinase, PKA coordinates diverse cellular processes [168, 169] As such, a considerable amount of work has been performed on exploring the effects of PKA on HIF-1α as a central regulator of the hypoxic response in tumor cells [178]. Before PKA itself was implicated as a possible effector of HIF-1α stability and activity, its activators were found to modulate HIF-1α target genes such as VEGF-A in lung cancer models [179]. PKA was then found to directly phosphorylate HIF-1α in endothelial cells under intermittent hypoxia [180]. The recent discovery of two putative PKA phosphorylation sites on HIF-1α Thr^{63} and Ser^{692} were shown to promote its

stabilization independently of prolyl hydroxylation in rat cardiomyocytes [181]. Within the context of PKA-HIF-1α, much of the focus has been placed on models of congestive heart failure, as PKA plays an important role for signal transduction through β-adrenergic receptors in cardiomyocytes. Most recently, inhibition of β-adrenergic receptors was found to reduce the hypoxia-induced stabilization of HIF-1α in primary human endothelial cells [182].

Although less extensive, there has been evidence that hypoxia and HIF-1α may affect PKA activity. First, in a model of melanoma it was demonstrated that the PKA scaffold protein AKAP12v2 is a direct transcriptional target of HIF-1α, and its hypoxic induction effectively enhances the migratory capacity of melanoma cells [183]. At the organelle level, hypoxia can promote the ubiquitination and degradation of the mitochondrial AKAP121, therefore attenuating PKA-CREB signal transduction to the outer mitochondrial membrane during brain ischemia [184]. Finally, in A549 lung cancer cells it was shown that long-term (two days) hypoxic incubation can increase the relative expression of *PRKACA,* indicating that this may occur independently of HIF-1α transcriptional regulation [185].

In GH-secreting pituitary tumor cells, neither hypoxia nor HIF-1α overexpression affected *Prkarca* expression, but dramatically repressed the transcription of *Prkar2B*. Furthermore, this repression was essential for the stimulatory action of hypoxia and HIF-1α on the downstream PKA readouts CREB and GH synthesis. The stimulatory effect of HIF-1α on PKA activity in GH-secreting pituitary tumors cells was found to occur specifically through suppression of RIIβ.

In contrast to many other protein kinases which are regulated by the turnover of an activation loop phosphate, PKA is regulated by the composition of its holoenzyme structure, which determines its activation potential by cAMP [186]. As such, PKA activity can be dysregulated as a result of altered patterns of regulatory subunit expression [153, 154].

As no significant alterations in intracellular cAMP levels under hypoxia were observed, it can be hypothesized that the suppression of *Prkar2b* expression is the sole trigger of overactive PKA under hypoxic conditions.

No significant correlation was found between HIF-1α expression and the gsp status in patients with acromegaly, but this may be due to the relatively low number of cases (n=21) included in the study. Interestingly, it was observed that $G_{s\alpha}$ transcript levels positively correlated with HIF-1α protein expression. Further investigation into the

possibility of HIF-1α-mediated $G_{s\alpha}$ expression may provide insight into the sequence of events promoting both HIF-1α and PKA activation.

The possibility of a feed-forward loop between HIF-1α and PKA tumors may be of significant interest in regards to examining non-genomic mechanisms of PKA activation in acromegaly, but also other disease entities.

5.4. HRE-independent transcriptional regulation by HIF-1α

We found that HIF-1α downregulates *Prkar2b* transcription but we did not detect any direct binding to its promoter. While HIF-1α can directly activate the transcription of a multitude of target genes via its constitutive DNA binding domain (CGTC), its role in transcriptional repression remains less well-characterized. Genome-wide association studies of HIF-1α DNA binding and transcription profiling have shown that HIF-1α dependent gene suppression most commonly occurs through indirect mechanisms such as that HIF-1α directly activates the transcription of gene products which themselves act to suppress the transcription of the further genes [122, 123]. A less well characterized mechanism is through the ability of HIF-1α to physically interact with and sequester transcription factors from their target promoter sequence. In this context HIF-1α was shown compete with Sp1 for c-Myc, resulting in the transcriptional repression of the Myc target gene MutSα [124]. The *PRKAR2B* promoter has GC-rich regions with Sp1 binding sites [155, 156]. HIF-1α physically interacts with and therefore decreases Sp1 binding from the *PRKAR2B* promoter therefore supporting the concept of HIF-1α-mediated transcriptional repression beyond the HRE-dependent regulation of gene expression. This effect of HIF-1α occurs solely by sequestering Sp1 and does not affect total Sp1 levels. These results may implicate a general mechanism through which HIF-1α could suppress the transcription of genes with GC-rich promoters.

5.5. Conclusion

The present study shows that hypoxia, an environmental stressor, can alter the activity of an important regulatory kinase. In GH-secreting pituitary tumors, HIF-1α therefore links the tumor microenvironment to the secretory behavior and the response of hypoxic tumor cells to pharmacological treatment. Evidence arising from cardiovascular models pointing towards the ability of PKA to stabilize and activate HIF-1α raises the question of a feed-forward loop between HIF-1α and PKA. Further investigations into the nature of HIF-1α -PKA interactions may therefore be of significant interest in developing targeted pharmacological therapy for patients suffering from acromegaly.

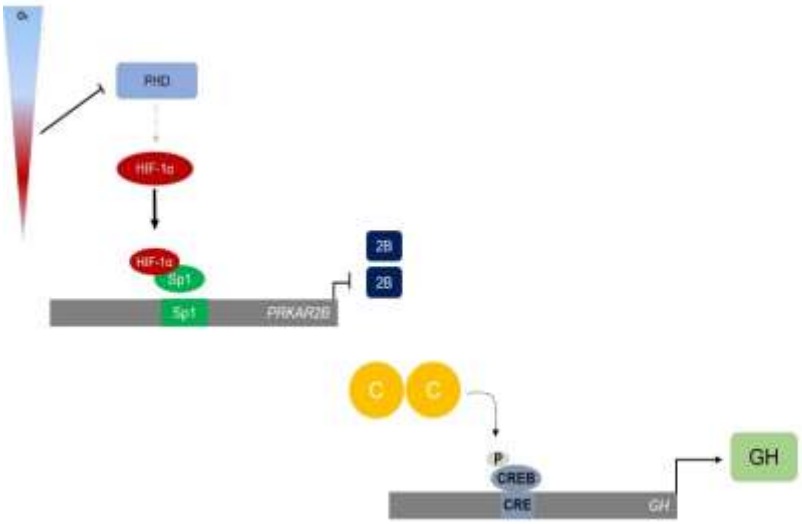

Figure 5.1. Proposed mechanism of HIF-1α's action on GH synthesis. HIF-1α is stabilized under conditions of intratumoral hypoxia. HIF-1α translocates to the nucleus and sequesters Sp1 from the promoter of PRKAR2B. When PRKAR2B transcription is decreased, the catalytic subunits of PKA are free to phosphorylate CREB which initiates transcription of growth hormone.

6. REFERENCES

1. Allaerts, W., P. Carmeliet, and C. Denef, *New perspectives in the function of pituitary folliculo-stellate cells.* Mol Cell Endocrinol, 1990. **71**(2): p. 73-81.
2. Asa, S.L. and S. Ezzat, *Molecular determinants of pituitary cytodifferentiation.* Pituitary, 1999. **1**(3-4): p. 159-68.
3. Scully, K.M. and M.G. Rosenfeld, *Pituitary development: regulatory codes in mammalian organogenesis.* Science, 2002. **295**(5563): p. 2231-5.
4. Cohen, L.E., *Genetic regulation of the embryology of the pituitary gland and somatotrophs.* Endocrine, 2000. **12**(2): p. 99-106.
5. Seeburg, P.H., *The human growth hormone gene family: nucleotide sequences show recent divergence and predict a new polypeptide hormone.* DNA, 1982. **1**(3): p. 239-49.
6. Alatzoglou, K.S. and M.T. Dattani, *Genetic causes and treatment of isolated growth hormone deficiency-an update.* Nat Rev Endocrinol, 2010. **6**(10): p. 562-76.
7. Strobl, J.S. and M.J. Thomas, *Human growth hormone.* Pharmacol Rev, 1994. **46**(1): p. 1-34.
8. Bloch, B., et al., *Immunohistochemical detection of growth hormone-releasing factor in brain.* Nature, 1983. **301**(5901): p. 607-8.
9. Steyn, F.J., et al., *Neuroendocrine Regulation of Growth Hormone Secretion.* Compr Physiol, 2016. **6**(2): p. 687-735.
10. Cataldi, M., et al., *Relationship between hypophyseal portal GHRH and somatostatin and peripheral GH levels in the conscious sheep.* J Endocrinol Invest, 1994. **17**(9): p. 717-22.
11. Giustina, A. and J.D. Veldhuis, *Pathophysiology of the neuroregulation of growth hormone secretion in experimental animals and the human.* Endocr Rev, 1998. **19**(6): p. 717-97.
12. Soya, H. and M. Suzuki, *A possible role of hypothalamic somatostatin in the maintenance of rat pituitary responsiveness to growth hormone-releasing factor.* Endocrinology, 1990. **126**(1): p. 285-91.
13. Goldsmith, P.C., et al., *Ultrastructural localization of somatostatin in pancreatic islets of the rat.* Endocrinology, 1975. **97**(4): p. 1061-4.
14. Patel, Y.C., et al., *Multiple gene transcripts of the somatostatin receptor SSTR2: tissue selective distribution and cAMP regulation.* Biochem Biophys Res Commun, 1993. **192**(1): p. 288-94.
15. Theodoropoulou, M. and G.K. Stalla, *Somatostatin receptors: from signaling to clinical practice.* Front Neuroendocrinol, 2013. **34**(3): p. 228-52.
16. Daughaday, W.H. and P. Rotwein, *Insulin-like growth factors I and II. Peptide, messenger ribonucleic acid and gene structures, serum, and tissue concentrations.* Endocr Rev, 1989. **10**(1): p. 68-91.
17. Junnila, R.K., et al., *The GH/IGF-1 axis in ageing and longevity.* Nat Rev Endocrinol, 2013. **9**(6): p. 366-76.
18. Romero, C.J., et al., *Insulin-like growth factor 1 mediates negative feedback to somatotroph GH expression via POU1F1/CREB binding protein interactions.* Mol Cell Biol, 2012. **32**(21): p. 4258-69.
19. Berelowitz, M., et al., *Somatomedin-C mediates growth hormone negative feedback by effects on both the hypothalamus and the pituitary.* Science, 1981. **212**(4500): p. 1279-81.
20. Jones, J.I. and D.R. Clemmons, *Insulin-like growth factors and their binding proteins: biological actions.* Endocr Rev, 1995. **16**(1): p. 3-34.
21. Bermann, M., et al., *Negative feedback regulation of pulsatile growth hormone secretion by insulin-like growth factor I. Involvement of hypothalamic somatostatin.* J Clin Invest, 1994. **94**(1): p. 138-45.

22. Skiba, N.P. and H.E. Hamm, *How Gsalpha activates adenylyl cyclase.* Nat Struct Biol, 1998. **5**(2): p. 88-92.
23. Mellon, P.L., et al., *Regulation of transcription by cyclic AMP-dependent protein kinase.* Proc Natl Acad Sci U S A, 1989. **86**(13): p. 4887-91.
24. Adams, J.A. and S.S. Taylor, *Energetic limits of phosphotransfer in the catalytic subunit of cAMP-dependent protein kinase as measured by viscosity experiments.* Biochemistry, 1992. **31**(36): p. 8516-22.
25. Kim, C., et al., *PKA-I holoenzyme structure reveals a mechanism for cAMP-dependent activation.* Cell, 2007. **130**(6): p. 1032-43.
26. Kapiloff, M.S., M. Rigatti, and K.L. Dodge-Kafka, *Architectural and functional roles of A kinase-anchoring proteins in cAMP microdomains.* J Gen Physiol, 2014. **143**(1): p. 9-15.
27. Gonzalez, G.A. and M.R. Montminy, *Cyclic AMP stimulates somatostatin gene transcription by phosphorylation of CREB at serine 133.* Cell, 1989. **59**(4): p. 675-80.
28. Bodner, M., et al., *The pituitary-specific transcription factor GHF-1 is a homeobox-containing protein.* Cell, 1988. **55**(3): p. 505-18.
29. Ingraham, H.A., et al., *A tissue-specific transcription factor containing a homeodomain specifies a pituitary phenotype.* Cell, 1988. **55**(3): p. 519-29.
30. McCormick, A., et al., *Regulation of the pituitary-specific homeobox gene GHF1 by cell-autonomous and environmental cues.* Nature, 1990. **345**(6278): p. 829-32.
31. Gaiddon, C., et al., *Constitutively active G(S) alpha-subunits stimulate Pit-1 promoter activity via a protein kinase A-mediated pathway acting through deoxyribonucleic acid binding sites both for Pit-1 and for adenosine 3',5'-monophosphate response element-binding protein.* Endocrinology, 1996. **137**(4): p. 1286-91.
32. Cohen, L.E., et al., *CREB-independent regulation by CBP is a novel mechanism of human growth hormone gene expression.* J Clin Invest, 1999. **104**(8): p. 1123-30.
33. Nelson, C., et al., *Activation of cell-specific expression of rat growth hormone and prolactin genes by a common transcription factor.* Science, 1988. **239**(4846): p. 1400-5.
34. Tansey, W.P., et al., *Distance-dependent interactions between basal, cyclic AMP, and thyroid hormone response elements in the rat growth hormone promoter.* J Biol Chem, 1993. **268**(20): p. 14906-11.
35. Tsaneva-Atanasova, K., et al., *Mechanism of spontaneous and receptor-controlled electrical activity in pituitary somatotrophs: experiments and theory.* J Neurophysiol, 2007. **98**(1): p. 131-44.
36. Clayton, R.N., *Sporadic pituitary tumours: from epidemiology to use of databases.* Baillieres Best Pract Res Clin Endocrinol Metab, 1999. **13**(3): p. 451-60.
37. Buurman, H. and W. Saeger, *Subclinical adenomas in postmortem pituitaries: classification and correlations to clinical data.* Eur J Endocrinol, 2006. **154**(5): p. 753-8.
38. Parent, A.D., B. Brown, and E.E. Smith, *Incidental pituitary adenomas: a retrospective study.* Surgery, 1982. **92**(5): p. 880-3.
39. Daly, A.F., M.A. Tichomirowa, and A. Beckers, *The epidemiology and genetics of pituitary adenomas.* Best Pract Res Clin Endocrinol Metab, 2009. **23**(5): p. 543-54.
40. Molitch, M.E., *Clinical manifestations of acromegaly.* Endocrinol Metab Clin North Am, 1992. **21**(3): p. 597-614.
41. Giustina, A., et al., *Criteria for cure of acromegaly: a consensus statement.* J Clin Endocrinol Metab, 2000. **85**(2): p. 526-9.
42. Lavrentaki, A., et al., *Epidemiology of acromegaly: review of population studies.* Pituitary, 2017. **20**(1): p. 4-9.
43. Holdaway, I.M., M.J. Bolland, and G.D. Gamble, *A meta-analysis of the effect of lowering serum levels of GH and IGF-I on mortality in acromegaly.* Eur J Endocrinol, 2008. **159**(2): p. 89-95.
44. Brue, T. and F. Castinetti, *The risks of overlooking the diagnosis of secreting pituitary adenomas.* Orphanet J Rare Dis, 2016. **11**(1): p. 135.

45. Wilson, L.S., J.L. Shin, and S. Ezzat, *Longitudinal assessment of economic burden and clinical outcomes in acromegaly.* Endocr Pract, 2001. **7**(3): p. 170-80.
46. Ronchi, C.L., et al., *Landscape of somatic mutations in sporadic GH-secreting pituitary adenomas.* Eur J Endocrinol, 2016. **174**(3): p. 363-72.
47. Valimaki, N., et al., *Whole-Genome Sequencing of Growth Hormone (GH)-Secreting Pituitary Adenomas.* J Clin Endocrinol Metab, 2015. **100**(10): p. 3918-27.
48. Vasilev, V., et al., *Familial pituitary tumor syndromes.* Endocr Pract, 2011. **17 Suppl 3**: p. 41-6.
49. Schernthaner-Reiter, M.H., G. Trivellin, and C.A. Stratakis, *MEN1, MEN4, and Carney Complex: Pathology and Molecular Genetics.* Neuroendocrinology, 2016. **103**(1): p. 18-31.
50. Stratakis, C.A., L.S. Kirschner, and J.A. Carney, *Clinical and molecular features of the Carney complex: diagnostic criteria and recommendations for patient evaluation.* J Clin Endocrinol Metab, 2001. **86**(9): p. 4041-6.
51. Hernandez-Ramirez, L.C., et al., *Landscape of Familial Isolated and Young-Onset Pituitary Adenomas: Prospective Diagnosis in AIP Mutation Carriers.* J Clin Endocrinol Metab, 2015. **100**(9): p. E1242-54.
52. Vierimaa, O., et al., *Pituitary adenoma predisposition caused by germline mutations in the AIP gene.* Science, 2006. **312**(5777): p. 1228-30.
53. Katznelson, L., et al., *Acromegaly: an endocrine society clinical practice guideline.* J Clin Endocrinol Metab, 2014. **99**(11): p. 3933-51.
54. Buchfelder, M. and S. Schlaffer, *Surgical treatment of pituitary tumours.* Best Pract Res Clin Endocrinol Metab, 2009. **23**(5): p. 677-92.
55. Vance, M.L. and A.G. Harris, *Long-term treatment of 189 acromegalic patients with the somatostatin analog octreotide. Results of the International Multicenter Acromegaly Study Group.* Arch Intern Med, 1991. **151**(8): p. 1573-8.
56. Newman, C.B., et al., *Safety and efficacy of long-term octreotide therapy of acromegaly: results of a multicenter trial in 103 patients--a clinical research center study.* J Clin Endocrinol Metab, 1995. **80**(9): p. 2768-75.
57. Ezzat, S., et al., *Octreotide treatment of acromegaly. A randomized, multicenter study.* Ann Intern Med, 1992. **117**(9): p. 711-8.
58. Bruns, C., et al., *SOM230: a novel somatostatin peptidomimetic with broad somatotropin release inhibiting factor (SRIF) receptor binding and a unique antisecretory profile.* Eur J Endocrinol, 2002. **146**(5): p. 707-16.
59. van der Hoek, J., et al., *A single-dose comparison of the acute effects between the new somatostatin analog SOM230 and octreotide in acromegalic patients.* J Clin Endocrinol Metab, 2004. **89**(2): p. 638-45.
60. Silverstein, J.M., *Hyperglycemia induced by pasireotide in patients with Cushing's disease or acromegaly.* Pituitary, 2016. **19**(5): p. 536-43.
61. Giustina, A., et al., *Pegvisomant in acromegaly: an update.* J Endocrinol Invest, 2017.
62. Lamberts, S.W., J.C. Reubi, and E.P. Krenning, *Somatostatin analogs in the treatment of acromegaly.* Endocrinol Metab Clin North Am, 1992. **21**(3): p. 737-52.
63. Freda, P.U., et al., *Long-acting somatostatin analog therapy of acromegaly: a meta-analysis.* J Clin Endocrinol Metab, 2005. **90**(8): p. 4465-73.
64. Bevan, J.S., *Clinical review: The antitumoral effects of somatostatin analog therapy in acromegaly.* J Clin Endocrinol Metab, 2005. **90**(3): p. 1856-63.
65. Melmed, S., et al., *A critical analysis of pituitary tumor shrinkage during primary medical therapy in acromegaly.* J Clin Endocrinol Metab, 2005. **90**(7): p. 4405-10.
66. Daniel, P.M., *The blood supply of the hypothalamus and pituitary gland.* Br Med Bull, 1966. **22**(3): p. 202-8.
67. Lafont, C., et al., *Cellular in vivo imaging reveals coordinated regulation of pituitary microcirculation and GH cell network function.* Proc Natl Acad Sci U S A, 2010. **107**(9): p. 4465-70.

68. Bonnefont, X., et al., *Revealing the large-scale network organization of growth hormone-secreting cells.* Proc Natl Acad Sci U S A, 2005. **102**(46): p. 16880-5.
69. Jugenburg, M., et al., *Vasculature in Nontumorous Hypophyses, Pituitary Adenomas, and Carcinomas: A Quantitative Morphologic Study.* Endocr Pathol, 1995. **6**(2): p. 115-124.
70. Viacava, P., et al., *Microvascular density and vascular endothelial growth factor expression in normal pituitary tissue and pituitary adenomas.* J Endocrinol Invest, 2003. **26**(1): p. 23-8.
71. Turner, H.E., et al., *Angiogenesis in pituitary adenomas and the normal pituitary gland.* J Clin Endocrinol Metab, 2000. **85**(3): p. 1159-62.
72. Erroi, A., et al., *Microvasculature of human micro- and macroprolactinomas. A morphological study.* Neuroendocrinology, 1986. **43**(2): p. 159-65.
73. Schechter, J., *Ultrastructural changes in the capillary bed of human pituitary tumors.* Am J Pathol, 1972. **67**(1): p. 109-26.
74. Wilson, W.R. and M.P. Hay, *Targeting hypoxia in cancer therapy.* Nat Rev Cancer, 2011. **11**(6): p. 393-410.
75. Michiels, C., *Physiological and pathological responses to hypoxia.* Am J Pathol, 2004. **164**(6): p. 1875-82.
76. Buttgereit, F. and M.D. Brand, *A hierarchy of ATP-consuming processes in mammalian cells.* Biochem J, 1995. **312 (Pt 1)**: p. 163-7.
77. Gardner, L.B., et al., *Hypoxia inhibits G1/S transition through regulation of p27 expression.* J Biol Chem, 2001. **276**(11): p. 7919-26.
78. Krtolica, A., N.A. Krucher, and J.W. Ludlow, *Hypoxia-induced pRB hypophosphorylation results from downregulation of CDK and upregulation of PP1 activities.* Oncogene, 1998. **17**(18): p. 2295-304.
79. Thomlinson, R.H. and L.H. Gray, *The histological structure of some human lung cancers and the possible implications for radiotherapy.* Br J Cancer, 1955. **9**(4): p. 539-49.
80. Vaupel, P., M. Hockel, and A. Mayer, *Detection and characterization of tumor hypoxia using pO2 histography.* Antioxid Redox Signal, 2007. **9**(8): p. 1221-35.
81. Jain, R.K., *Normalization of tumor vasculature: an emerging concept in antiangiogenic therapy.* Science, 2005. **307**(5706): p. 58-62.
82. Semenza, G.L., *Hypoxia, clonal selection, and the role of HIF-1 in tumor progression.* Crit Rev Biochem Mol Biol, 2000. **35**(2): p. 71-103.
83. Erler, J.T., et al., *Hypoxia-mediated down-regulation of Bid and Bax in tumors occurs via hypoxia-inducible factor 1-dependent and -independent mechanisms and contributes to drug resistance.* Mol Cell Biol, 2004. **24**(7): p. 2875-89.
84. Graeber, T.G., et al., *Hypoxia-mediated selection of cells with diminished apoptotic potential in solid tumours.* Nature, 1996. **379**(6560): p. 88-91.
85. Rouschop, K.M., et al., *The unfolded protein response protects human tumor cells during hypoxia through regulation of the autophagy genes MAP1LC3B and ATG5.* J Clin Invest, 2010. **120**(1): p. 127-41.
86. Lum, J.J., R.J. DeBerardinis, and C.B. Thompson, *Autophagy in metazoans: cell survival in the land of plenty.* Nat Rev Mol Cell Biol, 2005. **6**(6): p. 439-48.
87. Fischer, K., et al., *Inhibitory effect of tumor cell-derived lactic acid on human T cells.* Blood, 2007. **109**(9): p. 3812-9.
88. Cairns, R.A., I.S. Harris, and T.W. Mak, *Regulation of cancer cell metabolism.* Nat Rev Cancer, 2011. **11**(2): p. 85-95.
89. Kamphorst, J.J., et al., *Hypoxic and Ras-transformed cells support growth by scavenging unsaturated fatty acids from lysophospholipids.* Proc Natl Acad Sci U S A, 2013. **110**(22): p. 8882-7.
90. Cairns, R.A., T. Kalliomaki, and R.P. Hill, *Acute (cyclic) hypoxia enhances spontaneous metastasis of KHT murine tumors.* Cancer Res, 2001. **61**(24): p. 8903-8.
91. Postovit, L.M., et al., *Oxygen-mediated regulation of tumor cell invasiveness. Involvement of a nitric oxide signaling pathway.* J Biol Chem, 2002. **277**(38): p. 35730-7.

92. Rofstad, E.K., et al., *Hypoxia promotes lymph node metastasis in human melanoma xenografts by up-regulating the urokinase-type plasminogen activator receptor.* Cancer Res, 2002. **62**(6): p. 1847-53.
93. Hill, R.P., D.T. Marie-Egyptienne, and D.W. Hedley, *Cancer stem cells, hypoxia and metastasis.* Semin Radiat Oncol, 2009. **19**(2): p. 106-11.
94. Pennacchietti, S., et al., *Hypoxia promotes invasive growth by transcriptional activation of the met protooncogene.* Cancer Cell, 2003. **3**(4): p. 347-61.
95. Yang, M.H., et al., *Direct regulation of TWIST by HIF-1alpha promotes metastasis.* Nat Cell Biol, 2008. **10**(3): p. 295-305.
96. Luo, D., et al., *Mouse snail is a target gene for HIF.* Mol Cancer Res, 2011. **9**(2): p. 234-45.
97. Zhang, W., et al., *HIF-1alpha Promotes Epithelial-Mesenchymal Transition and Metastasis through Direct Regulation of ZEB1 in Colorectal Cancer.* PLoS One, 2015. **10**(6): p. e0129603.
98. Chen, J., et al., *Hypoxia potentiates Notch signaling in breast cancer leading to decreased E-cadherin expression and increased cell migration and invasion.* Br J Cancer, 2010. **102**(2): p. 351-60.
99. Sahlgren, C., et al., *Notch signaling mediates hypoxia-induced tumor cell migration and invasion.* Proc Natl Acad Sci U S A, 2008. **105**(17): p. 6392-7.
100. Copple, B.L., *Hypoxia stimulates hepatocyte epithelial to mesenchymal transition by hypoxia-inducible factor and transforming growth factor-beta-dependent mechanisms.* Liver Int, 2010. **30**(5): p. 669-82.
101. Gray, L.H., et al., *The concentration of oxygen dissolved in tissues at the time of irradiation as a factor in radiotherapy.* Br J Radiol, 1953. **26**(312): p. 638-48.
102. Teicher, B.A., J.S. Lazo, and A.C. Sartorelli, *Classification of antineoplastic agents by their selective toxicities toward oxygenated and hypoxic tumor cells.* Cancer Res, 1981. **41**(1): p. 73-81.
103. Nordsmark, M., et al., *Prognostic value of tumor oxygenation in 397 head and neck tumors after primary radiation therapy. An international multi-center study.* Radiother Oncol, 2005. **77**(1): p. 18-24.
104. Brizel, D.M., et al., *Tumor oxygenation predicts for the likelihood of distant metastases in human soft tissue sarcoma.* Cancer Res, 1996. **56**(5): p. 941-3.
105. Movsas, B., et al., *Hypoxic prostate/muscle pO2 ratio predicts for biochemical failure in patients with prostate cancer: preliminary findings.* Urology, 2002. **60**(4): p. 634-9.
106. Fyles, A., et al., *Tumor hypoxia has independent predictor impact only in patients with node-negative cervix cancer.* J Clin Oncol, 2002. **20**(3): p. 680-7.
107. Bos, R., et al., *Levels of hypoxia-inducible factor-1alpha independently predict prognosis in patients with lymph node negative breast carcinoma.* Cancer, 2003. **97**(6): p. 1573-81.
108. Wang, G.L., et al., *Hypoxia-inducible factor 1 is a basic-helix-loop-helix-PAS heterodimer regulated by cellular O2 tension.* Proc Natl Acad Sci U S A, 1995. **92**(12): p. 5510-4.
109. Wang, G.L. and G.L. Semenza, *Purification and characterization of hypoxia-inducible factor 1.* J Biol Chem, 1995. **270**(3): p. 1230-7.
110. Jiang, B.H., et al., *Dimerization, DNA binding, and transactivation properties of hypoxia-inducible factor 1.* J Biol Chem, 1996. **271**(30): p. 17771-8.
111. Jiang, B.H., et al., *Transactivation and inhibitory domains of hypoxia-inducible factor 1alpha. Modulation of transcriptional activity by oxygen tension.* J Biol Chem, 1997. **272**(31): p. 19253-60.
112. Koivunen, P., et al., *An endoplasmic reticulum transmembrane prolyl 4-hydroxylase is induced by hypoxia and acts on hypoxia-inducible factor alpha.* J Biol Chem, 2007. **282**(42): p. 30544-52.
113. Landazuri, M.O., et al., *Analysis of HIF-prolyl hydroxylases binding to substrates.* Biochem Biophys Res Commun, 2006. **351**(2): p. 313-20.
114. Appelhoff, R.J., et al., *Differential function of the prolyl hydroxylases PHD1, PHD2, and PHD3 in the regulation of hypoxia-inducible factor.* J Biol Chem, 2004. **279**(37): p. 38458-65.

115. Berra, E., et al., *HIF prolyl-hydroxylase 2 is the key oxygen sensor setting low steady-state levels of HIF-1alpha in normoxia.* Embo j, 2003. **22**(16): p. 4082-90.
116. Huang, L.E., et al., *Regulation of hypoxia-inducible factor 1alpha is mediated by an O2-dependent degradation domain via the ubiquitin-proteasome pathway.* Proc Natl Acad Sci U S A, 1998. **95**(14): p. 7987-92.
117. Ohh, M., et al., *Ubiquitination of hypoxia-inducible factor requires direct binding to the beta-domain of the von Hippel-Lindau protein.* Nat Cell Biol, 2000. **2**(7): p. 423-7.
118. Tanimoto, K., et al., *Mechanism of regulation of the hypoxia-inducible factor-1 alpha by the von Hippel-Lindau tumor suppressor protein.* Embo j, 2000. **19**(16): p. 4298-309.
119. Ivan, M., et al., *HIFalpha targeted for VHL-mediated destruction by proline hydroxylation: implications for O2 sensing.* Science, 2001. **292**(5516): p. 464-8.
120. Semenza, G.L., *Targeting HIF-1 for cancer therapy.* Nat Rev Cancer, 2003. **3**(10): p. 721-32.
121. Semenza, G.L., *Defining the role of hypoxia-inducible factor 1 in cancer biology and therapeutics.* Oncogene, 2010. **29**(5): p. 625-34.
122. Mole, D.R., et al., *Genome-wide association of hypoxia-inducible factor (HIF)-1alpha and HIF-2alpha DNA binding with expression profiling of hypoxia-inducible transcripts.* J Biol Chem, 2009. **284**(25): p. 16767-75.
123. Krishnamachary, B., et al., *Hypoxia-inducible factor-1-dependent repression of E-cadherin in von Hippel-Lindau tumor suppressor-null renal cell carcinoma mediated by TCF3, ZFHX1A, and ZFHX1B.* Cancer Res, 2006. **66**(5): p. 2725-31.
124. Koshiji, M., et al., *HIF-1alpha induces genetic instability by transcriptionally downregulating MutSalpha expression.* Mol Cell, 2005. **17**(6): p. 793-803.
125. Zhong, H., et al., *Overexpression of hypoxia-inducible factor 1alpha in common human cancers and their metastases.* Cancer Res, 1999. **59**(22): p. 5830-5.
126. Talks, K.L., et al., *The expression and distribution of the hypoxia-inducible factors HIF-1alpha and HIF-2alpha in normal human tissues, cancers, and tumor-associated macrophages.* Am J Pathol, 2000. **157**(2): p. 411-21.
127. Eckle, T., et al., *Hypoxia-inducible factor-1 is central to cardioprotection: a new paradigm for ischemic preconditioning.* Circulation, 2008. **118**(2): p. 166-75.
128. Bosch-Marce, M., et al., *Effects of aging and hypoxia-inducible factor-1 activity on angiogenic cell mobilization and recovery of perfusion after limb ischemia.* Circ Res, 2007. **101**(12): p. 1310-8.
129. Semenza, G.L., *Hypoxia-inducible factor 1 and cardiovascular disease.* Annu Rev Physiol, 2014. **76**: p. 39-56.
130. Semenza, G.L., *HIF-1 mediates metabolic responses to intratumoral hypoxia and oncogenic mutations.* J Clin Invest, 2013. **123**(9): p. 3664-71.
131. Harris, A.L., *Hypoxia--a key regulatory factor in tumour growth.* Nat Rev Cancer, 2002. **2**(1): p. 38-47.
132. Seagroves, T.N., et al., *Transcription factor HIF-1 is a necessary mediator of the pasteur effect in mammalian cells.* Mol Cell Biol, 2001. **21**(10): p. 3436-44.
133. Ryan, H.E., et al., *Hypoxia-inducible factor-1alpha is a positive factor in solid tumor growth.* Cancer Res, 2000. **60**(15): p. 4010-5.
134. Krishnamachary, B., et al., *Regulation of colon carcinoma cell invasion by hypoxia-inducible factor 1.* Cancer Res, 2003. **63**(5): p. 1138-43.
135. Feldser, D., et al., *Reciprocal positive regulation of hypoxia-inducible factor 1alpha and insulin-like growth factor 2.* Cancer Res, 1999. **59**(16): p. 3915-8.
136. Chiavarina, B., et al., *Metabolic reprogramming and two-compartment tumor metabolism: opposing role(s) of HIF1alpha and HIF2alpha in tumor-associated fibroblasts and human breast cancer cells.* Cell Cycle, 2012. **11**(17): p. 3280-9.
137. Gilkes, D.M., G.L. Semenza, and D. Wirtz, *Hypoxia and the extracellular matrix: drivers of tumour metastasis.* Nat Rev Cancer, 2014. **14**(6): p. 430-9.

138. Cox, T.R., et al., *LOX-mediated collagen crosslinking is responsible for fibrosis-enhanced metastasis.* Cancer Res, 2013. **73**(6): p. 1721-32.
139. Schietke, R., et al., *The lysyl oxidases LOX and LOXL2 are necessary and sufficient to repress E-cadherin in hypoxia: insights into cellular transformation processes mediated by HIF-1.* J Biol Chem, 2010. **285**(9): p. 6658-69.
140. Semenza, G.L., *Evaluation of HIF-1 inhibitors as anticancer agents.* Drug Discov Today, 2007. **12**(19-20): p. 853-9.
141. Bacon, A.L. and A.L. Harris, *Hypoxia-inducible factors and hypoxic cell death in tumour physiology.* Ann Med, 2004. **36**(7): p. 530-9.
142. Hayward, B.E., et al., *Imprinting of the G(s)alpha gene GNAS1 in the pathogenesis of acromegaly.* J Clin Invest, 2001. **107**(6): p. R31-6.
143. Michel, G., et al., *Site-directed mutagenesis studies of the hypoxia-inducible factor-1alpha DNA-binding domain.* Biochim Biophys Acta, 2002. **1578**(1-3): p. 73-83.
144. Mayo, K.E., *Molecular cloning and expression of a pituitary-specific receptor for growth hormone-releasing hormone.* Mol Endocrinol, 1992. **6**(10): p. 1734-44.
145. Struthers, R.S., et al., *Somatotroph hypoplasia and dwarfism in transgenic mice expressing a non-phosphorylatable CREB mutant.* Nature, 1991. **350**(6319): p. 622-4.
146. Hagiwara, M., et al., *Transcriptional attenuation following cAMP induction requires PP-1-mediated dephosphorylation of CREB.* Cell, 1992. **70**(1): p. 105-13.
147. Canettieri, G., et al., *Attenuation of a phosphorylation-dependent activator by an HDAC-PP1 complex.* Nat Struct Biol, 2003. **10**(3): p. 175-81.
148. Michael, L.F., et al., *The phosphorylation status of a cyclic AMP-responsive activator is modulated via a chromatin-dependent mechanism.* Mol Cell Biol, 2000. **20**(5): p. 1596-603.
149. Yamamoto, K.K., et al., *Phosphorylation-induced binding and transcriptional efficacy of nuclear factor CREB.* Nature, 1988. **334**(6182): p. 494-8.
150. Reimann, E.M., D.A. Walsh, and E.G. Krebs, *Purification and properties of rabbit skeletal muscle adenosine 3',5'-monophosphate-dependent protein kinases.* J Biol Chem, 1971. **246**(7): p. 1986-95.
151. Sandberg, M., et al., *Molecular cloning, cDNA structure and deduced amino acid sequence for a type I regulatory subunit of cAMP-dependent protein kinase from human testis.* Biochem Biophys Res Commun, 1987. **149**(3): p. 939-45.
152. Scott, J.D., et al., *The molecular cloning of a type II regulatory subunit of the cAMP-dependent protein kinase from rat skeletal muscle and mouse brain.* Proc Natl Acad Sci U S A, 1987. **84**(15): p. 5192-6.
153. Handschin, J.C. and U. Eppenberger, *Altered cellular ratio of type I and type II cyclic AMP-dependent protein kinase in human mammary tumors.* FEBS Lett, 1979. **106**(2): p. 301-4.
154. Basso, F., et al., *Comparison of the effects of PRKAR1A and PRKAR2B depletion on signaling pathways, cell growth, and cell cycle control of adrenocortical cells.* Horm Metab Res, 2014. **46**(12): p. 883-8.
155. Kadonaga, J.T., et al., *Isolation of cDNA encoding transcription factor Sp1 and functional analysis of the DNA binding domain.* Cell, 1987. **51**(6): p. 1079-90.
156. Kurten, R.C., et al., *Identification and characterization of the GC-rich and cyclic adenosine 3',5'-monophosphate (cAMP)-inducible promoter of the type II beta cAMP-dependent protein kinase regulatory subunit gene.* Mol Endocrinol, 1992. **6**(4): p. 536-50.
157. Weidemann, A. and R.S. Johnson, *Biology of HIF-1alpha.* Cell Death Differ, 2008. **15**(4): p. 621-7.
158. Bertout, J.A., S.A. Patel, and M.C. Simon, *The impact of O2 availability on human cancer.* Nat Rev Cancer, 2008. **8**(12): p. 967-75.
159. Pugh, C.W. and P.J. Ratcliffe, *Regulation of angiogenesis by hypoxia: role of the HIF system.* Nat Med, 2003. **9**(6): p. 677-84.
160. Semenza, G.L., *HIF-1 and tumor progression: pathophysiology and therapeutics.* Trends Mol Med, 2002. **8**(4 Suppl): p. S62-7.

161. Klatte, T., et al., *Hypoxia-inducible factor 1 alpha in clear cell renal cell carcinoma.* Clin Cancer Res, 2007. **13**(24): p. 7388-93.
162. Swinson, D.E., et al., *Hypoxia-inducible factor-1 alpha in non small cell lung cancer: relation to growth factor, protease and apoptosis pathways.* Int J Cancer, 2004. **111**(1): p. 43-50.
163. Baba, Y., et al., *HIF1A overexpression is associated with poor prognosis in a cohort of 731 colorectal cancers.* Am J Pathol, 2010. **176**(5): p. 2292-301.
164. Eberhard, A., et al., *Heterogeneity of angiogenesis and blood vessel maturation in human tumors: implications for antiangiogenic tumor therapies.* Cancer Res, 2000. **60**(5): p. 1388-93.
165. Asa, S.L., et al., *Evidence for growth hormone (GH) autoregulation in pituitary somatotrophs in GH antagonist-transgenic mice and GH receptor-deficient mice.* Am J Pathol, 2000. **156**(3): p. 1009-15.
166. Amieux, P.S., et al., *Compensatory regulation of RIalpha protein levels in protein kinase A mutant mice.* J Biol Chem, 1997. **272**(7): p. 3993-8.
167. Brandon, E.P., et al., *Defective motor behavior and neural gene expression in RIIbeta-protein kinase A mutant mice.* J Neurosci, 1998. **18**(10): p. 3639-49.
168. Taylor, S.S., et al., *PKA: a portrait of protein kinase dynamics.* Biochim Biophys Acta, 2004. **1697**(1-2): p. 259-69.
169. Skalhegg, B.S. and K. Tasken, *Specificity in the cAMP/PKA signaling pathway. Differential expression,regulation, and subcellular localization of subunits of PKA.* Front Biosci, 2000. **5**: p. D678-93.
170. Sandrini, F., et al., *Regulatory subunit type I-alpha of protein kinase A (PRKAR1A): a tumor-suppressor gene for sporadic thyroid cancer.* Genes Chromosomes Cancer, 2002. **35**(2): p. 182-92.
171. Tsigginou, A., et al., *PRKAR1A gene analysis and protein kinase A activity in endometrial tumors.* Endocr Relat Cancer, 2012. **19**(4): p. 457-62.
172. Kirschner, L.S., et al., *Mutations of the gene encoding the protein kinase A type I-alpha regulatory subunit in patients with the Carney complex.* Nat Genet, 2000. **26**(1): p. 89-92.
173. Beuschlein, F., et al., *Constitutive activation of PKA catalytic subunit in adrenal Cushing's syndrome.* N Engl J Med, 2014. **370**(11): p. 1019-28.
174. Lania, A.G., et al., *Proliferation of transformed somatotroph cells related to low or absent expression of protein kinase a regulatory subunit 1A protein.* Cancer Res, 2004. **64**(24): p. 9193-8.
175. Boikos, S.A. and C.A. Stratakis, *Molecular genetics of the cAMP-dependent protein kinase pathway and of sporadic pituitary tumorigenesis.* Hum Mol Genet, 2007. **16 Spec No 1**: p. R80-7.
176. Yin, Z., et al., *Pituitary-specific knockout of the Carney complex gene Prkar1a leads to pituitary tumorigenesis.* Mol Endocrinol, 2008. **22**(2): p. 380-7.
177. Sandrini, F., et al., *PRKAR1A, one of the Carney complex genes, and its locus (17q22-24) are rarely altered in pituitary tumours outside the Carney complex.* J Med Genet, 2002. **39**(12): p. e78.
178. Kietzmann, T., D. Mennerich, and E.Y. Dimova, *Hypoxia-Inducible Factors (HIFs) and Phosphorylation: Impact on Stability, Localization, and Transactivity.* Front Cell Dev Biol, 2016. **4**: p. 11.
179. Pullamsetti, S.S., et al., *Phosphodiesterase-4 promotes proliferation and angiogenesis of lung cancer by crosstalk with HIF.* Oncogene, 2013. **32**(9): p. 1121-34.
180. Toffoli, S., et al., *Intermittent hypoxia changes HIF-1alpha phosphorylation pattern in endothelial cells: unravelling of a new PKA-dependent regulation of HIF-1alpha.* Biochim Biophys Acta, 2007. **1773**(10): p. 1558-71.
181. Bullen, J.W., et al., *Protein kinase A-dependent phosphorylation stimulates the transcriptional activity of hypoxia-inducible factor 1.* Sci Signal, 2016. **9**(430): p. ra56.
182. Cheong, H.I., et al., *Hypoxia sensing through beta-adrenergic receptors.* JCI Insight, 2016. **1**(21): p. e90240.

183. Finger, E.C., et al., *Hypoxic induction of AKAP12 variant 2 shifts PKA-mediated protein phosphorylation to enhance migration and metastasis of melanoma cells.* Proc Natl Acad Sci U S A, 2015. **112**(14): p. 4441-6.
184. Carlucci, A., et al., *Proteolysis of AKAP121 regulates mitochondrial activity during cellular hypoxia and brain ischaemia.* Embo j, 2008. **27**(7): p. 1073-84.
185. Shaikh, D., et al., *cAMP-dependent protein kinase is essential for hypoxia-mediated epithelial-mesenchymal transition, migration, and invasion in lung cancer cells.* Cell Signal, 2012. **24**(12): p. 2396-406.
186. Taylor, S.S., et al., *Assembly of allosteric macromolecular switches: lessons from PKA.* Nat Rev Mol Cell Biol, 2012. **13**(10): p. 646-58.

7. Appendix

7.1. Abbreviations

[^{3}H]-TdR	Tritiated thymidine incorporation assay
ABC	Avidin-Biotin Complex
ACRO	Acromegaly-associated pituitary adenomas
ACTH	Adrenocorticotropin
ATP	Adenosin-5'-triphosphate
BSA	Bovine serum albumin
cAMP	cyclic adenosine monophosphate
ChIP	Chromatin immunoprecipitation
Co-IP	Co-immunoprecipitation
CREB	cAMP response element binding protein
DAB	3,3'-Diaminobenzidine
DDW	Double distilled water
DMEM	Dulbecco's Modified Eagle's Medium
DTT	Dithiothreitol
EDTA	Ethylenediaminetetraacetic acid
FACS	Fluoresence-activated cell sorting
FCS	Fetal calf serum
GH	Growth hormone
GHRH	Growth hormone releasing hormone
H_2O_2	Hydrogen peroxide
HEPES	2-(4-Hydroxyethyl)-1-peperazinyl)-ethanolsulforic acid
HIF1-α	Hypoxia-inducible factor 1α
I-2	Inhibitor 2 (specific for PP1)
IGF-1	Insuline-like growth factor
IHC	Immunohistochemistry
kD	Kilodalton (molecular weight)
NaCl	Sodium Chloride
NaOH	Sodium hydroxide
NFPA	Non-functioning pituitary adenoma
NP-40	Nonidet P-40
ONPG	o-Nitrophenyl-β-D-galactopyranosid
PBS	Phosphate buffered saline
Pit1	Pituitary transcription factor 1
PP1	Protein phosphatase 1
PRL	Prolactin
PVDF	Polyvinylidene fluoride
RIA	Radioimmunoassay
RLA	Relative luciferase activity
RT-PCR	Reverse transcriptase polymerase chain reaction
Rx	Reaction
SDS	Sodium dodecyl sulphate
SDS-PAGE	SDS polyacrylamide gel electrophoresis

SSA	Somatostatin analogs
Sstr	Somatostatin receptor
TEMED	Tetramethylethylenediamine
TBS	Tris buffered saline
TBST	TBS with 0.1% Tween-20
WT	Wild type

8. Acknowledgements

The last years spent working in the AG Stalla have probably been the most colorful and formative of my life. There are many people who have helped me push through the difficult times, celebrate the good ones and learn from all of them. At the risk of getting sappy and cliché, here we go:

Marily, thank you for taking me under your wing and giving me the chance to not just finish my PhD, but to learn, thrive and still be my weird self while doing it. Looking forward, I'm excited about the possibilities we will have to continue to work together setting up the Berlin-Munich Connection! You are a dear mentor and friend.

The AG Besoffenen (you know who you are!): oh man, where to start! Thank you for putting up with my inexperience in the lab (ie "lets run 15 blots at once to test antibody concentrations!"), for helping me learn and for always having time to listen. Thank you for all of the loud cafeteria afternoons and Tacos y Tequila nights. I don't think there will ever be such a fun, intelligent, inspiring and caring group as you guys.

Thank you to Mathias for your encouragement, help in the lab and the great inspiring discussions.

Ulrich, thank you for supporting me in the lab and making sure things run smoothly!

Thank you to Prof. Stalla for giving me the opportunity to work in the lab and for inspiring me to finish quickly.

Mom and Dad, thank you for always having my back and supporting my endeavors. You are the absolute greatest and I'm having a hard time expressing that in words now. I love you!

To everyone outside the lab, thank you for your understanding and for sticking with me through these last crazy years. I am grateful for each and every one of you.

Last but not least, thank you to the color purple for helping me through writers block.